UC Riverside
UC Riverside Electronic Theses and Dissertations

Title
Assessing the Role of Estrogen Signaling in the Developmental Toxicity of Oil in Fish

Permalink
https://escholarship.org/uc/item/1mm4t7n9

Author
Diamante, Graciel

Publication Date
2017

Peer reviewed|Thesis/dissertation

eScholarship.org Powered by the California Digital Library
University of California

UNIVERSITY OF CALIFORNIA
RIVERSIDE

Assessing the Role of Estrogen Signaling in the Developmental Toxicity of Oil in Fish

A Dissertation submitted in partial satisfaction
of the requirements for the degree of

Doctor of Philosophy

in

Environmental Toxicology

by

Graciel Y. Diamante

September 2017

Dissertation Committee:

Dr. Daniel Schlenk, Chairperson
Dr. David Volz
Dr. Morris Maduro

Copyright by
Graciel Y. Diamante
2017

The Dissertation of Graciel Y. Diamante is approved:

Committee Chairperson

University of California, Riverside

ACKNOWLDEGEMENTS

The work presented in this thesis would not have been possible without the support, guidance and help of my mentors, family and friends. I would first like to thank my major advisor Dr. Daniel Schlenk for accepting me into his lab and for his continual support and mentorship throughout my graduate career. He has helped me become a better researcher and scientist. When I first came to the lab, I was inexperienced in aquatic toxicology research. However, he encouraged me to attend the Society of Environmental Toxicology and Chemistry conference, which captivated my interest in this field. Furthermore, beyond the training I received in the lab, Dr. Schlenk has taught me the importance of collaboration, teamwork, and networking in academia and science.

I would also like to acknowledge all my past and current committee members, Dr. Dave Volz, Dr. Morris Maduro and Dr. Nicole zur Nieden for all their advice and suggestion during the course of this project. I would especially like to thank Dr. Volz for his help on my projects as well as taking time out of his busy schedule to discuss career options. Additionally, I want to express my gratitude to our collaborators in the University of Miami, Dr. Martin Grosell and his lab members, and the entire RECOVER Consortium, for their technical assistants and intellectual contributions to the project.

During my time at UCR I have been fortunate enough to make many new friends to share this journey. I would like to thank Hailey Choi and Allison Kupsco for their support and friendship since my first year at UCR. We all started grad school at UCR in 2012. We went through the ups and downs of classes and research together, and I am

extremely grateful to have shared those moments with each of them. We have become not only colleagues but great friends. Being a part of the Schlenk lab has also introduced me to many people from all over the world. I would like to thank Gabrielle do Amaral e Silva Müller, Juliane Freitas, Flávia Yamamoto and Eloise Lemaire for all the amazing and memorable moments I got to enjoy. Of course, I would also like to thank the current members of the Schlenk and Volz labs, especially Luisa Bertotto, Marissa Giroux and Sara Vliet. Even though I have only known them for a couple of years, we have become good friends. Thank you to Luisa and Marissa for making the lab a happy place to work. I would also like to thank Dr. Elvis Xu for his help on the RECOVER project and always answering my bioinformatics questions.

And last but not least, I would especially like to family and friends for all their love, support and patience for the last 5 years. I would like to thank my grandma, parents, sister, aunts, uncles, cousins and best friends for being my escape for the weekends. Thank you to my mom, dad and sister Camille for always being there and showing me there is more to life then grad school. I would also like to thank Hovik for everything, I could not have done this without you by side.

DEDICATION

I dedicate this dissertation to my parents and grandparents who have taught me the importance of hard work, diligence, respect and integrity.

ABSTRACT OF THE DISSERTATION

Assessing the Role of Estrogen Signaling in the Developmental Toxicity of Oil in Fish

by

Graciel Y. Diamante

Doctor of Philosophy, Graduate Program in Environmental Toxicology
University of California, Riverside, September 2017
Dr. Daniel Schlenk, Chairperson

Oil spills are one of the primary sources of polycyclic aromatic hydrocarbons (PAHs) in marine environments. PAHs are subject to biotic and abiotic weathering that can alter their physical and chemical characteristics. Due to photochemical reactions and microbial activity PAHs can undergo oxidation forming oxygenated products that can have severe effects on marine life and the environment. Previous studies have indicated that weathered oil can cause greater developmental toxicity than source oil. Among the PAHs found in crude oil, chrysene is one of the most persistent in the water column and can undergo photo-oxidation to produce oxygenated derivatives such as 2-hydroxychrysene and 6-hydroxychrysene, which possess respective estrogenic and antiestrogenic properties. The endocrine system regulates many signaling processes that control the development of cardiovascular immune, reproductive and central nervous systems. The integrated role of various biological systems and the interaction between

organs can make it difficult to assess the effects of endocrine disrupting compounds (EDCs) especially when a series of signaling events need to occur in a precise spatio-temporal manner during embryogenesis. To assess the role of estrogen signaling in the effects of hydroxychrysene, estradiol toxicity was first characterized using zebrafish. Here we showed that although disruption of estrogen signaling can result in significant malformations, the toxic effects of 2-hydroxychrysene and 6-hydroxychrysene were not directly mediated through this pathway. Additionally, studies evaluating microRNA regulation of mRNA expression, indicated disruption of ion transport may be critical step in the cardiovascular toxicity caused by oil. These findings raise the need to utilize genomic and epigenomic tools to identify mechanisms that are involved in the toxicity of these compounds to assess the potential risks of oil spills on fish populations.

Table of Contents

Title		Page
Introduction		1
Chapter 1:	Contribution of G protein-coupled estrogen receptor 1 (GPER) to 17β-estradiol-induced developmental toxicity in zebrafish	62
Chapter 2:	Developmental Toxicity Of Hydroxylated Chrysene Metabolites in Zebrafish Embryos	94
Chapter 3:	Regulation of microRNAs in mahi-mahi (*Coryphaena hippurus*) exposed to Deepwater Horizon oil	128
Conclusion		180

List of figures in the Introduction

Figure 0-1	Endocrine system network.	30
Figure 0-2	The hypothalamus–pituitary complex	31
Figure 0-3	Diagram of the major steps involved in thyroid hormone (T3 and T4) synthesis and secretion.	32
Figure 0-4	Thyroid receptor activation pathways.	33
Figure 0-5	Diagram of the steroid biosynthesis pathway.	34
Figure 0-6	Sex steroid hormones synthesis in the testis and the ovary.	35
Figure 0-7	Androgen receptor activation pathway.	36
Figure 0-8	The classical genomic activity of estrogens is mediated through the signaling of nuclear estrogen receptors (ERs).	37
Figure 0-9	Functional domains of the nuclear estrogen receptors.	38
Figure 0-10	Rapid non-genomic signaling of G-protein coupled estrogen receptors (GPER).	39
Figure 0-11	Zebrafish cardiac development.	40
Figure 0-12	Aryl hydrocarbon receptor pathway.	41

List of figures in Chapter 1

Figure 1-1	Effects of 17β–Estradiol (E2) on cardiac development and mRNA levels of GPER in zebrafish embryos at different times during development.	79
Figure 1-2	Effects of E2 on the expression of *lrrc10* in zebrafish embryos at different times during development.	80
Figure 1-3	Effects of E2 on the expression of *hand2* in zebrafish embryos at different times during development.	81
Figure 1-4	Effects of G1 exposure on cardiac development and expression of *lrrc10, hand2* and *gper* in zebrafish embryos.	82
Figure 1-5	Effects of GPER agonist G1 and GPER antagonist G36 co-exposure on deformities and the expression of *lrrc10, hand2* and *gper* in zebrafish embryos.	83
Figure 1-6	Effects of co-exposure to E2 and GPER antagonist G36 on deformities and the expression of *lrrc10, hand2* and *gper* in zebrafish embryos.	84
Figure 1-7	Percent of cardiac deformities after co-exposure of ER antagonist ICI 182, 780 with 17β–Estradiol (E2).	85
Figure 1-8	Images of sublethal malformations were observed after treatment with E2, including curved body axis, yolk-sac edema and pericardial edema at 76 hpf.	86
Figure 1-9	Effects of E2 on *vtg* expression in zebrafish embryos at 76 hpf.	87
Figure 1-10	Effects on Ca^{2+} levels in zebrafish embryos after 17β–Estradiol (E2) and G1 exposure.	88
Figure 1-11	Levels of cAMP in zebrafish embryos after 17β–Estradiol (E2) and G1.	89

List of tables in Chapter 2

Table 2-1	Effects of 2-hydroxychrysene, 6-hydroxychrysene, phenanthrene, chrysene and 17β–estradiol on survival and development of zebrafish embryos at 76 hpf after a 74hr exposure.	113-114

List of figures in Chapter 2

Figure 2-1	Effects of 2-hydroxychrysene, 6-hydroxychrysene, phenanthrene, chrysene and 17β–estradiol on spinal development of zebrafish embryos at 76 hpf after a 74 h exposure.	115
Figure 2-2	Effects of 2-hydroxychrysene, 6-hydroxychrysene, phenanthrene, chrysene and 17β–estradiol on eye development of zebrafish embryos at 76 hpf after a 74 h exposure.	116
Figure 2-3	Effects of 2-hydroxychrysene, 6-hydroxychrysene, Phenanthrene, Chrysene and 17β–Estradiol on cardiac development of zebrafish embryos at 76 hpf after a 74 h exposure.	117
Figure 2-4	Effects of 2-hydroxychrysene and 6-hydroxychrysene on pericardial area of zebrafish embryos at 76 hpf after a 74 h exposure.	118
Figure 2-5	Effects of 2-hydroxychrysene, 6-hydroxychrysene, Phenanthrene, Chrysene and 17β–Estradiol on circulation of zebrafish embryos at 76 hpf after a 74 h exposure.	119
Figure 2-6	Effects of 2-hydroxychrysene and 6-hydroxychrysene on hemoglobin levels in zebrafish embryos at 76 hpf after a 74 h exposure.	120
Figure 2-7	Effects of 2- and 6-hydroxychrysene on estrogen pathway signaling in zebrafish embryos at 76 hpf after a 74 hr exposure.	121
Figure 2-8	Effects of 2- and 6-hydroxychrysene on *rho, nxc1, vegfa, sema, runx1 and gata1* expression in zebrafish embryos at 76 hpf after a 74 h exposure.	122

List of tables in Chapter 3

Table 3-1	Upregulated and downregulated miRNA after slick and source oil exposure using both methods.	149
Table 3-2	List of differentially expressed miRNA at all 3 stages after source and slick oil exposure observed using both methods.	151
Table 3-3	List of differentially expressed miRNA at all 3 stages after source and slick oil exposure using the Fugu-guided approach method	152
Table 3-4	List of differentially expressed miRNA at all 3 stages after source and slick oil exposure using the phylogenetic-guided approach method.	153-156
Table 3-5	Enriched IPA cardiovascular disease of differentially expressed miRNA and inversely correlated genes at the 48 hpf stage after slick oil treatment using both methods.	160-161
Table 3-6	Enriched IPA cardiovascular disease of differentially expressed miRNA and inversely correlated genes at the 96 hpf stage after slick oil treatment using both methods.	162-164
Table 3-7	Enriched IPA ophthalmic disease of differentially expressed miRNA and inversely correlated genes at the 96 hpf stage after slick oil treatment using the both methods.	166-167
Table 3-8	Top cellular component and molecular function terms at the 96 hpf stage after source oil treatment using DAVID.	170-171
Table 3-9	Top cellular component and molecular function terms at the 96 hpf stage after slick oil treatment using DAVID.	172-173

List of figures in Chapter 3

Figure 3-1	Schematic of bioinformatics pipeline.	146
Figure 3-2	Transcript expression profiles of miRNAs using the phylogenetic-guided approach and Fugu-guided approach method	147-148

Figure 3-3	Venn Diagrams of differentially expressed miRNA at the 3 different stages after slick and source oil exposure.	150
Figure 3-4	Visual distribution of the number of differentially expressed mRNA correlated to differentially miRNA identified using IPA at 24 hpf.	157
Figure 3-5	Visual distribution of the number of differentially expressed mRNA correlated to differentially miRNA identified using IPA 48 hpf	158
Figure 3-6	Visual distribution of the number of differentially expressed mRNA correlated to differentially miRNA identified using IPA at 96 h	159
Figure 3-7	Ingenuity Pathway Analysis of correlated miRNA and mRNA network 96 hpf after slick oil exposure.	165
Figure 3-8	GO analysis of enriched biological processes of the correlated differentially expressed mRNA at 96 hpf after source oil exposure.	168
Figure 3-9	GO analysis of enriched biological processes of the correlated differentially expressed mRNA at 96 hpf after slick oil exposure.	169
Figure 3-10	Comparison of relative fold change of miRNA in 96 hpf larvae after slick oil exposure as determined by miRNAseq and qPCR.	174

Introduction

The endocrine system is a network of cellular signaling tissues that secrete hormones into the circulatory system. When a hormone binds to its receptor on/in a target tissue, it typically initiates a signaling cascade. Activation of the hormone receptor can have multiple downstream physiological effects, including regulation of the immune system, reproduction, behavior, and development (Figure 0-1).

The ability of the endocrine system to control cellular processes requires close coordination with the central nervous system (CNS). The primary link between the CNS and the endocrine system is the hypothalamus. It is organized into groups of neuronal bodies that can receive signals from the brain or afferent signals from the viscera, which then initiate the release of specific factors to the anterior or posterior portions of the pituitary gland. The magnocellular neurons release oxytocin (OT), vasopressin (AVP) and neurophysins (NP) to the posterior pituitary. The parvocellular neurons release corticotropin-releasing hormone (CRH), dopamine (DA), growth hormone-releasing hormone (GHRH), gonadotropin releasing hormone (GnRH), and thyrotropin-releasing hormone (TRH) to the anterior pituitary (Figure 0-2). The hypothalamus also releases inhibitory factors such as the gonadotropin-inhibitory hormone (GnIH) and somatostatin (SS) (Ubuka et al. 2013). The hormones produced by pituitary cells are typically released into the circulation, eventually reaching a diverse array of targets which elicit either the synthesis or release of a multitude of downstream factors.

Endocrine signaling can be negatively influenced by a host of factors including contaminants (DeRosa et al. 1998; Crisp et al. 1998; Sumpter 1998). Given the importance of the endocrine system to reproduction, most studies have focused on this apical endpoint. However, endocrine disrupting chemicals (EDCs) have also been shown to have adverse developmental, neurological and more recently cardiovascular effects (Panzica et al. 2007; Waye and Trudeau 2011; Frye et al. 2012; Gao and Wang 2014). In an attempt to better regulate endocrine endpoints, the US Environmental Protection Agency established the Endocrine Disruptor Screening Program (EDSP) to identify chemicals that adversely affect the estrogen, androgen, thyroid and steroid biosynthesis pathways in a biological system. Consequently, background on these four pathways will be initially the focus of this chapter with subsequent emphasis on steroid signaling. The goal of this review is to highlight the role of the different endocrine pathways in regulating the cardiovascular system and to present the challenges in evaluating EDCs during development.

Thyroid hormone synthesis and signaling pathways

Thyrotropin-releasing hormone signaling

Thyroid signaling is initiated when TRH reaches the pituitary and targets thyrotrophic cells that synthesize and release of the glycoprotein, thyroid-stimulating hormone (TSH). TRH binds to a subfamily of $G_{q/11}$ protein-coupled receptors, activating phospholipase C (PLC) that cleaves phosphatidylinositol 4,5-bisphosphate (PIP_2) into

two secondary messengers; inositol 1,4,5-trisphosphate (IP3) and diacylglycerol (DAG). Each of the secondary messengers will cause an influx of intracellular Ca^{2+} initiating the release of TSH to the blood stream where it will target the thyroid gland (Hsieh and Martin 1992). TSH regulates energy storage and consumption throughout development and during adulthood. TSH also binds to a group of G_s protein-coupled receptors on the membrane of thyroid cells activating adenylate cyclase (AC) and forming cyclic 3'5'-adenosine monophosphate (cAMP). Increases in cAMP can activate the protein kinase A (PKA) signaling pathways, which are involved in the production and secretion of thyroid hormones: 3,3'3,5'-Triiodo-L-thyronine (T_3) and L-thyroxine (T_4) (Brent 1994; Mullur et al. 2014).

Thyroid hormone synthesis

T_3 and T_4 are both synthesized in the follicles of the thyroid gland, derived from iodinated tyrosine. Blood-borne iodide is transported to the lumen of the thyroid follicle where it is oxidized to iodine by thyroperoxidase. Diet is another source of iodine, which is absorbed in the small intestine and transported to the thyroid. As a part of this process, thyroglobulin (Tg) is synthesized in the endoplasmic reticulum of thyroid gland cells and further processed in the Golgi apparatus. Tg is secreted into the colloid space, where the tyrosine residues undergo iodination (Kim and Arvan 1991 and 1993). Iodinated Tg will re-enter the cell by receptor-mediated endocytosis. After Tg is internalized, the endosome will fuse with lysosomes allowing the formation of T_3 and T_4 through the cleavage of Tg (Figure 0-3). The resulting thyroid hormones will then diffuse into the bloodstream (Kostrouch et al. 1991; Seljelid et al. 1970; Brix and Herzog 1994; Dunn et al. 1991).

Approximately 85% of the hormone released is T_4 and is predominantly converted to the more biologically active thyroid hormone T_3, by 5'-monodeiodinase in multiple organs such as the liver (Klein and Danzi 2007). In the bloodstream, T_4 and T_3 are transported by several thyroid hormone binding plasma proteins to ensure the supply of thyroid hormones to the cells (Herzog 1983; Kostrouch et al. 1993). Thyroxine-binding globulin, transthyretin and albumin are plasma proteins that transport of T_4 and T_3 in the bloodstream (Ingenbleek and Young 1994). The degradation and synthesis of thyroid hormones are highly regulated by available iodine, which influence the synthesis of Tg. TSH can increase the transport of iodine into the cells leading to a rise of thyroid hormone levels, which control TSH release through negative feedback (Breen et al. 1997).

Thyroid hormone signaling

Thyroid hormones play an important role in growth, development and metabolism. T_3 and T_4 bind to a superfamily of thyroid hormone receptors (TRs) that act as transcription factors. Unbound thyroid receptor is associated with a co-repressor protein that prevents it from initiating transcription. Upon binding of T_3 or T_4, the receptor will undergo a conformational change allowing it to bind to thyroid regulatory elements (TREs), upstream the promoter region of target genes. TRs also dimerize with retinoid X receptors (RXRs) and bind TREs (Figure 0-4). RXRs are widely distributed throughout different tissues and can interact with other receptors allowing TR crosstalk with additional regulatory pathways. At the plasma membrane, thyroid hormones can

bind to receptors on integrin avB3 leading to downstream effects on ion exchange such as Na^+ and H^+ (Cheng et al. 2010).

Steroid hormone synthesis and signaling pathways

Gonadotropin releasing hormone

Another factor released from the hypothalamus is GnRH, which regulates steroid synthesis and signaling. To mediate its role in reproduction, GnRH can bind to a $G_{q/11}$ protein-coupled receptor, found in gonadotrophic cells of the pituitary gland. Binding of GnRH to the membrane bound receptor will cause the G-protein to undergo a conformational change resulting in the activation of phospholipase C leading to the mobilization Ca^{2+}. Influx of Ca^{2+} ions initiates a cascade of signaling events including the production and secretion of two glycoproteins, luteinizing hormone (LH) and follicle-stimulating hormone (FSH). Each hormone plays a major role in reproduction by inducing steroidogenesis, spermatogenesis, folliculogenesis and ovulation. The increased levels of sex steroid hormones in the blood can cause a negative feedback decreasing the release of GnRH from the hypothalamus, which will affect the secretion of LH and FSH from the anterior pituitary gland.

FSH and LH have gender-specific roles in regulating reproduction. In females, FSH stimulates the growth of granulosa cells, which regulates follicular maturation and the production of estradiol (E2) by inducing CYP19 (Padmanabhan et al. 1991). In addition to enhancing proliferation of sertoli cells in the testis, FSH stimulates

spermatogenesis by inducing androgen binding-protein (ABP) in sertoli cells (Hansson et al. 1975). ABP aids in the intracellular transport of hormones such as testosterone, dihydrotestosterone and E2 (Meachem et al. 1996). Under the control of circulating testosterone and E2, FSH is also regulated by several transforming growth factor β (TGF-β) proteins: activin and inhibin (Gregory and Kaiser 2004). Activin increases the secretion of FSH and inhibin diminishes the release of FSH in females (Ling et al. 1986; De Jong 1988).

In females, an increase in circulating LH levels enhances ovulation and development of the corpus luteum, which secretes progesterone during the luteal phase of the ovarian cycle. In theca cells of the ovary, LH signaling initiates the conversion of cholesterol to androgens, which are precursors for estrogen synthesis via cytochrome P450 aromatase (CYP19). In males, LH is involved in the production of testosterone in the testis (Hu et al. 2010). Increased levels of testosterone will activate a negative feedback loop by inhibiting the release of GnRH and ultimately LH in the hypothalamus.

Steroid hormone synthesis

Production of steroid hormones can occur in several different tissues utilizing multiple forms of the cytochrome p450 monooxygenases or the hydroxysteroid dehydrogenase families of proteins (Payne and Hales 2004). Cytochrome p450 enzymes are a group of heme containing enzymes that are found in all organisms. They are not only important for steroid synthesis but also catalyze the biotransformation of endogenous as well as exogenous chemicals (Klingenberg 1958; Omiecinski et al. 2011). Hydroxysteroid dehydrogenases belong to a family of alcohol dehydrogenases with tissue

specific expression throughout development (Voutilainen and Miller 1986; Kayes-Wandover and White 2000; Mellon and Griffin 2002; Payne and Hales 2004). Steroid hormones are derived from the parent compound cholesterol. Intermediary products include aldosterone, cortisol, estrogens and androgens.

The first step in steroidogenesis occurs in the mitochondrial membrane, where the side chain moiety from cholesterol is cleaved, forming pregnenolone (Miller 2002 and 2008). Pregnenolone can either be hydroxylated by cytochrome p450 17 (CYP17) to form 17-hydroxypregnenolone or is converted into progesterone by 3β-hydroxysteroid dehydrogenase (3β-HSD). 17-Hydroxypregnenolone and progesterone are both precursors for androstenedione but under different pathways. 17-Hydroxypregnenolone is converted via CYP17 to dehydroepiandrosterone (DHEA), which is formed into androstenedione by an oxidoreductase known as 3β-HSD. Alternatively, progesterone may undergo hydroxylation by CYP17 into 17-hydroxyprogesterone, which is subsequently converted into androstenedione then into estrone or testosterone by CYP19 or by 17β-HSD, respectively. Estrone and testosterone are both precursors for E2. Estrone can be hydrolyzed to E2 by 17β-HSD and testosterone can be converted into E2 by CYP19 (Figure 0-5). The conversion of cholesterol to androstenedione and testosterone primarily occur in either the theca cells and granulosa cells of the ovaries or in the Leydig cells of the testis (Figure 0-6). Conversion of androstenedione to estrone and testosterone to estradiol occur in the granulosa cell of the ovaries (Figure 0-6).

Estrogens and androgens are synthesized in both males and females. However, differences in concentration and hormone receptor expression contribute to the difference

between the sexes. In males, androgens are the main steroid hormones that regulate reproduction and physiology. In Leydig cells, testosterone is rapidly created from androstenedione due to the high expression of 17β-HSD (Andersson et al. 1996; O'Shaughnessy et al. 2000). However, estradiol is also present in males and is produced in mammalian testis (Stumpf 1969). Estrogen has an essential role in reproduction as well as Leydig cell development and function (Khan et al. 1998; Abney 1999). In addition to its roles normal male physiology, estrogens have a role in regulating steroidogenesis (Melner and Abney 1980a and 1980b; Kalla et al. 1980). Studies have shown that estradiol can inhibit enzymes important for steroid production such as 17α-hydroxylase in males (Brinkmann et al. 1980; Abney 1999). The biosynthesis of androgens in females occurs in the ovary and in the adrenal gland (Lebbe and Woodruff 2013). The production of androgens in theca cells is primarily under LH regulation (Baird et al. 1981). Low levels of LH have been shown to result in the increased production of androgens (Campbell et al. 1998). Maintaining the appropriate amounts of androgens in female is important in sexual development and bone formation.

Since steroid hormones play a significant role in vertebrate physiology and development, there are essential mechanisms that have evolved to help maintain hormonal homeostasis. Steroidogenic acute regulatory protein (StAR) alters the production of steroid hormones through the manipulation of cholesterol transport in the cell (Miller 1999 and 2007). Steroidogenesis can also be regulated transcriptionally through the expression of the above steroidogenic enzymes (Hiroi et al. 2004). Recent

evidence has shown that these enzymes can also be epigenetically regulated (Martinez-Arguelles and Papadopoulos 2010).

Signaling of steroid hormones

Steroids hormones such as androgens and estrogens, initiate receptor activation by binding to intracellular or membrane bound receptors. When initially described in the late 1960s to early 1970s, estrogenic activation was characterized by the binding of E2 to a classical intracellular receptor (Jensen et al. 1968; Jensen and Desombre 1973). These intracellular steroid receptors belong to a superfamily of nuclear receptors that can either stimulate or inhibit the transcription of specific gene targets through genomic interactions. In addition to nuclear receptor activation, steroid hormones can also induce non-genomic signals that initiate the production of secondary messengers. Increases in secondary messengers can also control the expression of genes through a variety of additional downstream signal transduction pathways. The primary difference between genomic and non-genomic pathways is that the latter does not require the entry of hormones into the cell but rather mediates their action through receptors at the cell membrane.

Signaling of Androgens

Androgens initiate activity by binding to cytosolic androgen receptors (ARs) (Chang et al. 1988a and 1988b; Gobinet et al. 2002). One of the most well studied androgens that bind to ARs is testosterone (Benten et al. 1999). After the binding of testosterone to an AR, the receptor undergoes a conformational change exposing the DNA binding domain. The ligand- receptor complex then moves to the nucleus and

activates the expression of genes by binding to androgen-response elements (AnRE) (Jenster et al. 1991; Chang et al. 1995). Once bound to the DNA, the complex can recruit co-activators that initiate chromatin structure modifications, which allow RNA polymerases access to initiate transcription (Wang et al. 2005; McKenna and O'Malley 2002) (Figure 0-7).

AR is expressed in several tissues of all vertebrates (de Waal et al. 2008; Gustafsson and Pousette 1975; Chang et al. 1988b). The expression of AR is dependent on age and reproductive stage of an organism. In rats, aside from the reproductive organs of both male and female, AR is expressed in the pancreas, liver, thyroid gland and heart in varying degrees (Gustafsson and Pousette 1975; Takeda et al. 1990; Kimura et al. 1993). ARs regulate the expression of enzymes important for metabolism, cell differentiation, growth and detoxification (Sahlin et al. 1994; Hossain et al. 2008). Androgens can also initiate rapid non-genomic effects through secondary messengers (Foradori et al. 2008). Studies in mouse have shown that testosterone can induce an influx of extracellular Ca^{2+} following activation of the phospholipase C pathway and the downstream effectors, calmodulin and extracellular signal-regulated kinase (ERK) (Benten et al. 1999; Mellstrom and Naranjo 2001; Estrada et al. 2003).

Signaling of Estrogens

Estrogens can induce biological effects by binding to G-protein coupled receptors or nuclear receptors (Hall et al. 2001; Prossnitz et al. 2008). Of the different estrogens, E2 is the strongest endogenous agonist for estrogen receptors (Kuiper et al. 1997; Heldring et al. 2007). The classical pathway of estrogen signaling regulates gene

transcription by binding to the nuclear estrogen receptor (ER). In the absence of a ligand, heat shock proteins inhibit ERs. When E2 binds to the receptor, it will induce a conformational change causing the release of the inhibitory factors and initiating dimerization with another molecule of ligand-ER complex. The activation of ER also results in the exposure of the DNA binding domain in the receptor that binds to estrogen response elements (EREs) in the promoting region of ER-regulated genes. Each response element has a specific palindromic DNA sequence (AGGTCAnnnTGACCT).

Activated ER can also induce transcription by regulating proteins involved in chromatin modification and recruitment of the transcriptional machinery (Pinzone et al. 2004; Heldring et al. 2007) (Figure 0-8). The two main forms of nuclear estrogen receptors are ERα and ERβ. ERα was the first estrogen receptor that was described in the 1960s in humans (Jensen 1962). Then in 1993, an ERα knockout mice was created and soon after ERβ was discovered (Lubahn et al. 1993; Kuiper et al. 1996). Both ERs are highly conserved in structure and in DNA binding domains (Heldring et al. 2007). Expression of these receptors depends on tissue type and developmental stage.

ERs have 6 different structural regions (A-F) that have various physiological functions. For instance in humans, region E is the site for ligand binding, while region C allows for DNA binding. Each region is stabilized by region D. Region E also has a ligand dependent transcription activation function (AF-2), while domain A/B has a ligand independent transcription activation function (AF-1) (Figure 0-9). AF-2 binds a family of co-activator proteins called p160s, which includes GRIP1, TIF1 and SRC-1. These co-activators then recruit other transcriptional factors such as CREB binding proteins and

p300. Together these proteins can induce histone modification and allow the recruitment of the transcription machinery complex. Unlike AF-2, less is known about the activity for AF-1 (Webb et al. 1998).

Genes lacking ERE sequences can still be regulated by E2, further showing the diversity of estrogen signaling. ERs can also be transcriptional regulators by interacting with other proteins to induce expression. For example, ER can interact with activation protein 1 (AP-1) and affect the expression of genes that contain AP-1 binding sites (Figure 0-8). AP-1 is a complex of proteins that consist of different combinations of FOS and JUN proteins. AP-1 binding sites are found in promoters of genes essential for many cellular processes like cell division and death. Interaction between ER and AP-1 sites has been shown to induce transcription of ovalbumin, cyclin D1 and IGF genes (Gaub et al. 1990; Umayahara et al. 1994; Liu et al. 2002). ER and AP-1 protein interactions are dependent on the receptor subtype and the AF domain (Webb et al. 1999).

There are also genes that only contain imperfect sequences or half of the ERE sequence in their promoting regions (Duan et al. 1998; Petz and Nardulli 2000). Genes with unique EREs include low-density lipoprotein receptor (*LDLR*) and *c-fos*, and are regulated through an ER-Sp1 complex (Weisz and Rosales 1990). Studies in breast cancer cells have shown that ERα-Sp1 can induce genes involved in cell cycle progression and proliferation (Kim et al. 2005). Similar to the signaling pathways induced by ER/AP-1, the actions of the ER/Sp1 complex are also dependent on receptor type. E2 signaling is also involved in the regulatory functions of NF-KB and GATA1.

Interaction of ER with NF-KB has been shown to have a role in bone metabolism by affecting the transcription of interleukin 6 (*il-6*) (Stein and Yang et al. 1995).

Similar to other steroid hormones the effects of estrogen can also occur through non-genomic interactions mediated through secondary messengers such as Ca^{2+} and cAMP (Figure 0-10) (Szego and Davis 1967; Pietras and Szego, 1975). E2 membrane signaling is complex and quite controversial. These rapid changes in levels of Ca^{2+} and cAMP can be induced by E2 binding to membrane bound receptors such as a transmembrane, G-protein coupled estrogen receptor (GPER) (Revelli et al. 1998; Revankar et al. 2005; Thomas et al. 2005) (Figure 0-10). GPER has been found on the plasma membrane as well as the outer surfaces of intracellular organelles such as the endoplasmic reticulum (Thomas et al. 2005; Revankar et al. 2005; Funakoshi et al. 2006). Although rapid production of secondary messengers is the predominant effect produced, GPER activation alters downstream gene expression (Vivacqua et al. 2012). Estrogen induced increases of cAMP has been observed in uterine, mammary gland, and breast cancer cells (Szego and Davis 1967; Aronica et al. 1994). In breast cancer cells, E2 was shown to bind to GPER, and activate adenylyl cyclase (AC) and increase cAMP levels (Thomas et al. 2005). A study in vascular smooth muscle cells has shown that E2 can promote apoptosis by inhibition of PKA via GPER (Ding et al. 2009). GPER signaling can also activate the phosphoinositide 3-kinase (PI3K) pathway (Ding et al. 2009). PI3K/AKT regulates cellular proliferation and suppression of apoptosis (Datta et al. 1997 and 1999). GPER induced apoptosis in vascular cells has been shown to be via ERK signaling (Ding et al. 2009). Estrogen mediated-ERK activity has been described to

involve EGFR transactivation (Daub et al. 1996; Filardo et al. 2000). The EGF pathway is important in regulating meiosis, mitosis and cellular differentiation (Carpenter and Cohen 1979). Binding of GPER has been shown to induce the mobilization of Ca^{2+} ions into the cytosol by its interaction with EGFR (Figure 0-10) (Revankar et al2005).

While differences are present between the genomic and non-genomic regulatory pathways of estrogens, overlap also occurs. For example, cyclin D1 (*CCND1*) expression is regulated by AP-1, but studies have shown that E2 can induce *CCND1* transcription via cAMP, which was linked to the activation of PKA (Castro-Rivera et al. 2001). The ability of estrogen to regulate the transcription of genes such as *CCND1* by several mechanisms further shows the complexity of estrogen signaling pathways. Additionally, the interaction of ERα and GPER is required for estrogen induced pathways in ovarian cancer cells (Albanito et al. 2007).

Role of the Endocrine System on the Cardiovascular System

Hormones play a key role in a diverse number of signaling pathways in different organ systems like the cardiovascular system. Thyroid hormone receptors are expressed in many different tissues such as the brain, heart, kidney and liver (Cheng et al. 2010). In the heart, changes in the concentration of both T_3 and T_4 can cause changes in cardiac output, myocyte contraction, as well as oxygen consumption (Kahaly and Dillmann 2005; Biondi et al. 2002; Danzi and Klein 2002). However, in cardiac myocytes, T_3 initiates most of the signaling because of limited deiodination in these cells (Everts et al. 1996).

T_3 can initiate signaling in cardiac myocytes by binding to TR or RXR and regulate the expression of multiple genes involved in cardiac function (Brent 1994). Expression of cardiac genes such myosin heavy chain, sarcoplasmic reticulum Ca^{2+} ATPase (SERCA) and phospholamban (PLB) are regulated by TR (Hartong et al. 1994; Kiss et al. 1994; Klein and Danzi 2007). Myosins are important parts of muscle fibers and aid in muscle contraction. During muscle relaxation, cytosolic Ca^{2+} is remobilized into the sarcoplasmic reticulum by SERCA under PLB regulation. Thyroid hormones can also mediate physiological effects by non-genomic pathways in cardiac cells. T_3 can alter membrane channels that control ion influxes such as Ca^{2+} essential for proper cardiac function (Davis and Davis 2002). In mice, treatment of vascular endothelial cells with T_3 led to the phosphorylation of protein kinase B (AKT) and endothelial nitric oxide synthase (eNOS), a protein involved in synthesis of nitric oxide (NO), which regulates contraction, heart rate and myocyte contractility (Hiroi et al. 2006).

Steroid hormones have also been shown to have cardiac effects. In addition to reproductive tissues, testosterone has also been shown to impact macrophages, cardiac myocytes and neuroblastoma cells (Ceballos et al. 1999; Estrada et al. 2006a and 2006b). Androgen-induced Ca^{2+} influxes cause cell proliferation, cell death by apoptosis or necrosis (Estrada et al. 2006b). In cardiac myocytes, activation of a G-protein coupled receptor by testosterone causes an increase in intracellular Ca^{2+} (Vicencio et al. 2006). In rabbits, the non-genomic effects of androgens have been shown to affect the relaxation of coronary arteries and the aorta in rabbit (Yue et al. 1995). Xiao et al. (2015) showed that testosterone could have a protective role in cardiac myocytes by decreasing cell death via

AR. Although androgens have been linked to cardiac health, the role of androgen signaling on the heart has not been fully characterized (Liu et al. 2003; Kaushik et al. 2010).

As with androgens, estrogens can regulate of non-reproductive organ systems, including the cardiovasculature system (Murphy 2011), often having a protective role against cardiovascular diseases (Mendelsohn and Karas 1999; Deschamps and Murphy 2009). For example, estrogen therapy has been linked to decreasing cardiac arrhythmias in postmenopausal women (Cagnacci et al. 1992), and estrogens can affect blood flow by regulating the metabolism of cholesterol and reduce arterial plaque formation (Chow 1995). The role of the estrogen pathway on cardiovascular function is complex (Meyer et al. 2009 and 2011). Activation of GPER also prevents the opening of mitochondria permeability transition pores, which may reduce intracellular Ca^{2+} levels during ischemia-reperfusion injury (Hausenloy and Yellon 2003; Bopassa et al. 2010). Contraction of cardiac myocytes is dependent upon rapid fluctuations in intracellular Ca^{2+}. Studies in mice have shown that the number of L-type Ca^{2+} channels is maintained by E2 (Johnson et al. 1997). L-Type Ca^{2+} channels are one of the most abundant calcium channels found in cardiac cells and transport Ca^{2+} into the cytosol (Catterall 1991). Signaling pathways via estrogen can also impact the cardiovascular system by regulating the expression of nitric oxide synthase (NOS), a protein that catalyzes the production of NO (Chambliss and Shaul 2002). NO targets vascular endothelial cells and modulates myocardial contractility.

Endocrine Disrupting Chemicals

The ability of hormones to affect an important network like the cardiovascular system, shows the complex and integral role of the endocrine system in normal organismal physiology. Biological processes that are required for normal development and function of organ systems can be influenced not only by endogenous molecules but as well as exogenous agents. Environmental contaminants can alter the endocrine system signaling (DeRosa et al. 1998; Crisp et al. 1998; Sumpter 1998). Endocrine disrupting chemicals (EDCs) include a host of compounds such as pesticides, steroid hormones and pharmaceutical agents, which can enter water bodies through municipal discharge of wastewater, as well as agricultural, industrial and urban runoff (Ternes et al. 1999; Purdom et al. 1994; Larsson et al. 1999). The presence of EDCs in the environment has become a major concern due to the potential risks they pose to exposed populations.

EDCs can alter endocrine pathways by mimicking endogenous hormones and binding to specific receptors, either as an agonist or as an antagonist. The synthesis or clearance of endogenous hormones may also be altered by EDCs. Moreover, some EDCs can have multiple modes of action. For example, bisphenol-A (BPA), an industrial plasticizer, acts on several endocrine pathways by binding to estrogen, androgen and thyroid receptors (Kuiper et al. 1997; Moriyama et al. 2002; Zoeller et al. 2005; Sohoni and Sumpter 1998; Lee et al. 2003). As described above each of these pathways have roles in the cardiovascular system. Epidemiological evidence has correlated exposure to BPA with increased cardiovascular risks (Melzer et al. 2010). Identification of the

specific pathway affected by toxicants such as BPA can be especially challenging, due to the significant amount of cross-talk between endocrine pathways.

Hormones have also been suggested to play a role in cardiac development, and exposure to EDCs during embryogenesis can have significant effects that may impair the fitness of the organism. The heart serves a critical role in a developing organism. Consequently, impairment of endocrine pathways at sensitive life stages may significantly alter cardiac development and cause multiple lethal and sublethal effects that may not be observed until later life stages. Due to the complex nature of the evaluating EDCs, researchers have established and benefitted from the use of zebrafish as a model organism.

Zebrafish as a Model for Cardiac development

Zebrafish (*Danio rerio*) has been a useful model in better understanding developmental toxicology. Traditionally, toxicants were screened for developmental effects using rodents, which bring certain limitations owing to their high cost of use and protracted developmental time, both of which limit the ability to evaluate the impacts of toxicants at sensitive stages. Zebrafish can be easily maintained and cultured in a laboratory setting. Due to its transparent embryos, visual analysis of organogenesis can be measured throughout embryonic development. The zebrafish development toxicity assay (ZEDTA) has evaluated the teratogenicity of hundreds of compounds with high predictive ability (Ball et al. 2014). Large-scale mutagenesis screens have allowed the

classification of important genes involved in the development of many organs such as the heart (Haffter et al. 1996; Driever et al. 1996; Chen et al. 1996). To further explore zebrafish development, small molecule screens have also been conducted to investigate both time and dose effects (Peterson et al. 2000; Mathew et al. 2007).

Many of the genes involved in development are highly conserved between zebrafish and humans allowing it to serve not only as a general vertebrate model, but also one that can be utilized in human health biomedical research (Lam et al. 2006). There are several transgenic strains that have greatly contributed to developmental biology research (Veldman and Lin 2008; Ni et al. 2012). One of the first strains developed was a GFP labeled *gata1* gene that allows the study of erythrocyte development (Long et al. 1997). Transgenic zebrafish models have also been generated to study human diseases. A transgenic zebrafish line containing the mutated human cardiac sodium channel gene *scn5a* was developed as an arrhythmia model (Huttner et al. 2013).

The development of zebrafish is rapid; embryos hatch approximately 72 hrs after fertilization. The release of eggs by fecund females is driven by light and the eggs are then externally fertilized immediately. Zebrafish development is divided into several stages: zygotic, cleavage, blastula, gastrula, segmentation, pharyngula, and the hatching period (Kimmel et al. 1995). Zebrafish are not dependent on a functional cardiovascular system for the first five days of its development, allowing phenotypic analysis after genetic alterations or chemical exposure. Although the cardiovascular system of zebrafish is different from mammals, early cardiac development has many similarities. The many

complex processes that occur during cardiovascular development in zebrafish has been extensively reviewed (Stainier 2001; Staudt and Stainier, 2012).

Myocardial and endocardial progenitor cell formation is one of the earliest events in cardiac development and many of the genes and pathways involved are highly conserved among vertebrates. Cardiac progenitor cells that will later differentiate into myocardial and endocardial cells are derived from mesodermal cells (Figure 0-11). At around 3 hours post fertilization (hpf), cardiac progenitor cells are found on the marginal zone of the embryo. One of the earliest genes to be expressed in cardiac cells and is thought to be a key player in cardiac differentiation is *gata5*. It has been shown to initiate and can regulate expression of *nkx2.5* during cardiac cell specification (Reiter et al. 1999). NKX2.5 is crucial for myocardial differentiation in zebrafish (Chen and Fishman 1996). Several mutation studies have identified that *nodal* and *bmp* signaling also affects *nkx2.5* expression. Mutations on *nodal* and *bmp* result in a decrease in *nkx2.5* expression which could be restored by forcible expression of GATA5 (Reiter et al. 2001; Kishimoto et al. 1997). NKX2.5 homologs have been identified in pre-cardiac mesoderm cells of other organisms such as mice and frogs (Lints et al. 1993; Tonissen et al. 1994). Another important gene in cardiac differentiation is helix–loop–helix transcription factor (*hand2*) (Yelon et al. 2000). *Hand2* also contains the binding site for GATA transcription factors in its promoter region (McFadden et al. 2000). Hand2 deficient embryos result in a decrease in myocyte cell number (Yelon et al. 2000). The differentiation of endocardial cells is less understood compared to that of myocardial cells. One of the genes that is

important for endocardial cell formation is *clouche (clo)*. Mutations in this gene have been shown to block endocardial and blood cell differentiation (Stainier et al. 1995).

Starting from mid to late gastrula and during the segmentation period, cardiac precursor cells move towards anterior lateral plate mesoderm (ALPM) (~16 hpf) and then fuse in the midline (~19 hpf) (Figure 0-11). When cardiac cells reach the ALPM they continue to further differentiate (De Pater et al. 2009). The myocardial cells will further differentiate into ventricular or atrial myocytes by expression of different myosin heavy chain genes. *Grinch,* which encode a G-protein coupled receptor, is expressed in the marginal zone and the ALPM, while its ligand apelin are found in the midline and (Scott et al. 2007; Zeng et al. 2007). Grinch-Appelin signaling has been shown to be important for cardiac cell migration during gastrulation. Fibronectin is an essential factor in cell migration and cardiac fusion. Mutation in the fibronectin gene (*natter*) has been demonstrated to disrupt the movement of cells to the midline (Trinh and Stainier 2004). Levels of fibronectin are balanced and regulated by *hand2* (Garavito-Aguilar et al. 2010). A gene mutation known as Miles apart (*mil*), and its ligand regulator two of hearts (*toh*), is reported crucial for cell movement to the midline (Kupperman et al. 2000; Osborne et al. 2008). Endocardial cells will migrate towards the midline with the aid of the transcription factor *tal1* (Bussmann et al. 2007). VEGF signaling is also required for endocardial movement in order to coat the interior heart tube. Interaction between the endocardial and myocardial cells is also important. Endocardial cells may play a role in myocardial cell migration to form the outer layers of the cardiac cone (Staudt and Stainier 2012).

After the fusion of the two bilateral cardiac primordia (~19 hpf), the heart forms a disc-like structure in the midline that will form the primitive heart tube (~26 hpf). The myocardial disc will rotate forming the venous pole at the left side of the midline, while the arterial pole remains at the midline (Figure 0-11). The myocardial cells originating from the right field will involute towards the ventral side into the anterior region of the embryo. Mutations to *has* and *nok* have been shown to alter cell polarity and interfere with heart tube formation (Rohr et al. 2006; 2008). Both *nodal* and *bmp* signaling also help regulate this well-organized process (Bakkers 2011). *Bmp4* is asymmetrically expressed with high amounts on the left field (Chen et al. 1997). Along with the left rotation of the disc, the heart subsequently undergoes extension.

After formation of the cardiac tube, at ~36 hpf, the heart tube loops to form a two-chambered organ with an inner and outer curvature (Figure 0-11). The ventricle will bend to the right side of the midline while the future atrium remains in place. This second rotation is also regulated by asymmetric gene expression. The venous and arterial poles will rotate at different degrees. Then the chambers will obtain their curvature by undergoing a process called cardiac ballooning. Natriuretic peptide type A (*nppa*) expression sets the outer curvature of the myocardium (Auman et al. 2007). Several molecular events are required for ventricular specification, which will form the major pumping chamber. Alterations in several genes such as *gata5* and *hand2* specifically produce altered ventricle formation (Reiter et al 1999; Yelon et al. 2000).

Another important step in heart development is the atrioventricular canal (AVC) and valve formation. This starts at ~36 hpf and continues until about 4 days post

fertilization when the valve leaflets are formed. The AVC is formed at the border between the two cardiac chambers. AVC specification is observed when restriction of *bmp4* and *versican* expression is limited to the AVC myocardial cells, and *notch1b* is limited to the endocardial cells (Westin and Lardelli, 1997; Walsh and Stainier 2001). Cardiac valves are essential in maintaining the direction of blood flow from the ventricle to the atrium. Valve development starts with the formation of an endocardium cushion in the atrioventricular canal. Endothelial cells will take a cuboidal shape and start to express *dm-grasp* (Beis et al. 2005; Bakkers 2011). The molecular signaling of valve formation involves communication between the myocardial and endocardial layers via *nodal*, *nfat* and *tgf-B* pathways. After hatching, the endocardial cushion will enlarge and differentiate to form the atrioventricular valve leaflets. Blood flow also plays a role in valve development. Molecular changes that occur during valvulogenesis can be stimulated by physical changes of blood flow. The sheer stress produced from the oscillating flow induces the transcription of *klf2*, which regulates *notch* expression and enhances valve formation (Vermot et al. 2009; Timmerman et al. 2004).

As the heart is developing from a tube to a looped structure, it contains layers of two different cell types (the myocardial and endocardial cells) (Figure 0-11). However, a third layer arises from the surrounding cells called the epicardium. This cell layer forms a surface around the entire heart. *Bmp4* signaling from the myocardium layer induces epicardial specification (Liu and Stainier 2010). Expression of *wt1*, *tbx18* and *tcf21* are the molecular markers for the epicardial cell population (Serluca 2008). The epithelial layer that surrounds the heart protects it from injury. After injury, the epicardial cells

respond by increasing the expression of *tbx18* causing epithelial to mesenchyme transition, which will move into the injured myocardium layer forming a vascular network to promote repair (Lepilina et al. 2006; Kim et al. 2010).

Contractions are first observed at the venous pole of the developing heart (~24 hpf). Contractions initially occur at an irregular rhythm until the heart tube is fully formed. As the heart continues to develop, the contractions continue to increase and occur in a sequential pattern. The cells that maintain this pulse are located at the inner atrial node. *Islet-1* regulates the activity of pacemaker cells, which is seen at 48 hpf (Tessadori et al. 2012). Before the heart starts to contract in a peristaltic pattern, there is a decrease in pulse in the canal myocardium. This delay disappears in zebrafish that lack an endothelium suggesting that this event is initiated from signals from the endocardial cells (Milan et al. 2006). Transcription factor *tbx2b*, which is expressed in the myocardium of the AV canal is also required for the conduction delay as well as marking fast and slow conducting cells. *Bmp4* can regulate expression of *tbx2b*, which are both regulated by Wnt signaling in the AV canal myocardium (Verhoeven et al. 2011).

Cardiotoxicity in the Zebrafish

The growing use zebrafish and detailed studies on its cardiovascular development have greatly contributed in characterizing the effects of cardiac toxicants. 2,3,7,8-Tetrachlorodibenzo-*p*-dioxin (TCDD), a polychlorinated dibenzo-*p*-dioxin congener, is known to target the cardiovascular system. TCDD mediates its toxicity by binding with

high affinity to the aryl hydrocarbon receptor (AhR) in the cytoplasm. Activated AhR will move to the nucleus and form a dimer with the aryl hydrocarbon receptor nuclear translocator (ARNT). The AhR/ARNT dimer can then bind to xenobiotic response elements (XRE) and regulate transcription of specific genes (Denison et al. 1988a and 1988b; Schmidt and Bradfield 1996; Rowlands and Gustafsson 1997). AhR regulates the genes involved in chemical metabolism such as cyp1A (Fujisawa-Sehara et al. 1987; Telakowski-Hopkins et al. 1988; Denison et al. 1988a) (Figure 0-12).

AhR also has an important role in the development of several organs, including the heart (Gonzalez and Fernandez-Salguero 1998; Antkiewics et al. 2006). Disruption of the AhR pathway results in cardiovascular defects. Ahr-null mice resulted in an increase in heart weight that is associated with myocyte hypertrophy (Thackaberry et al. 2002; Lund et al. 2003). Furthermore, over activation of AhR by TCDD causes heart size defects and dys-regulation in myocyte proliferation and heart rate (Hornung et al. 1999; Walker and Catron 2000; Thackaberry et al. 2005). Other effects include looping malformations, pericardial edema, and decreases in myocyte number have also been associated to TCDD toxicity (Henry et al. 1997; Antkiewics et al. 2006; Carney et al. 2006). Further evidence that the developmental effects of TCDD were mediated through AhR comes from the observation that malformations in wildtype mice were reversed with a loss of function mutation of the *ahr* and *arnt* genes (Walisser et al. 2004). However, there is growing evidence that TCDD toxicity isn't dependent on activation of *cyp1a* (Carney et al. 2004).

Since the genome is well annotated for zebrafish, many researchers have used this model to uncover other AhR targets during development. Handley-Goldstone et al. 2005 showed exposure to TCDD can alter the expression of genes that form the sarcomere, which is important for contraction. To further elucidate specific targets of AhR/ARNT, transcriptional changes were also temporally assessed in heart tissue of zebrafish after TCDD exposure (Carney et al. 2006). The genes that were dys-regulated were involved in xenobiotic metabolism, cell division and proliferation, as well as ion transport. Along with the gene alterations, there was a significant reduction in cardiac function, heart size and looping defects (Carney et al. 2006).

Another group of compounds that have been shown to activate the AhR and cause cardiac defects are polycyclic aromatic hydrocarbons (PAHs). PAHs are byproducts formed from incomplete combustion of organic matter. Mixtures of PAHs can also be found in fossil fuels such as crude oil and coal. Many studies have shown that exposure to crude oil can result in several malformations and sublethal effects (Incardona et al. 2013, 2014 and 2015). Some of the abnormal phenotypes that have been observed after exposure to PAH mixtures are pericardial edema, yolk sac edema, and curved body axis (Incardona et al. 2004; Heintz et al. 1999). Effects on heart rate (bradycardia) have also been described after PAH exposure (Incardona et al. 2004). To determine the specific compounds that cause toxicity, zebrafish embryos were exposed to a host of individual PAHs with subsequent evaluation of development (Incardona et al. 2004; 2006 and 2011). These studies showed that individual PAHs can induce toxicity with differing severity. Three-ring PAHs such as phenanthrene and dibenzothiophene caused more

severe effects compared to pyrene, as well as different deformities. Phenanthrane and dibenzothiophene showed effects on cardiac conduction while pyrene resulted in anemia and loss of peripheral circulation showing that ring number is an important characteristic in PAH toxicity (Incardona et al. 2004).

Studies have also been done to evaluate the molecular mechanism of cardiac toxicity of individual PAHs. Research on PAHs has been primarily focused on AhR activation (Jayasundara et al. 2015). However, growing evidence suggests that certain PAHs can induce toxicity independent of AhR (Incardona et al. 2005; Goodale et al. 2013). AhR morpholinos were able to prevent the cardiac toxicity seen in zebrafish embryos treated with pyrene, but not phenanthrene or dibenzothiophene (Incardona et al. 2005). This further shows that other pathways may also be involved in PAH cardiac induced toxicity, and warrants further investigation especially those that are known to interact with the AhR pathway.

Compounds that alter the endocrine system can also cause cardiotoxic effects. Estrogenic compounds have also been shown to change Ca^{2+} homeostasis in cardiomyocyte cells. E2 and BPA can alter Ca^{2+} regulation, promoting cardiac arrhythmias in rodents (Yan et al. 2011). Levels of BPA measured in the urine from adults in the U.S were associated with increased risk of myocardial infarction (Lang et al. 2008), coronary artery disease (Melzer et al. 2010) and hypertension (Shankar et al. 2012). Zebrafish embryos exposed to BPA (15mg/L) caused pericardial edema, indicating an effect on the development of cardiovascular system (Duan et al. 2008). Although research has established the role of the endocrine system on cardiovascular

maintenance and function, its specific role in development remains unclear and warrants further investigation. Exposure to 17β-estradiol (3 μM) has also shown to result in pericardial edema as well as other defects (Chandrasekar et al. 2010). GPER has been suggested to have a role in heart development in zebrafish. Exposure to the GPER agonist G1 resulted in cardiac malformations (Jayasinghe and Volz 2012; Diamante et al., 2017). However, minimal studies have been done to further elucidate this as a potential pathway for cardiac toxicity. However, examining estrogen signaling can be multifaceted because of the great deal of crosstalk between several pathways. In addition, the AhR and ER signaling have been shown to interact, leading to another potential mechanism for cardiotoxicity (Matthews and Gustafsson 2006). Activated AhR has been shown to recruit ERs to promoter regions and to affect normal estrogen signaling (Matthews et al. 2005). The exact role of ER to AhR regulated genes needs to be further examined.

Conclusion

The endocrine system plays a vital role in many cellular processes that are important for maintaining normal physiological functions. The thyroid, androgen and estrogen pathways not only have the ability to signal to their specific receptors, but can crosstalk with other pathways that add to the complexity of the signaling cascades that are induced. Therefore, studying the molecular effects of EDCs on an organism can become quite complicated, even more so when assessing their effects during development. With the numerous pathways that are endocrine regulated along with the

additional complexity of cellular processes occurring during development, assessing toxicity at these intricate times brings about more difficulties. Therefore, despite numerous studies showing the effects of hormones on development, the specific molecular pathways responsible for these phenotypic effects remain unclear. Using the zebrafish as a model organism may help bridge the gaps.

The zebrafish has become a popular model for developmental and toxicological research. It has played a role in obtaining the current knowledge we have about the cardiotoxic effects of dioxins and PAHs. However, there are still many compounds that need to be further studied to better assess their potential to negatively affect embryo development. Estrogens have been well studied in terms of their effect on reproduction, but their role in embryo development and cardiovascular functions are now being examined. Using zebrafish as a tool can aid in the study of the role of estrogens on heart development. These findings will be essential in elucidating the mechanisms of toxicity of xenoestrogens. Future research needs to be able to match the molecular events of toxicity to a specific time point in the very complex timeline of development. A detailed mechanistic understanding of the normal role of endocrine system and the ability of EDCs to induce cardiac effects during development may help to address the toxicity of other environmental contaminants.

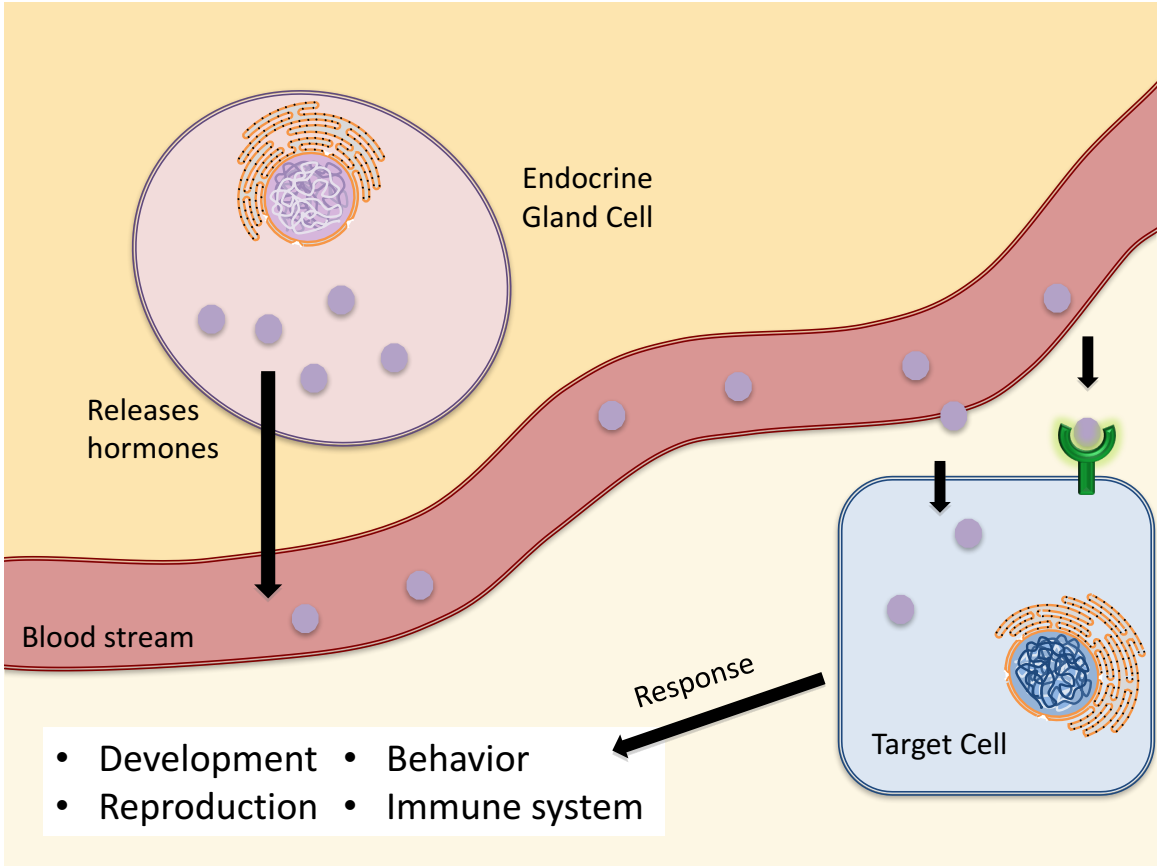

Figure 0-1: Endocrine system network. The endocrine system is a network of glands that synthesize and secrete hormones as chemical messages. These hormones are released into the circulatory system to reach a target organ. Upon binding to a specific receptor, the hormones can induce signal transduction events that regulate many physiological functions.

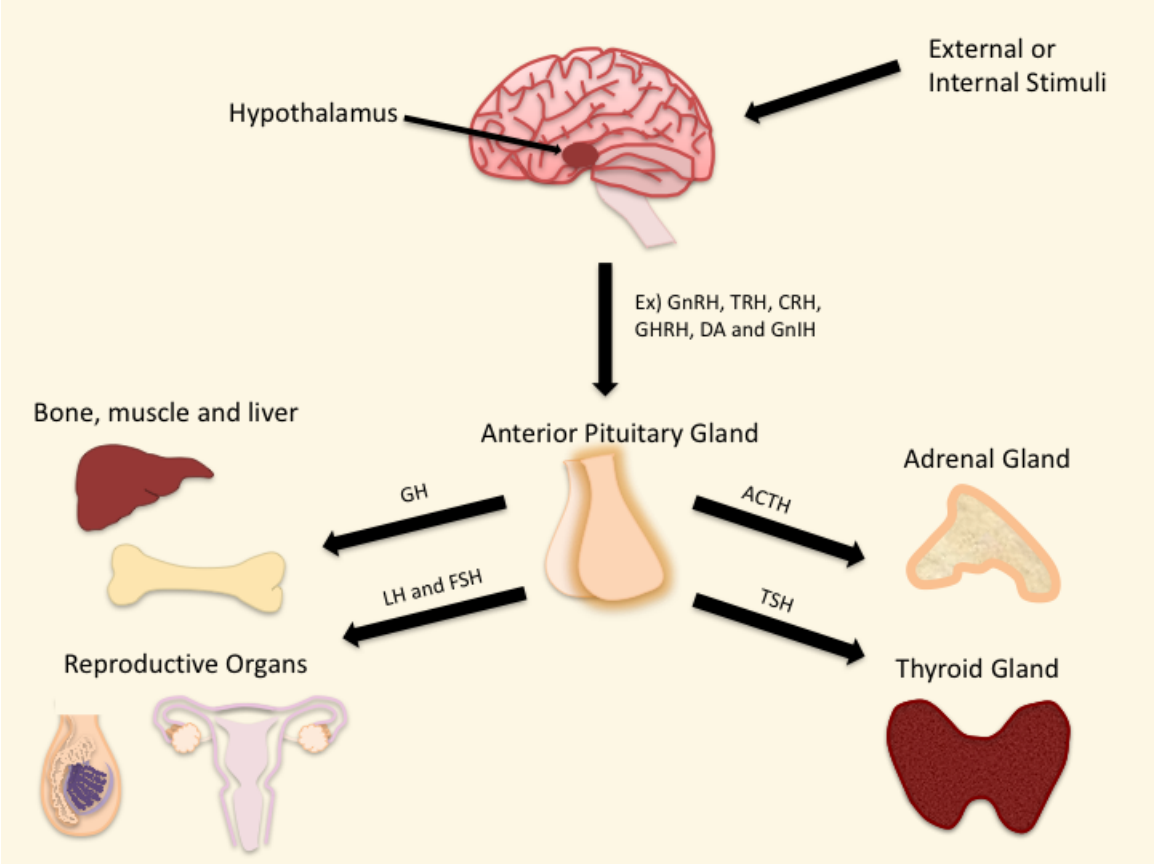

Figure 0-2: The hypothalamus–pituitary complex. Hormone signaling and synthesis begins at the hypothalamus. Specialized cells in the hypothalamus release hormones that either inhibit or promote release of other hormones from the anterior lobe of the pituitary. The hormones that target the anterior pituitary include corticotropin-releasing hormone (CRH), dopamine (DA), growth hormone-releasing hormone (GHRH), gonadotropin releasing hormone (GnRH), thyroid-releasing hormone (TRH) and gonadotropin-inhibitory hormone (GnIH). These hormones then initiate or inhibit the synthesis of hormones from the pituitary gland such as luteinizing hormone (LH), follicle-stimulating hormone (FSH), thyroid-stimulating hormone (TSH), growth hormone (GH) and adrenocorticotropic hormone (ACTH) that have unique functions in specific target organs.

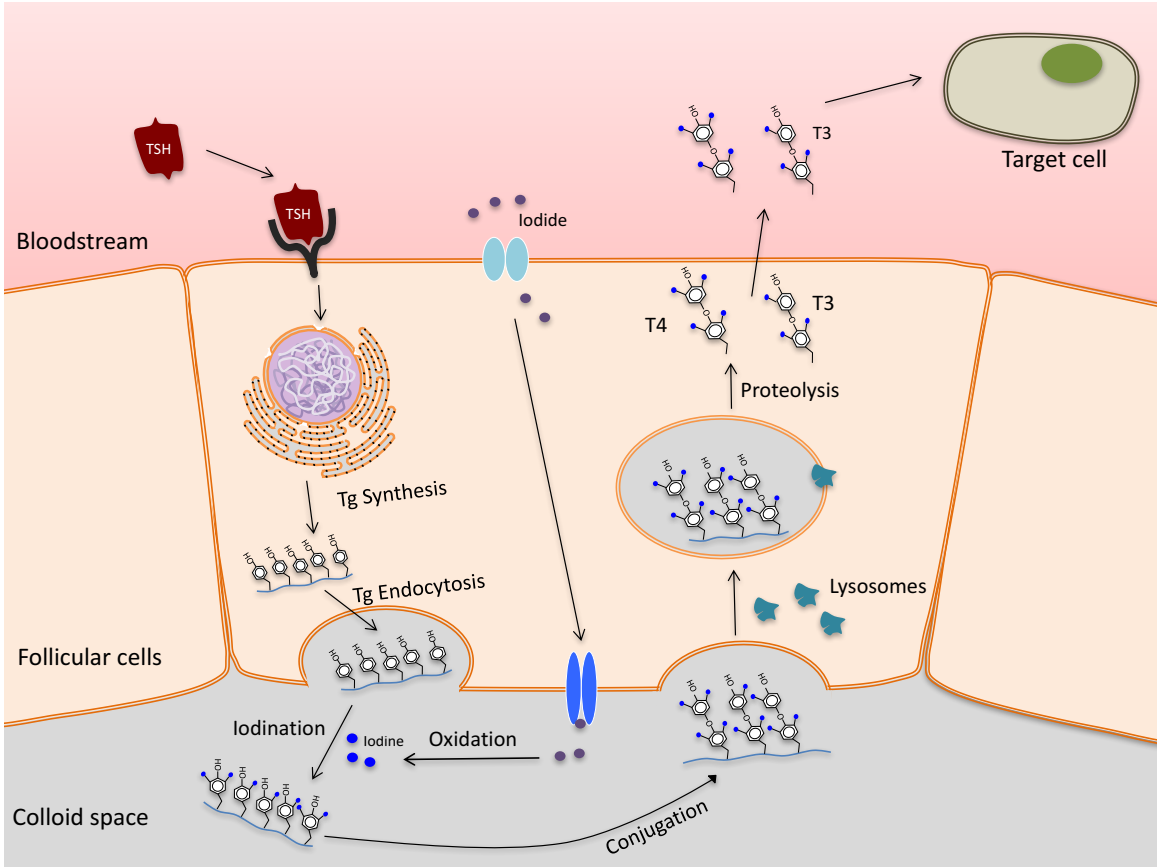

Figure 0-3: Diagram of the major steps involved in thyroid hormone (T3 and T4) synthesis and secretion. Thyroid hormones are formed in follicles lined by a single layer of follicular cells. Thyroglobulin (Tg) is formed in the endoplasmic reticulum and then secreted into the colloid where it undergoes iodination. Iodinated residues of tyrosine are then conjugated. Processed thyroglobulin will re-enter the cell by endocytosis and broken down by proteases to yield T3 and T4.

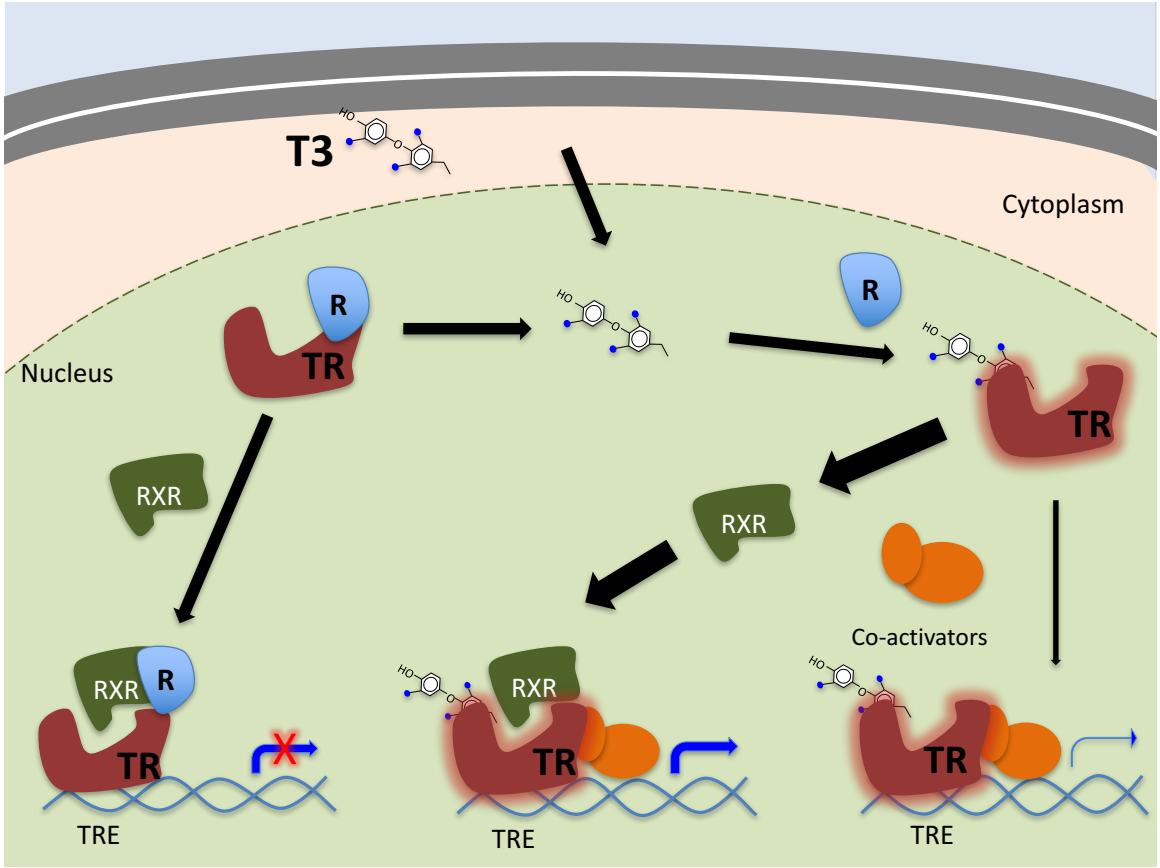

Figure 0-4: Thyroid receptor activation pathways. In the nucleus, thyroid hormones can bind to thyroid receptors (TRs), which recruit co-activator protein. An activated TR can then activate the transcription of thyroid response element (TRE) containing genes. TRs form heterodimers with retinoid X receptors (RXRs) and bind to TREs located in the promoter regions of target genes. In the absence of the ligand, the RXR–TR heterodimer interact with repressor proteins (R) to inhibit target gene transcription.

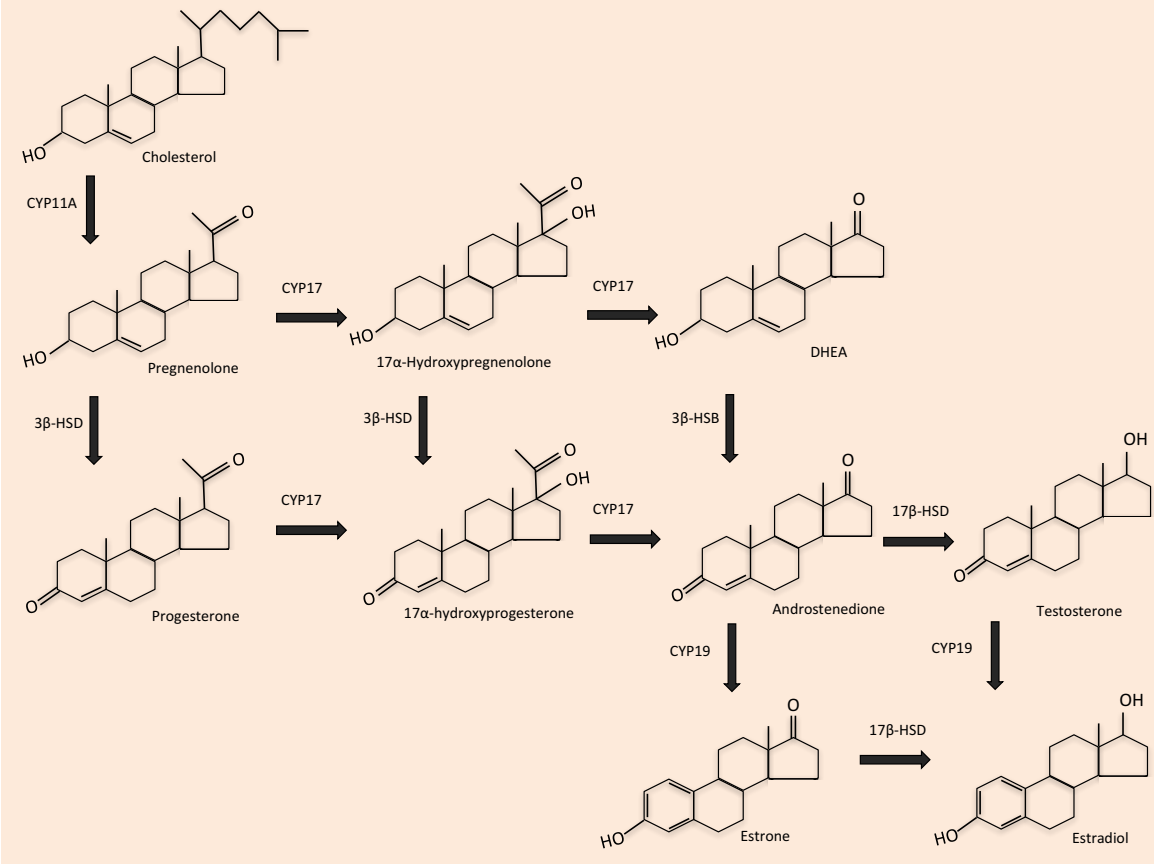

Figure 0-5: Diagram of the steroid biosynthesis pathway along with the enzymes involved in each step. 17β-Hydroxysteroid dehydrogenase (17β-HSD), 3β-Hydroxysteroid dehydrogenase (3β-HSD), cytochrome P450 family 11 subfamily A (cyp11A), cytochrome P450 Family 17 (cyp17) and cytochrome P450 Family 19 (cyp19).

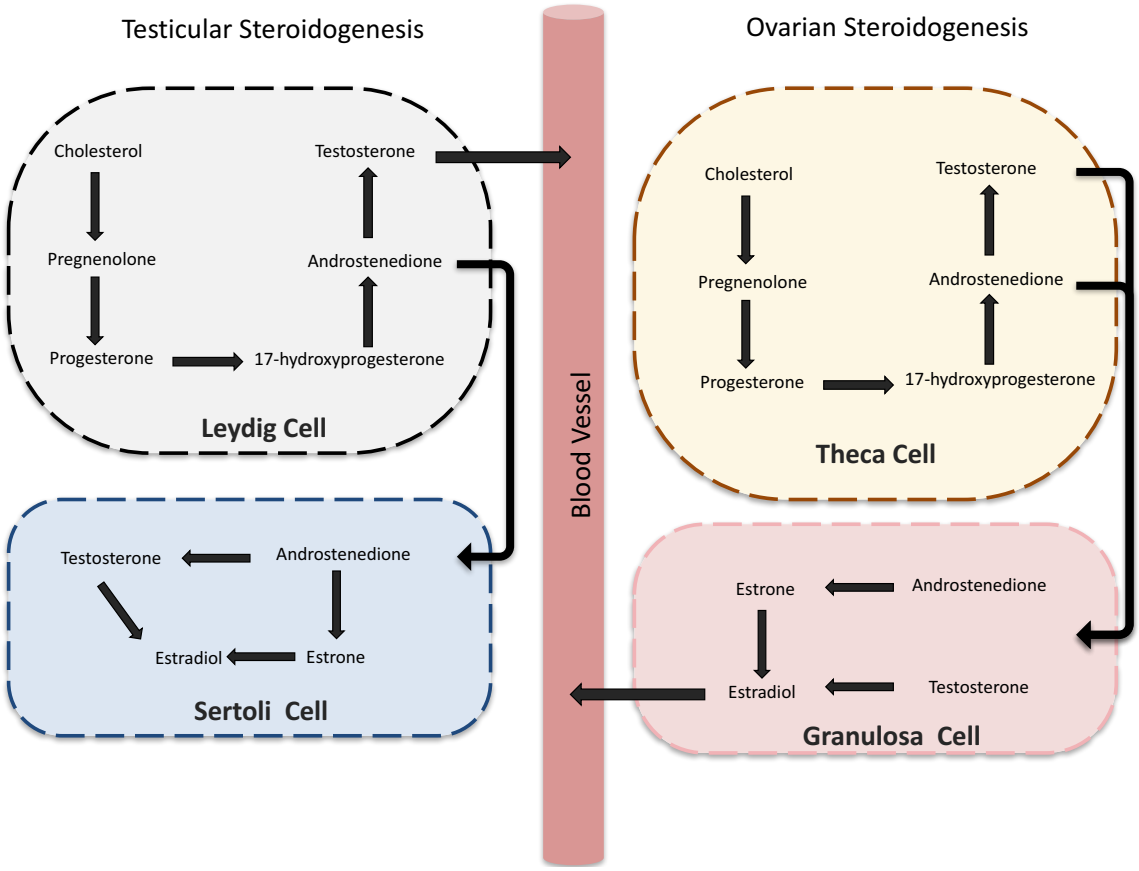

Figure 0-6. Sex steroid hormones synthesis in the testis and the ovary. Conversion of cholesterol to the primary sex steroid hormones in the testis and the ovary. This process requires both the theca cells and granulosa cells of the ovaries and the Leydig cells and Sertoli cells of testis.

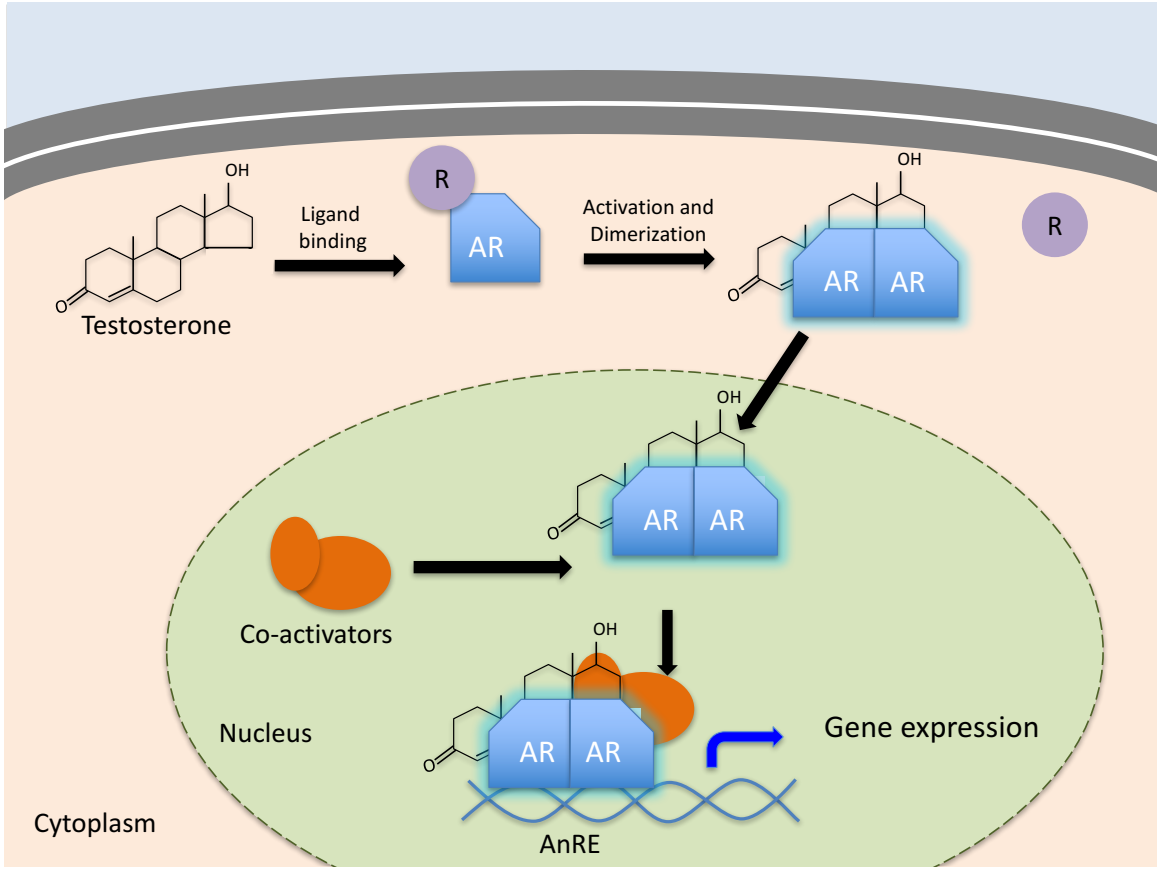

Figure 0-7: Androgen receptor activation pathway. In the absence of its ligand, androgen receptors (ARs) are bound to repressors (R) that inhibit its transport to the nucleus. Testosterone-bound ARs form dimers that translocate into the nucleus to initiate the transcription of AR-regulated genes. Activated ARs will recruit co-activators and bind to androgen response element (ARE) upstream the promoter region of target genes.

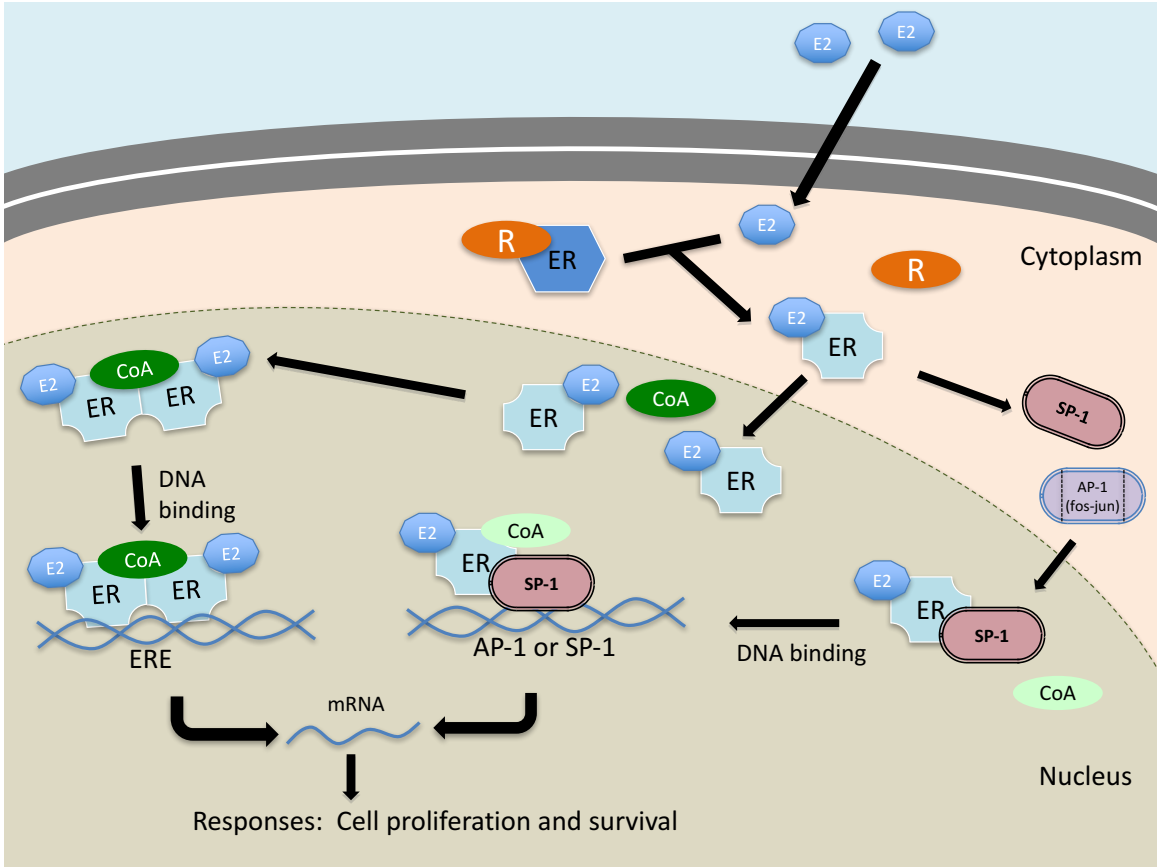

Figure 0-8: The classical genomic activity of estrogens is mediated through the signaling of nuclear estrogen receptors (ERs). Unbound ER is bound to repressor proteins (R). 17β-estradiol (E2) binding induces formation of ER dimers, which relocate into the nucleus. After dimerization, ERs recruits co-activators (CoA) and binds to estrogen response elements (ERE) on DNA. ERs also associate with other transcription factors such as specificity Protein 1 (Sp1) and activating protein-1 (AP-1) to induce transcription of target genes.

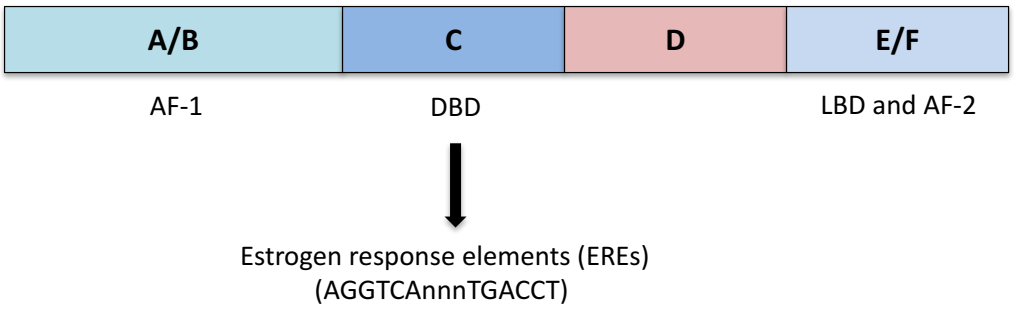

Figure 0-9: Functional domains of the nuclear estrogen receptors. Both ERα and ERβ have four main functional domains. Domain C harbors a DNA-binding domain (DBD) while the ligand-binding domain (LBD) is located in E/F. The two transcriptional activation functions (AF-1 and AF-2) of the ERs are in A/B and E/F.

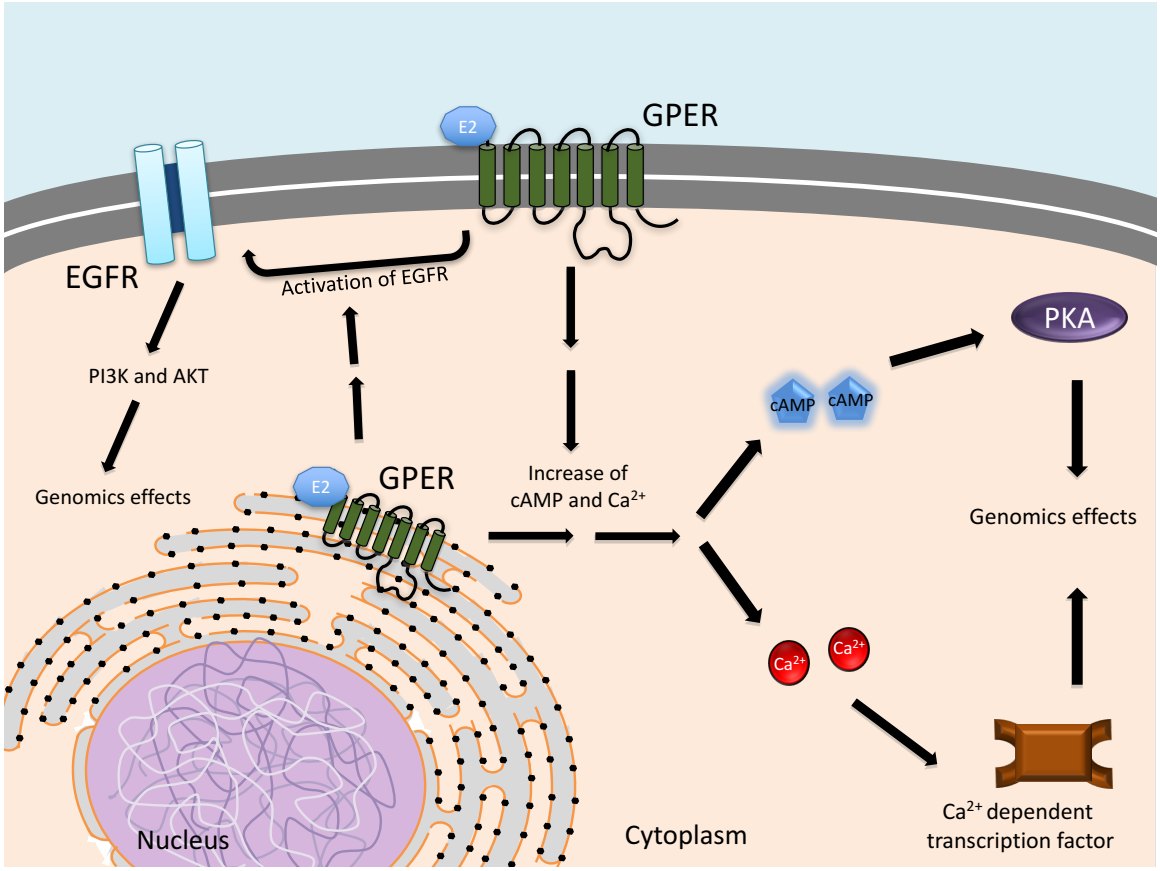

Figure 0-10: Rapid non-genomic signaling of G-protein coupled estrogen receptors (GPER). Binding of 17β-estradiol (E2) to GPER can activate the epidermal growth factor receptor (EGFR) leading to the initiation of other signal transduction pathways such as PI3K/AKT that can have downstream genomic effects. Activation of GPER can also lead to an increase in the conversion of adenosine triphosphate (ATP) to cyclic adenosine monophosphate (cAMP) as well as the release of Ca^{2+} in the cytosol. Accumulation of cAMP in the cytoplasm can activate protein kinase A (PKA), which can phosphorylate transcription factors to regulate transcription. Increased levels of Ca^{2+} can lead to the activation of different transcription factors.

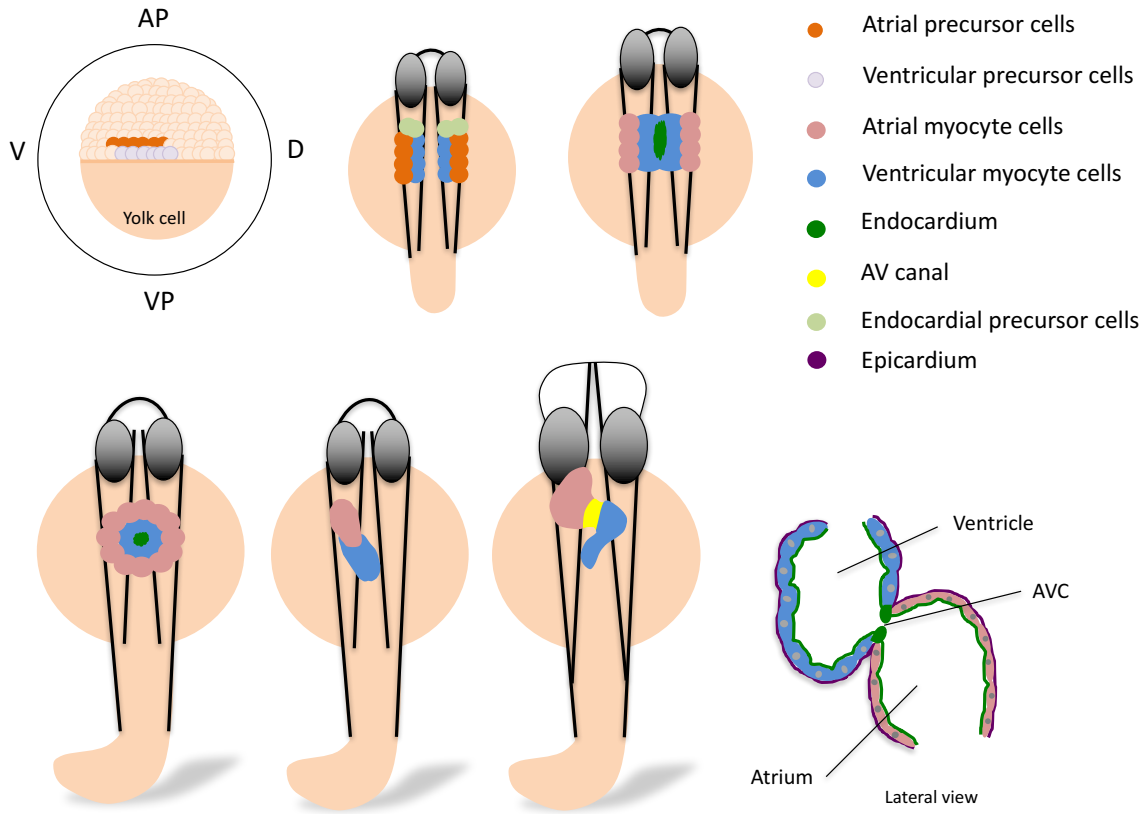

Figure 0-11: Zebrafish cardiac development. Cardiac progenitor cells are located bilaterally in the lateral marginal zone. The cardiac progenitor cells move dorsally towards the mid-line to end up in the anterior later plate mesoderm (ALPM). The pre-endocardial and myocardial cells migrate towards the mid-line. When the bilateral heart fields fuse at the mid-line, they form a cardiac disc structure with the endocardial cells forming the inner layer and the ventricular and atrial myocytes at the periphery of the disc. Cardiac morphogenesis transforms the cardiac disc into a cardiac tube. When the linear heart tube forms, the venous pole is located at the anterior left and the arterial pole is fixed at the mid-line. The heart tube will then loop with 2 distinct chambers. The heart will continue to develop and form an epicardium and valve leaflets at the atrioventricular canal (AVC). Ventral side (V), dorsal side (D)

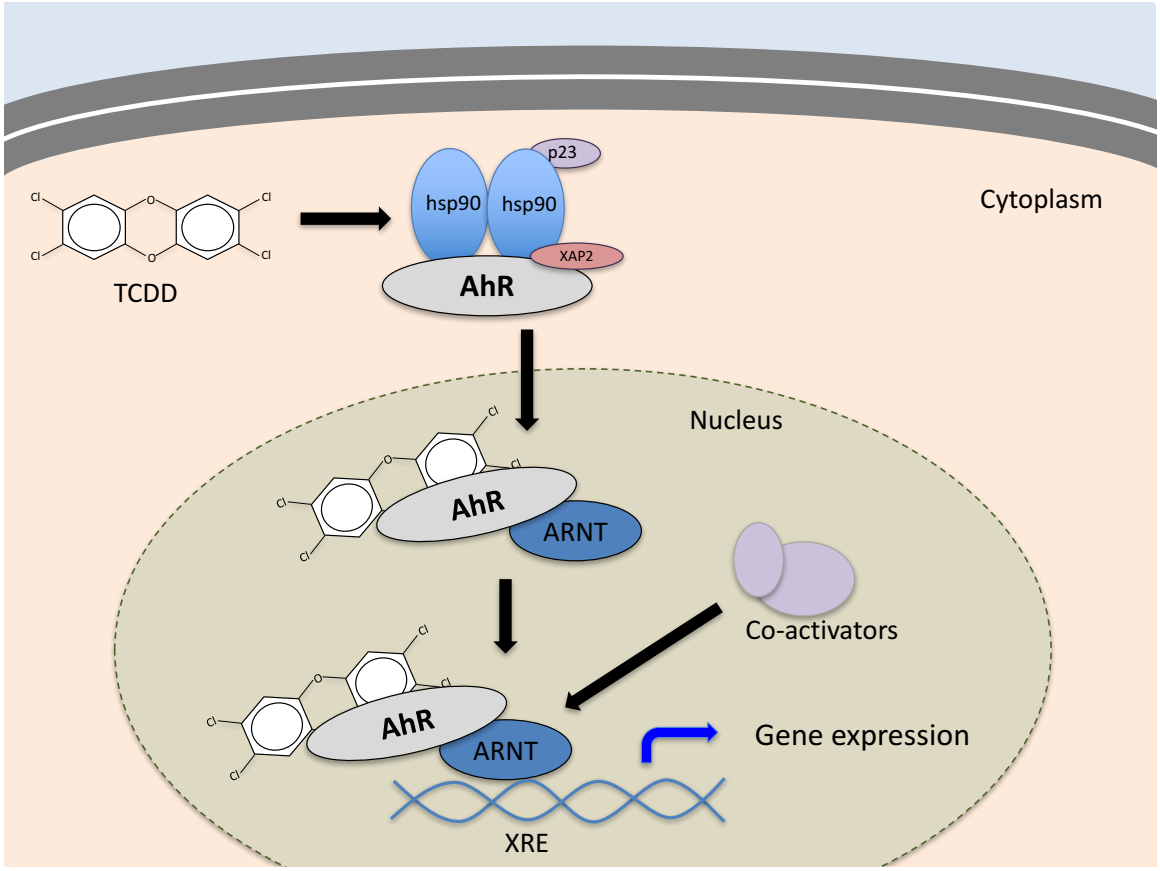

Figure 0-12: Aryl hydrocarbon receptor pathway. In the absence of bound ligand, aryl hydrocarbon receptor (AHR) resides in a complex with heat shock protein 90 (HSP90), the co-chaperone protein X-associated protein 2 (XAP2), and p23. When bound to an agonist ligand such as 2,3,7,8-tetrachlorodibenzo-p-dioxin (TCDD), the AHR complex translocates to the nucleus, resulting in HSP90 displacement. AHR binds to the AHR nuclear translocator (ARNT), leading to AHR–ARNT heterodimer formation. This heterodimer is capable of binding to a xenobiotic responsive element (XRE). Both AHR and ARNT can recruit co-activators, leading to the transcription of a wide variety of genes such as cytochrome P450 1A1 (CYP1A1).

References

Abney TO (1999) The potential roles of estrogens in regulating Leydig cell development and function: a review. Steroids 64(9):610-7

Albanito L, Madeo A, Lappano R, Vivacqua A, Rago V, Carpino A, Oprea TI, Prossnitz ER, Musti AM, Andò S, Maggiolini M (2007) G protein-coupled receptor 30 (GPR30) mediates gene expression changes and growth response to 17beta-estradiol and selective GPR30 ligand G-1 in ovarian cancer cells. Cancer Res. 67(4):1859-66.

Andersson S, Geissler WM, Wu L, Davis DL, Grumbach MM, New MI, Schwarz HP, Blethen SL, Mendonca BB, Bloise W, Witchel SF, Cutler GB Jr, Griffin JE, Wilson JD, Russel DW (1996) Molecular genetics and pathophysiology of 17 beta-hydroxysteroid dehydrogenase 3 deficiency. J Clin Endocrinol Metab 81(1):130-6

Antkiewicz DS, Peterson RE, Heideman W (2006) Blocking expression of AHR2 and ARNT1 in zebrafish larvae protects against cardiac toxicity of 2,3,7,8-tetrachlorodibenzo-p-dioxin. Toxicol Sci 94(1):175-82

Aronica SM, Kraus WL, Katzenellenbogen BS (1994) Estrogen action via the cAMP signaling pathway: stimulation of adenylate cyclase and cAMP-regulated gene transcription. Proc Natl Acad Sci USA 91(18): 8517-21

Auman HJ, Coleman H, Riley HE, Olale F, Tsai HJ, Yelon D (2007) Functional modulation of cardiac form through regionally confined cell shape changes. PLoS Biol 5(3):e53

Baird DT, Swanston IA and McNeilly AS (1981) Secretion of androgens and estrogens by the preovulatory follicle in the ewe. Biology of Reproduction 24:1013-25

Bakkers J (2011) Zebrafish as a model to study cardiac development and human cardiac disease. Cardiovasc Res 91(2):279-88

Ball JS, Stedman DB, Hillegass JM, Zhang CX, Panzica-Kelly J, Coburn A, Enright BP, Tornesi B, Amouzadeh HR, Hetheridge M, Gustafson AL, Augustine-Rauch KA (2014) Fishing for teratogens: a consortium effort for a harmonized zebrafish developmental toxicology assay. Toxicol Sci 139(1):210-9

Beis D, Bartman T, Jin SW, Scott IC, D'Amico LA, Ober EA, Verkade H, Frantsve J, Field HA, Wehman A, Baier H, Tallafuss A, Bally-Cuif L, Chen JN, Stainier DY, Jungblut B (2005) Genetic and cellular analyses of zebrafish atrioventricular cushion and valve development. Development 132(18):4193-204

Benten WP, Lieberherr M, Stamm O, Wrehlke C, Guo Z, Wunderlich F (1999) Testosterone signaling through internalizable surface receptors in androgen receptor-free macrophages. Mol Biol Cell 10(10):3113-23

Biondi B, Palmieri EA, Lombardi G, Fazio S (2002) Effects of thyroid hormone on cardiac function: the relative importance of heart rate, loading conditions, and myocardial contractility in the regulation of cardiac performance in human hyperthyroidism. J Clin Endocrinol Metab 87(3):968-74

Bopassa JC, Eghbali M, Toro L, Stefani E (2010) A novel estrogen receptor GPER inhibits mitochondria permeability transition pore opening and protects the heart against ischemia-reperfusion injury. Am J Physiol Heart Circ Physiol 298(1): 16-23

Breen JJ, Hickok NJ, Guff JA. (1997) The rat TSH gene contains distinct response elements for regulation by retinoids and thyroid hormone. Mol Cell Endocrinol. 131:137–146

Brent GA (1994) The molecular basis of thyroid hormone action. N Engl J Med 331(13):847-53

Brinkmann AO, Leemborg FG, Roodnat EM, De Jong FH, Van der Molen HJ (1980) A Specific Action of Estradiol on Enzymes Involved in Testicular Steroidogenesis. Biol Reprod 23(4):801-9

Brix K, Herzog V (1994) Extrathyroidal release of thyroid hormones from thyroglobulin by J774 mouse macrophages. J Clin Invest 93(4):1388-96

Bussmann J, Bakkers J, Schulte-Merker S (2007) Early endocardial morphogenesis requires Scl/Tal1. PLoS Genet 3(8):e140

Cagnacci A, Soldani R, Puccini E, Fioretti P, Melis GB (1992) Lipid-independent therapeutic properties of transdermal 17 B-estradiol on cardiovascular diseases. Acta Obstet Gynecol Scand 71(8):639-41

Campbell BK, Baird DT, Webb R (1998) Effects of dose of LH on androgen production and luteinization of ovine theca cells cultured in a serum-free system. J Reprod Fertil 112(1):69-77

Carney SA, Chen J, Burns CG, Xiong KM, Peterson RE, Heideman W (2006) Aryl hydrocarbon receptor activation produces heart-specific transcriptional and toxic responses in developing zebrafish. Mol Pharmacol 70(2):549-61

Carney SA, Peterson RE, Heideman W (2004) 2,3,7,8-Tetrachlorodibenzo-p-dioxin activation of the aryl hydrocarbon receptor/aryl hydrocarbon receptor nuclear translocator

pathway causes developmental toxicity through a CYP1A-independent mechanism in zebrafish. Mol Pharmacol 66(3):512-21

Carpenter G, Cohen S (1979) Epidermal growth factor. Annu Rev Biochem 48:193-216

Castro-Rivera E, Samudio I, Safe S (2001) Estrogen regulation of cyclin D1 gene expression in ZR-75 breast cancer cells involves multiple enhancer elements. J Biol Chem 276(33):30853-61

Catterall WA (1991) Functional subunit structure of voltage-gated calcium channels. Science 253(5027):1499-500

Ceballos G, Figueroa L, Rubio I, Gallo G, Garcia A, Martinez A, Yañez R, Perez J, Morato T, Chamorro G (1999) Acute and nongenomic effects of testosterone on isolated and perfused rat heart. J Cardiovasc Pharmacol 33(5):691-7

Chambliss KL, Shaul PW (2002) Estrogen modulation of endothelial nitric oxide synthase. Endocr Rev 23(5):665-86

Chandrasekar G, Archer A, Gustafsson JA, Andersson Lendahl M (2010) Levels of 17b-Estradiol Receptors Expressed in Embryonic and Adult Zebrafish Following In Vivo Treatment of Natural or Synthetic Ligands. PLoS ONE 5(3): e9678

Chang C, Saltzman A, Yeh S, Young W, Keller E, Lee HJ, Wang C, Mizokami A (1995) Androgen receptor: an overview. Crit Rev Eukaryot Gene Expr 5(2):97-125

Chang CS, Kokontis J, Liao ST (1988a) Molecular cloning of human and rat complementary DNA encoding androgen receptors. Science 240(4850):324-6

Chang CS, Kokontis J, Liao ST (1988b) Structural analysis of complementary DNA and amino acid sequences of human and rat androgen receptors. Proc Natl Acad Sci U S A 85(19):7211-5

Chen JN, Fishman MC (1996) Zebrafish tinman homolog demarcates the heart field and initiates myocardial differentiation. Development 122(12):3809-16

Chen JN, Haffter P, Odenthal J, Vogelsang E, Brand M, van Eeden FJ, Furutani-Seiki M, Granato M, Hammerschmidt M, Heisenberg CP, Jiang YJ, Kane DA, Kelsh RN, Mullins MC, Nüsslein-Volhard C (1996) Mutations affecting the cardiovascular system and other internal organs in zebrafish. Development 123:293-302

Chen JN, van Eeden FJ, Warren KS, Chin A, Nüsslein-Volhard C, Haffter P, Fishman MC (1997) Left-right pattern of cardiac BMP4 may drive asymmetry of the heart in zebrafish. Development 124(21):4373-82

Cheng SY, Leonard JL, Davis PJ (2010) Molecular aspects of thyroid hormone actions. Endocr Rev 31(2):139-70

Chow MS (1995) Benefit/risk of estrogen therapy in cardiovascular disease: current knowledge and future challenges. J Clin Pharmacol 35(9 Suppl):11S-17S

Crisp TM, Clegg ED, Cooper RL, Wood WP, Anderson DG, Baetcke KP, Hoffmann JL, Morrow MS, Rodier DJ, Schaeffer JE, Touart LW, Zeeman MG, Patel YM (1998) Environmental endocrine disruption: an effects assessment and analysis. Environ Health Perspect 106 Suppl 1:11-56

Danzi S, Klein I (2002) Thyroid hormone-regulated cardiac gene expression and cardiovascular disease. Thyroid 12(6):467-72

Datta SR, Brunet A, Greenberg ME (1999) Cellular survival: a play in three Akts. Genes Dev 13(22):2905-27

Datta SR, Dudek H, Tao X, Masters S, Fu H, Gotoh Y, Greenberg ME (1997) Akt phosphorylation of BAD couples survival signals to the cell-intrinsic death machinery. Cell 91(2):231-41

Daub H, Weiss FU, Wallasch C, Ullrich A (1996) Role of transactivation of the EGF receptor in signalling by G-protein-coupled receptors. Nature 379(6565):557-60.
Davis PJ, Davis FB (2002) Nongenomic actions of thyroid hormone on the heart. Thyroid 12(6):459-66

De Jong FH (1988) Inhibin. Physiol Rev 68(2):555-607

De Pater E, Clijsters L, Marques SR, Lin YF, Garavito-Aguilar ZV, Yelon D, Bakkers J (2009) Distinct phases of cardiomyocyte differentiation regulate growth of the zebrafish heart. Development 136(10):1633-41

De Waal PP, Wang DS, Nijenhuis WA, Schulz RW, Bogerd J (2008) Functional characterization and expression analysis of the androgen receptor in zebrafish (Danio rerio) testis. Reproduction 136(2):225-34

Denison MS, Fisher JM, Whitlock JP Jr (1988a) Inducible, receptor-dependent protein-DNA interactions at a dioxin-responsive transcriptional enhancer. Proc Natl Acad Sci U S A 85(8):2528-32
Denison MS, Fisher JM, Whitlock JP Jr (1988b) The DNA recognition site for the dioxin-Ah receptor complex. Nucleotide sequence and functional analysis. J Biol Chem 263(33):17221-4

DeRosa C, Richter P, Pohl H, Jones DE (1998) Environmental exposures that affect the endocrine system: public health implications. J Toxicol Environ Health B Crit Rev 1(1):3-26

Deschamps AM, Murphy E (2009) Activation of a novel estrogen receptor, GPER, is cardioprotective in male and female rats. Am J Physiol Heart Circ Physiol 297(5): 1806-13

Diamante G, Menjivar-Cervantes N, Leung MS, Volz DC, Schlenk D (2017) Contribution of G protein-coupled estrogen receptor 1 (GPER) to 17β-estradiol-induced developmental toxicity in zebrafish. Aquat Toxicol. 186:180-187

Ding Q, Gros R, Limbird LE, Chorazyczewski J, Feldman RD (2009) Estradiol-mediated ERK phosphorylation and apoptosis in vascular smooth muscle cells requires GPR 30. Am J Physiol Cell Physiol 297(5):C1178-87

Driever W, Solnica-Krezel L, Schier AF, Neuhauss SC, Malicki J, Stemple DL, Stainier DY, Zwartkruis F, Abdelilah S, Rangini Z, Belak J, Boggs C (1996) A genetic screen for mutations affecting embryogenesis in zebrafish. Development 123:37-46

Duan R, Porter W, Safe S (1998) Estrogen-induced c-fos protooncogene expression in MCF-7 human breast cancer cells: role of estrogen receptor Sp1 complex formation. Endocrinology 139(4):1981-90

Duan Z, Zhu L, Zhu L, Kun Y, Zhu X (2008) Individual and joint toxic effects of pentachlorophenol and bisphenol A on the development of zebrafish (Danio rerio) embryo. Ecotoxicol Environ Saf 71(3):774-80

Dunn AD, Crutchfield HE, Dunn JT (1991) Proteolytic processing of thyroglobulin by extracts of thyroid lysosomes. Endocrinology 128(6):3073-80

Estrada M, Espinosa A, Müller M, Jaimovich E (2003) Testosterone stimulates intracellular calcium release and mitogen-activated protein kinases via a G protein-coupled receptor in skeletal muscle cells. Endocrinology 144(8):3586-97

Estrada M, Uhlen P, Ehrlich BE (2006a) Ca2+ oscillations induced by testosterone enhance neurite outgrowth. J Cell Sci 119(Pt 4):733-43

Estrada M, Varshney A, Ehrlich BE (2006b) Elevated testosterone induces apoptosis in neuronal cells. J Biol Chem 281(35):25492-501

Everts ME, Verhoeven FA, Bezstarosti K, Moerings EP, Hennemann G, Visser TJ, Lamers JM (1996) Uptake of thyroid hormones in neonatal rat cardiac myocytes. Endocrinology 137(10): 4235-42

Filardo EJ, Quinn JA, Bland KI, Frackelton AR Jr (2000) Estrogen-induced activation of Erk-1 and Erk-2 requires the G protein-coupled receptor homolog, GPR30, and occurs via trans-activation of the epidermal growth factor receptor through release of HB-EGF. Mol Endocrinol 14(10):1649-60

Foradori CD, Weiser MJ, Handa RJ (2008) Non-genomic actions of androgens. Front Neuroendocrinol 29(2):169-81

Frye CA, Bo E, Calamandrei G, Calzà L, Dessì-Fulgheri F, Fernández M, Fusani L, Kah O, Kajta M, Le Page Y, Patisaul HB, Venerosi A, Wojtowicz AK, Panzica GC (2012) Endocrine disrupters: a review of some sources, effects, and mechanisms of actions on behaviour and neuroendocrine systems. J Neuroendocrinol 24(1):144-59

Fujisawa-Sehara A, Sogawa K, Yamane M, Fujii-Kuriyama Y (1987) Characterization of xenobiotic responsive elements upstream from the drug-metabolizing cytochrome P-450c gene: A similarity to glucocorticoid regulatory elements. Nucleic Acids Res 15(10) :4179-91

Funakoshi T, Yanai A, Shinoda K, Kawano MM, Mizukami Y (2006) G protein-Coupled Receptor 30 Is an Estrogen Receptor in the Plasma Membrane. Biochem. Biophys. Res. Commun 346(3): 904-910

Gao X, Wang HS (2014) Impact of bisphenol a on the cardiovascular system - epidemiological and experimental evidence and molecular mechanisms. Int J Environ Res Public Health 11(8):8399-413

Garavito-Aguilar ZV, Riley HE, Yelon D (2010) Hand2 ensures an appropriate environment for cardiac fusion by limiting Fibronectin function. Development 137(19):3215-20

Gaub MP, Bellard M, Scheuer I, Chambon P, Sassone-Corsi P (1990) Activation of the ovalbumin gene by the estrogen receptor involves the fos-jun complex. Cell 63(6):1267-76

Gobinet J, Poujol N, Sultan C (2002) Molecular action of androgens. Mol Cell Endocrinol 198:15-24

Gonzalez FJ, Fernandez-Salguero P (1998) The aryl hydrocarbon receptor: studies using the AHR-null mice. Drug Metab Dispos 26(12):1194-8

Goodale BC, Tilton SC, Corvi MM, Wilson GR, Janszen DB, Anderson KA, Waters KM, Tanguay RL (2013) Structurally distinct polycyclic aromatic hydrocarbons induce

differential transcriptional responses in developing zebrafish. Toxicol Appl Pharmacol 272(3):656-70

Gregory SJ, Kaiser UB (2004) Regulation of gonadotropins by inhibin and activin. Semin Reprod Med 22(3):253-67

Gustafsson J, Pousette K (1975) Demonstration and partial characterization of cytosol receptors for testosterone. Biochemistry 14(14):3094-101

Haffter P, Granato M, Brand M, Mullins MC, Hammerschmidt M, Kane DA, Odenthal J, van Eeden FJ, Jiang YJ, Heisenberg CP, Kelsh RN, Furutani-Seiki M, Vogelsang E, Beuchle D, Schach U, Fabian C, Nüsslein-Volhard C (1996) The identification of genes with unique and essential functions in the development of the zebrafish, Danio rerio. Development 123:1-36

Hall JM, Couse JF, Korach KS (2001) The multifaceted mechanisms of estradiol and estrogen receptor signaling. J Biol Chem 276(40): 36869-72

Handley-Goldstone HM, Grow MW, Stegeman JJ (2005) Cardiovascular gene expression profiles of dioxin exposure in zebrafish embryos. Toxicol Sci 85(1):683-93

Hansson V, Weddington SC, Petrusz P, Ritzen EM, Nayfeh SN, French FS (1975) FSH stimulation of testicular androgen binding protein (ABP): comparison of ABP response and ovarian augmentation. Endocrinology. 1975 Aug;97(2):469-73

Hartong R, Wang N, Kurokawa R, Lazar MA, Glass CK, Apriletti JW, Dillmann WH (1994) Delineation of three different thyroid hormone-response elements in promoter of rat sarcoplasmic reticulum Ca2+ATPase gene. Demonstration that retinoid X receptor binds 5' to thyroid hormone receptor in response element 1. J Biol Chem 269(17):13021-9

Hausenloy DJ, Yellon DM (2003) The mitochondrial permeability transition pore: its fundamental role in mediating cell death during ischaemia and reperfusion. J Mol Cell Cardiol 35(4):339-41

Heintz RA, Short JW, Rice SD (1999) Sensitivity of fish embryos to weathered crude oil: II. Increased mortality of pink salmon (Oncorhynchus gorbuscha) embryos incubating downstream from weathered Exxon Valdez crude oil. Environ Toxicol Chem 18(3):494-503

Heldring N, Pike A, Andersson S, Matthews J, Cheng G, Hartman J, Tujague M, Ström A, Treuter E, Warner M, Gustafsson JA (2007) Estrogen receptors: how do they signal and what are their targets. Physiol Rev 87(3):905-31

Henry TR, Spitsbergen JM, Hornung MW, Abnet CC, Peterson RE (1997) Early life stage toxicity of 2,3,7,8-tetrachlorodibenzo-p-dioxin in zebrafish (Danio rerio). Toxicol Appl Pharmacol 142(1):56-68

Herzog V (1983) Transcytosis in thyroid follicle cells. J Cell Biol 97(3):607-17
Hiroi H, Christenson LK, Strauss JF 3rd (2004) Regulation of transcription of the steroidogenic acute regulatory protein (StAR) gene: temporal and spatial changes in transcription factor binding and histone modification. Mol Cell Endocrinol 215(1-2):119-26

Hiroi Y, Kim HH, Ying H, Furuya F, Huang Z, Simoncini T, Noma K, Ueki K, Nguyen NH, Scanlan TS, Moskowitz MA, Cheng SY, Liao JK (2006) Rapid nongenomic actions of thyroid hormone. Proc Natl Acad Sci U S A 103(38):14104-9

Hornung MW, Spitsbergen JM, Peterson RE (1999) 2,3,7,8-Tetrachlorodibenzo-p-dioxin alters cardiovascular and craniofacial development and function in sac fry of rainbow trout (Oncorhynchus mykiss). Toxicol Sci 47(1):40-51

Hossain MS, Larsson A, Scherbak N, Olsson PE, Orban L (2008) Zebrafish androgen receptor: isolation, molecular, and biochemical characterization. Biol Reprod 78(2):361-9

Hsieh KP, Martin TF (1992) Thyrotropin-releasing hormone and gonadotropin-releasing hormone receptors activate phospholipase C by coupling to the guanosine triphosphate-binding proteins Gq and G11. Mol Endocrinol 6(10):1673-81

Hu J, Zhang Z, Shen WJ, Azhar S (2010) Cellular cholesterol delivery, intracellular processing and utilization for biosynthesis of steroid hormones. Nutr Metab (Lond). 7:47
Huttner IG, Trivedi G, Jacoby A, Mann SA, Vandenberg JI, Fatkin D (2013) A transgenic zebrafish model of a human cardiac sodium channel mutation exhibits bradycardia, conduction-system abnormalities and early death. J Mol Cell Cardiol 61:123-32

Incardona JP, Carls MG, Holland L, Linbo TL, Baldwin DH, Myers MS, Peck KA, Tagal M, Rice SD, Scholz NL (2015) Very low embryonic crude oil exposures cause lasting cardiac defects in salmon and herring. Sci Rep 5:13499

Incardona JP, Carls MG, Teraoka H, Sloan CA, Collier TK, Scholz NL (2005) Aryl hydrocarbon receptor-independent toxicity of weathered crude oil during fish development. Environ Health Perspect 113(12):1755-62

Incardona JP, Collier TK, Scholz NL (2004) Defects in cardiac function precede morphological abnormalities in fish embryos exposed to polycyclic aromatic hydrocarbons. Toxicol Appl Pharmacol 196(2):191-205

Incardona JP, Day HL, Collier TK, Scholz NL (2006) Developmental toxicity of 4-ring polycyclic aromatic hydrocarbons in zebrafish is differentially dependent on AH receptor isoforms and hepatic cytochrome P4501A metabolism. Toxicol Appl Pharmacol 217(3):308-21

Incardona JP, Gardner LD, Linbo TL, Brown TL, Esbaugh AJ, Mager EM, Stieglitz JD, French BL, Labenia JS, Laetz CA, Tagal M, Sloan CA, Elizur A, Benetti DD, Grosell M, Block BA, Scholz NL (2014) Deepwater Horizon crude oil impacts the developing hearts of large predatory pelagic fish. Proc Natl Acad Sci U S A 111(15):E1510-8

Incardona JP, Linbo TL, Scholz NL (2011) Cardiac toxicity of 5-ring polycyclic aromatic hydrocarbons is differentially dependent on the aryl hydrocarbon receptor 2 isoform during zebrafish development. Toxicol Appl Pharmacol 257(2):242-9

Incardona JP, Swarts TL, Edmunds RC, Linbo TL, Aquilina-Beck A, Sloan CA, Gardner LD, Block BA, Scholz NL (2013) Exxon Valdez to Deepwater Horizon: comparable toxicity of both crude oils to fish early life stages. Aquat Toxicol 142-143:303-16

Ingenbleek Y, Young V (1994) Transthyretin (prealbumin) in health and disease: nutritional implications. Annu Rev Nutr 14:495-533

Jayasinghe BS, Volz DC (2012) Aberrant ligand-induced activation of G protein-coupled estrogen receptor 1 (GPER) results in developmental malformations during vertebrate embryogenesis. Toxicol Sci 125(1): 262-73

Jayasundara N, Van Tiem Garner L, Meyer JN, Erwin KN, Di Giulio RT (2015) AHR2-Mediated transcriptomic responses underlying the synergistic cardiac developmental toxicity of PAHs. Toxicol Sci 143(2):469-81

Jensen EV (1962) On the mechanism of estrogen action. Perspect Biol Med 6:47–54
Jensen EV, Desombre ER (1973) Estrogen-receptor interaction: estrogenic hormones effect transformation of specific receptor proteins to a biologically active form. Science 182:126-134

Jensen EV, Suzuki T, Kawashima T, Stumpf WE, Jungblut PW, DeSombre ER (1968) A two-step mechanism for the interaction of estradiol with rat uterus. Proc Natl Acad Sci U S A 59(2):632-8

Jenster G, van der Korput HA, van Vroonhoven C, van der Kwast TH, Trapman J, Brinkmann AO (1991) Domains of the human androgen receptor involved in steroid binding, transcriptional activation, and subcellular localization. Mol Endocrinol 5(10):1396-404

Johnson BD, Zheng W, Korach KS, Scheuer T, Catterall WA, Rubanyi GM (1997) Increased expression of the cardiac L-type calcium channel in estrogen receptor-deficient mice. J Gen Physiol 110(2):135-40

Kahaly GJ, Dillmann WH (2005) Thyroid hormone action in the heart. Endocrine Rev 26(5):704-28

Kalla NR, Nisula BC, Menard R, Loriaux DL (1980) The effect of estradiol on Leydig cell testosterone biosynthesis. Endocrinology 106:35-39

Kaushik M, Sontineni SP, Hunter C (2010) Cardiovascular disease and androgens: a review. Int J Cardiol 142(1):8-14

Kayes-Wandover KM, White PC (2000) Steroidogenic enzyme gene expression in the human heart. J Clin Endocrinol Metab 85(7):2519-25

Khan SA, Ball RB, Hendry WJ 3rd (1998) Effects of neonatal administration of diethylstilbestrol in male hamsters: disruption of reproductive function in adults after apparently normal pubertal development. Biol Reprod 58(1):137-42

Kim J, Wu Q, Zhang Y, Wiens KM, Huang Y, Rubin N, Shimada H, Handin RI, Chao MY, Tuan TL, Starnes VA, Lien CL (2010) PDGF signaling is required for epicardial function and blood vessel formation in regenerating zebrafish hearts. Proc Natl Acad Sci U S A 107(40):17206-10

Kim K, Barhoumi R, Burghardt R, Safe S (2005) Analysis of estrogen receptor {α}-Sp1 interactions in breast cancer cells by fluorescence resonance energy transfer. Mol Endocrinol 19(4):843-54

Kim PS, Arvan P (1991) Folding and assembly of newly synthesized thyroglobulin occurs in a pre-Golgi compartment. J Biol Chem 266(19): 12412-18

Kim PS, Arvan P (1993) Hormonal regulation of thyroglobulin export from the endoplasmic reticulum of cultured thyrocytes. J Biol Chem 268(7): 4873-79

Kimmel CB, Ballard WW, Kimmel SR, Ullmann B, Schilling TF (1995) Stages of embryonic development of the zebrafish. Dev Dyn 203(3):253-310.

Kimura N, Mizokami A, Oonuma T, Sasano H, Nagura H (1993) Immunocytochemical localization of androgen receptor with polyclonal antibody in paraffin-embedded human tissues. J Histochem Cytochem 41(5):671-8

Kishimoto Y, Lee KH, Zon L, Hammerschmidt M, Schulte-Merker S (1997) The molecular nature of zebrafish swirl: BMP2 function is essential during early dorsoventral patterning. Development 124(22):4457-66

Kiss E, Jakab G, Kranias EG, Edes I (1994) Thyroid hormone-induced alterations in phospholamban protein expression: regulatory effects on sarcoplasmic reticulum Ca2+ transport and myocardial relaxation. Circ Res 75(2):245-251

Klein I, Danzi S (2007) Thyroid disease and the heart. Circulation 116(15):1725-35
Klingenberg M (1958) Pigments of rat liver microsomes. Arch Biochem Biophys 75(2):376-86

Kostrouch Z, Bernier-Valentin F, Munari-Silem Y, Rajas F, Rabilloud R, Rousset B (1993) Thyroglobulin molecules internalized by thyrocytes are sorted in early endosomes and partially recycled back to the follicular lumen. Endocrinology 132(6):2645-53

Kostrouch Z, Munari-Silem Y, Rajas F, Bernier-Valentin F, Rousset B (1991) Thyroglobulin internalized by thyrocytes passes through early and late endosomes. Endocrinology 129(4):2202-11

Kuiper GG, Carlsson B, Grandien K, Enmark E, Häggblad J, Nilsson S, Gustafsson JA (1997) Comparison of the ligand binding specificity and transcript tissue distribution of estrogen receptors alpha and beta. Endocrinology 138(3):863-70

Kuiper GG, Enmark E, Pelto-Huikko M, Nilsson S, Gustafsson JA (1996) Cloning of a novel receptor expressed in rat prostate and ovary. Proc Natl Acad Sci U S A 93(12):5925-30

Kupperman E, An S, Osborne N, Waldron S, Stainier DY (2000) A sphingosine-1-phosphate receptor regulates cell migration during vertebrate heart development. Nature 406:192-195

Lam SH, Winata CL, Tong Y, Korzh S, Lim WS, Korzh V, Spitsbergen J, Mathavan S, Miller LD, Liu ET, Gong Z (2006) Transcriptome kinetics of arsenic-induced adaptive response in zebrafish liver. Physiol Genomics 27(3):351-61

Lang IA, Galloway TS, Scarlett A, Henley WE, Depledge M, Wallace RB, Melzer D (2008) Association of urinary bisphenol A concentration with medical disorders and laboratory abnormalities in adults. JAMA 300(11):1303-10

Larsson DGJ, Adolfsson-Erici M, Parkkonen J, Pettersson M, Berg AH, Olsson PE, Förlin L (1999) Ethinyloestradiol - an undesired fish contraceptive? Aquat Toxicol 45(2-3):91-7

Lebbe M, Woodruff TK (2013) Involvement of androgens in ovarian health and disease. Mol Hum Reprod 19(12):828-37

Lee HJ, Chattopadhyay S, Gong EY, Ahn RS, Lee K (2003) Antiandrogenic effects of bisphenol A and nonylphenol on the function of androgen receptor. Toxicol Sci 75(1):40-6

Lepilina A, Coon AN, Kikuchi K, Holdway JE, Roberts RW, Burns CG, Poss KD (2006) A dynamic epicardial injury response supports progenitor cell activity during zebrafish heart regeneration. Cell 127(3):607-19

Ling N, Ying SY, Ueno N, Shimasaki S, Esch F, Hotta M, Guillemin R (1986) Pituitary FSH is released by a heterodimer of the beta-subunits from the two forms of inhibin. Nature 321(6072):779-82

Lints TJ, Parsons LM, Hartley L, Lyons I, Harvey RP (1993) Nkx-2. 5: a novel murine homeobox gene expressed in early heart progenitor cells and their myogenic descendants. Development 119(3):419-31

Liu J, Stainier DY (2010) Tbx5 and Bmp signaling are essential for proepicardium specification in zebrafish. Circ Res 106(12):1818-28

Liu MM, Albanese C, Anderson CM, Hilty K, Webb P, Uht RM, Price RH Jr, Pestell RG, Kushner PJ (2002) Opposing action of estrogen receptors alpha and beta on cyclin D1 gene expression. J Biol Chem. 277(27):24353-60

Liu PY, Death AK, Handelsman DJ (2003) Androgens and cardiovascular disease. Endocr Rev 24(3):313-40

Long Q, Meng A, Wang H, Jessen JR, Farrell MJ, Lin S (1997) GATA-1 expression pattern can be recapitulated in living transgenic zebrafish using GFP reporter gene. Development 124(20):4105-11

Lubahn DB, Moyer JS, Golding TS, Couse JF, Korach KS, Smithies O (1993) Alteration of reproductive function but not prenatal sexual development after insertional disruption of the mouse estrogen receptor gene. Proc Natl Acad Sci U S A 90(23):11162-6

Lund AK, Goens MB, Kanagy NL, Walker MK (2003) Cardiac hypertrophy in aryl hydrocarbon receptor null mice is correlated with elevated angiotensin II, endothelin-1, and mean arterial blood pressure. Toxicol Appl Pharmacol 193(2):177-87

Martinez-Arguelles DB, Papadopoulos V (2010) Epigenetic regulation of the expression of genes involved in steroid hormone biosynthesis and action. Steroids 75(7):467-76

Mathew LK, Sengupta S, Kawakami A, Andreasen EA, Löhr CV, Loynes CA, Renshaw SA, Peterson RT, Tanguay RL (2007) Unraveling tissue regeneration pathways using chemical genetics. J Biol Chem 282(48):35202-10

Matthews J, Gustafsson JA (2006) Estrogen receptor and aryl hydrocarbon receptor signaling pathways. Nucl Recept Signal 4:e016

Matthews J, Wihlén B, Thomsen J, Gustafsson JA (2005) Aryl hydrocarbon receptor-mediated transcription: ligand-dependent recruitment of estrogen receptor alpha to 2,3,7,8-tetrachlorodibenzo-p-dioxin-responsive promoters. Mol Cell Biol 25(13):5317-28

McFadden DG, Charité J, Richardson JA, Srivastava D, Firulli AB, Olson EN (2000) A GATA-dependent right ventricular enhancer controls dHAND transcription in the developing heart. Development 127(24):5331-41

McKenna NJ, O'Malley BW (2002) Combinatorial control of gene expression by nuclear receptors and coregulators. Cell 108(4):465-74

Meachem SJ, McLachlan RI, de Kretser DM, Robertson DM, Wreford NG (1996) Neonatal exposure of rats to recombinant follicle stimulating hormone increases adult Sertoli and spermatogenic cell numbers. Biol Reprod 54(1):36-44

Mellon SH, Griffin LD (2002) Neurosteroids: biochemistry and clinical significance. Trends Endocrinol Metab 13(1):35-43

Mellström B, Naranjo JR (2001) Mechanisms of Ca(2+)-dependent transcription. Curr Opin Neurobiol 11(3):312-9

Melner MH, Abney TO (1980a) The direct effect of 17β-estradiol on LH-stimulated testosterone production in hypophysectomized rats. J Steroid Biochem 13(2):203-10

Melner MH, Abney TO (1980b) Depletion of the cytoplasmic estrogen receptor in gonadotropin-desensitized testes. Endocrinology 107(5):1620-6

Melzer D, Rice NE, Lewis C, Henley WE, Galloway TS (2010) Association of urinary bisphenol a concentration with heart disease: evidence from NHANES 2003/06. PLoS One 5(1):e8673

Mendelsohn ME, Karas RH (1999) The protective effects of estrogen on the cardiovascular system. N Engl J Med 340(23):1801-11

Meyer MR, Haas E, Prossnitz ER, Barton M (2009) Non-genomic regulation of vascular cell function and growth by estrogen. Mol Cell Endocrinol 308(1-2):9-16

Meyer MR, Prossnitz ER, Barton M (2011) The G protein-coupled estrogen receptor GPER/GPR30 as a regulator of cardiovascular function. Vascul Pharmacol 55(1-3):17-25

Milan DJ, Giokas AC, Serluca FC, Peterson RT, MacRae CA (2006) Notch1b and neuregulin are required for specification of central cardiac conduction tissue. Development 133(6):1125-32

Miller WL (2002) Androgen biosynthesis from cholesterol to DHEA. Mol Cell Endocrinol (1-2):7-14

Miller WL (2007) StAR search—what we know about how the steroidogenic acute regulatory protein mediates mitochondrial cholesterol import. Mol Endocrinol 21(3):589–601

Miller WL (2008) Steroidogenic enzymes. Endocr Dev 13:1-18

Miller WL, Strauss JF 3rd. (1999) Molecular pathology and mechanism of action of the steroidogenic acute regulatory protein, StAR. J Steroid Biochem Mol Biol 69(1-6):131–41

Moriyama K, Tagami T, Akamizu T, Usui T, Saijo M, Kanamoto N, Hataya Y, Shimatsu A, Kuzuya H, Nakao K (2002) Thyroid hormone action is disrupted by bisphenol A as an antagonist. J Clin Endocrinol Metab 87(11):5185-90

Mullur R, Liu YY, Brent GA (2014) Thyroid Hormone Regulation of Metabolism. Physiol Rev 94(2):355–82

Murphy E (2011) Estrogen signaling and cardiovascular disease. Circ Res 109(6):687-96

Ni TT, Lu J, Zhu M, Maddison LA, Boyd KL, Huskey L, Ju B, Hesselson D, Zhong TP, Page-McCaw PS, Stainier DY, Chen W (2012) Conditional control of gene function by an invertible gene trap in zebrafish. Proc Natl Acad Sci U S A 109(38):15389-94

O'Shaughnessy PJ, Baker PJ, Heikkilä M, Vainio S, McMahon AP (2000) Localization of 17beta-hydroxysteroid dehydrogenase/17-ketosteroid reductase isoform expression in the developing mouse testis--androstenedione is the major androgen secreted by fetal/neonatal leydig cells. Endocrinology 141(7):2631-7

Omiecinski CJ, Vanden Heuvel JP, Perdew GH, Peters JM (2011) Xenobiotic metabolism, disposition, and regulation by receptors: from biochemical phenomenon to predictors of major toxicities. Toxicol Sci 120 Suppl 1:S49-75

Osborne N, Brand-Arzamendi K, Ober EA, Jin SW, Verkade H, Holtzman NG, Yelon D, Stainier DY (2008) The spinster homolog, two of hearts, is required for sphingosine 1-phosphate signaling in zebrafish. Curr Biol 18(23):1882-8

Padmanabhan V, Sairam MR, Hassing JM, Brown MB, Ridings JW, Beitins IZ (1991) Follicle-stimulating hormone signal transduction: role of carbohydrate in aromatase induction in immature rat Sertoli cells. Mol Cell Endocrinol 79(1-3):119-28.

Panzica GC, Viglietti-Panzica C, Mura E, Quinn MJ Jr, Lavoie E, Palanza P, Ottinger MA (2007) Effects of xenoextrogens on the differentiation of behaviorally-relevant neural circuits. Front Neuroendocrinol 28(4):179-200

Payne AH, Hales DB (2004) Overview of steroidogenic enzymes in the pathway from cholesterol to active steroid hormones. Endocr Rev 25(6):947-70

Peterson RT, Link BA, Dowling JE, Schreiber SL (2000) Small molecule developmental screens reveal the logic and timing of vertebrate development. Proc Natl Acad Sci U S A 97(24):12965-9

Petz LN, Nardulli AM (2000) Sp1 binding sites and an estrogen response element half-site are involved in regulation of the human progesterone receptor A promoter. Mol Endocrinol 14(7):972-85

Pietras RJ, Szego CM (1975) Endometrial cell calcium and oestrogen action. Nature 253(5490):357-9

Pinzone JJ, Stevenson H, Strobl JS, Berg PE (2004) Molecular and cellular determinants of estrogen receptor alpha expression. Mol Cell Biol 24(11):4605-12

Prossnitz ER, Arterburn JB, Smith HO, Oprea TI, Sklar LA, Hathaway HJ (2008) Estrogen signaling through the transmembrane G protein-coupled receptor GPR30. Annu Rev Physiol 70:165-90

Purdom CE, Hardiman PA, Bye VVJ, Eno NC, Tyler CR, Sumpter JP (1994) Estrogenic Effects of Effluents From Sewage Treatment Works. Chem Ecol 8:275- 85

Reiter JF, Alexander J, Rodaway A, Yelon D, Patient R, Holder N, Stainier DY (1999) Gata5 is required for the development of the heart and endoderm in zebrafish. Genes Dev 13(22):2983-95

Reiter JF, Verkade H, Stainier DY (2001) Bmp2b and Oep promote early myocardial differentiation through their regulation of gata5. Dev Biol 234(2):330-8

Revankar CM, Cimino DF, Sklar LA, Arterburn JB, Prossnitz ER (2005) A transmembrane intracellular estrogen receptor mediates rapid cell signaling. Science 307(5715): 1625-30

Revelli A, Massobrio M, Tesarik J (1998) Nongenomic actions of steroid hormones in reproductive tissues. Endocr Rev 19(1):3-17

Rohr S, Otten C, Abdelilah-Seyfried S (2008) Asymmetric involution of the myocardial field drives heart tube formation in zebrafish. Circ Res 102(2):e12-9

Rohr S, Bit-Avragim N, Abdelilah-Seyfried S (2006) Heart and soul/prkci and nagie oko/mpp5 regulate myocardial coherence and remodeling during cardiac morphogenesis. *Development*. 133: 107–115.

Rottbauer W, Wessels G, Dahme T, Just S, Trano N, Hassel D, Burns CG, Katus HA, Fishman MC (2006) Cardiac myosin light chain-2: a novel essential component of thick-myofilament assembly and contractility of the heart. Circ Res. 99(3):323-31

Rowlands JC, Gustafsson JA (1997) Aryl hydrocarbon receptor-mediated signal transduction. Crit Rev Toxicol 27(2):109-34

Sahlin L, Norstedt G, Eriksson H (1994) Androgen regulation of the insulin-like growth factor-I and the estrogen receptor in rat uterus and liver. J Steroid Biochem Mol Biol 51(1-2):57-66

Schmidt JV, Bradfield CA (1996) Ah receptor signaling pathways. Annu Rev Cell Dev Biol 12:55-89

Scott IC, Masri B, D'Amico LA, Jin SW, Jungblut B, Wehman AM, Baier H, Audigier Y, Stainier DY (2007) The g protein-coupled receptor agtrl1b regulates early development of myocardial progenitors. Dev Cell 12(3):403-13

Seljelid R, Reith A, Nakken KF (1970) The early phase of endocytosis in rat thyroid follicle cells. Lab Invest 23:595-605

Serluca FC (2008) Development of the proepicardial organ in the zebrafish. Dev Biol 315(1):18-27

Shankar A, Teppala S, Sabanayagam C (2012) Urinary bisphenol a levels and measures of obesity: results from the national health and nutrition examination survey 2003-2008. ISRN Endocrinol 2012:965243

Sohoni P, Sumpter JP (1998) Several environmental oestrogens are also anti-androgens. J Endocrinol 158(3):327-39

Stainier DY (2001) Zebrafish genetics and vertebrate heart formation. Nat Rev Genet 2(1):39-48

Stainier DY, Weinstein BM, Detrich HW 3rd, Zon LI, Fishman MC (1995) Cloche, an early acting zebrafish gene, is required by both the endothelial and hematopoietic lineages. Development 121(10):3141-50

Staudt D, Stainier D (2012) Uncovering the molecular and cellular mechanisms of heart development using the zebrafish. Annu Rev Genet 46:397-418

Stein B, Yang MX (1995) Repression of the interleukin-6 promoter by estrogen receptor is mediated by NF-kappa B and C/EBP beta. Mol Cell Biol 15(9):4971-9

Stumpf WE (1969) Nuclear concentration of 3H-estradiol in target tissues. Dry-mount autoradiography of vagina, oviduct, ovary, testis, mammary tumor, liver and adrenal. Endocrinology 85(1):31-7

Sumpter JP (1998) Xenoendorine disrupters--environmental impacts. Toxicol Lett 102-103:337-42

Szego CM, Davis JS (1967) Adenosine 3',5'-monophosphate in rat uterus: acute elevation by estrogen. Proc Natl Acad Sci U S A 58(4):1711-8

Takeda H, Chodak G, Mutchnik S, Nakamoto T, Chang C (1990) Immunohistochemical localization of androgen receptors with mono- and polyclonal antibodies to androgen receptor. J Endocrinol 126(1):17-25

Telakowski-Hopkins CA1, King RG, Pickett CB (1988) Glutathione S-transferase Ya subunit gene: identification of regulatory elements required for basal level and inducible expression. Proc Natl Acad Sci U S A 85(4):1000-4

Ternes TA, Stumpf M, Mueller J, Haberer K, Wilken RD, Servos M (1999) Behavior and occurrence of estrogens in municipal sewage treatment plants--I. Investigations in Germany, Canada and Brazil. Sci Total Environ 225(1-2):81-90

Tessadori F, van Weerd JH, Burkhard SB, Verkerk AO, de Pater E, Boukens BJ, Vink A, Christoffels VM, Bakkers J (2012) Identification and functional characterization of cardiac pacemaker cells in zebrafish. PLoS One 7(10):e47644

Thackaberry EA, Gabaldon DM, Walker MK, Smith SM (2002) Aryl hydrocarbon receptor null mice develop cardiac hypertrophy and increased hypoxia-inducible factor-1alpha in the absence of cardiac hypoxia. Cardiovasc Toxicol 2(4):263-74

Thackaberry EA, Jiang Z, Johnson CD, Ramos KS, Walker MK (2005) Toxicogenomic profile of 2,3,7,8-tetrachlorodibenzo-p-dioxin in the murine fetal heart: modulation of cell cycle and extracellular matrix genes. Toxicol Sci 88(1):231-41

Thomas P, Pang Y, Filardo EJ, Dong J (2005) Identity of an estrogen membrane receptor coupled to a G protein in human breast cancer cells. Endocrinology 146(2):624-32

Timmerman LA, Grego-Bessa J, Raya A, Bertrán E, Pérez-Pomares JM, Díez J, Aranda S, Palomo S, McCormick F, Izpisúa-Belmonte JC, de la Pompa JL (2004) Notch promotes epithelial-mesenchymal transition during cardiac development and oncogenic transformation. Genes Dev 18(1):99-115

Tonissen KF, Drysdale TA, Lints TJ, Harvey RP, Krieg PA (1994) XNkx-2. 5, a Xenopus gene related to Nkx-2. 5 and tinman: evidence for a conserved role in cardiac development. Dev Biol 162(1):325-8

Trinh LA, Stainier DY (2004) Fibronectin regulates epithelial organization during myocardial migration in zebrafish. Dev Cell 6(3):371-82

Ubuka T, Son YL, Bentley GE, Millar RP, Tsutsui K (2013) Gonadotropin-inhibitory hormone (GnIH), GnIH receptor and cell signaling. Gen Comp Endocrinol. 190:10-7

Umayahara Y, Kawamori R, Watada H, Imano E, Iwama N, Morishima T, Yamasaki Y, Kajimoto Y, Kamada T (1994) Estrogen regulation of the insulin-like growth factor I gene transcription involves an AP-1 enhancer. J Biol Chem 269(23):16433-42

Veldman MB, Lin S (2008) Zebrafish as a developmental model organism for pediatric research. Pediatr Res 64(5):470-6

Verhoeven MC, Haase C, Christoffels VM, Weidinger G, Bakkers J (2011) Wnt signaling regulates atrioventricular canal formation upstream of BMP and Tbx2. Birth Defects Res A Clin Mol Teratol 91(6):435-40

Vermot J, Forouhar AS, Liebling M, Wu D, Plummer D, Gharib M, Fraser SE (2009) Reversing blood flows act through klf2a to ensure normal valvulogenesis in the developing heart. PLoS Biol 7(11):e1000246

Vicencio JM, Ibarra C, Estrada M, Chiong M, Soto D, Parra V, Diaz-Araya G, Jaimovich E, Lavandero S (2006) Testosterone induces an intracellular calcium increase by a nongenomic mechanism in cultured rat cardiac myocytes. Endocrinology 147(3):1386-95

Vivacqua A, Romeo E, De Marco P, De Francesco EM, Abonante S, Maggiolini M (2012) GPER mediates the Egr-1 expression induced by 17β-estradiol and 4-

hydroxitamoxifen in breast and endometrial cancer cells. Breast Cancer Res Treat 133(3):1025-35

Voutilainen R, Miller WL (1986) Developmental expression of genes for the stereoidogenic enzymes P450scc (20,22-desmolase), P450c17 (17 alpha-hydroxylase/17,20-lyase), and P450c21 (21-hydroxylase) in the human fetus. J Clin Endocrinol & Metab 63(5):1145-50

Walisser JA, Bunger MK, Glover E, Bradfield CA (2004) Gestational exposure of Ahr and Arnt hypomorphs to dioxin rescues vascular development. Proc Natl Acad Sci U S A 101(47):16677-82

Walker MK, Catron TF (2000) Characterization of cardiotoxicity induced by 2,3,7, 8-tetrachlorodibenzo-p-dioxin and related chemicals during early chick embryo development. Toxicol Appl Pharmacol 167(3):210-21

Walsh EC, Stainier DY (2001) UDP-glucose dehydrogenase required for cardiac valve formation in zebrafish. Science. 293(5535):1670-3

Wang Q, Carroll JS, Brown M (2005) Spatial and temporal recruitment of androgen receptor and its coactivators involves chromosomal looping and polymerase tracking. Mol Cell 19(5):631-42

Waye A, Trudeau VL (2011) Neuroendocrine Disruption: More than Hormones are Upset. J Toxicol Environ Health B Crit Rev 14(5-7): 270–91

Webb P, Nguyen P, Shinsako J, Anderson C, Feng W, Nguyen MP, Chen D, Huang SM, Subramanian S, McKinerney E, Katzenellenbogen BS, Stallcup MR, Kushner PJ (1998) Estrogen receptor activation function 1 works by binding p160 coactivator proteins. Mol Endocrinol 12(10):1605-18

Webb P, Nguyen P, Valentine C, Lopez GN, Kwok GR, McInerney E, Katzenellenbogen BS, Enmark E, Gustafsson JA, Nilsson S, Kushner PJ (1999) The estrogen receptor enhances AP-1 activity by two distinct mechanisms with different requirements for receptor transactivation functions. Mol Endocrinol 13(10):1672-85

Weisz A, Rosales R (1990) Identification of an estrogen response element upstream of the human c-fos gene that binds the estrogen receptor and the AP-1 transcription factor. Nucleic Acids Res 18(17):5097-106

Westin J, Lardelli M (1997) Three novel Notch genes in zebrafish: implications for vertebrate Notch gene evolution and function. Dev Genes Evol 207(1):51-63

Xiao FY, Nheu L, Komesaroff P, Ling S (2015) Testosterone protects cardiac myocytes from superoxide injury via NF-κB signalling pathways. Life Sci 133:45-52

Yan S, Chen Y, Dong M, Song W, Belcher SM, Wang HS (2011) Bisphenol A and 17β-estradiol promote arrhythmia in the female heart via alteration of calcium handling. PLoS One 6(9):e25455

Yelon D, Ticho B, Halpern ME, Ruvinsky I, Ho RK, Silver LM, Stainier DY (2000) The bHLH transcription factor hand2 plays parallel roles in zebrafish heart and pectoral fin development. Development 127(12): 2573-82

Yue P, Chatterjee K, Beale C, Poole-Wilson PA, Collins P (1995) Testosterone relaxes rabbit coronary arteries and aorta. Circulation 91(4):1154-60

Zeng XX, Wilm TP, Sepich DS, Solnica-Krezel L (2007) Apelin and its receptor control heart field formation during zebrafish gastrulation. Dev Cell. 2007 Mar;12(3):391-402

Zoeller RT, Bansal R, Parris C (2005) Bisphenol-A, an environmental contaminant that acts as a thyroid hormone receptor antagonist in vitro, increases serum thyroxine, and alters RC3/neurogranin expression in the developing rat brain. Endocrinology 146(2):607-12

Chapter 1

Contribution of G protein-coupled estrogen receptor 1 (GPER) to 17β-estradiol-induced developmental toxicity in zebrafish

The text of this part of the thesis, in full, is a reprint of the material as it appears in the Journal of Aquatic Toxicology (186:180-187) published on May 2017.
Co-authors: Menjivar-Cervantes N, Leung MS, Volz DC, Schlenk D.

This research was made possible by a grant from The Gulf of Mexico Research Initiative. Grant No: SA-1520; Name: Relationship of Effects of Cardiac Outcomes in fish for Validation of Ecological Risk (RECOVER). GRIIDC DOI: 10.7266/N7P848X9. The study was also funded through the University of California, Riverside College of Natural and Agricultural Science US Department of Agriculture/Agricultural Experiment Station Resource Support Allocation Program.

Abstract

Exposure to 17B-estradiol (E2) influences the regulation of multiple signaling pathways, and E2-mediated disruption of signaling events during early development can lead to malformations such as cardiac defects. In this study, we investigated the potential role of the G-protein estrogen receptor 1 (GPER) in E2-induced developmental toxicity. Zebrafish embryos were exposed to E2 from 2 h post fertilization (hpf) to 76 hpf with subsequent transcriptional measurements of heart and neural crest derivatives expressed 2 (hand2), leucine rich repeat containing 10 (lrrc10), and gper at 12, 28 and 76 hpf. Alteration in the expression of lrrc10, hand2 and gper was observed at 12 hpf and 76 hpf, but not at 28 hpf. Expres- sion of these genes was also altered after exposure to G1 (a GPER agonist) at 76 hpf. Expression of lrrc10, hand2 and gper all coincided with the formation of cardiac edema at 76 hpf as well as other developmental abnormalities. While co-exposure of G1 with G36 (a GPER antagonist) rescued G1-induced abnormalities and altered gene expression, co-exposure of E2 with G36, or ICI 182,780 (an estrogen receptor antagonist) did not rescue E2-induced cardiac deformities or gene expression. In addition, no effects on the concen- trations of downstream ER and GPER signaling molecules (cAMP or calcium) were observed in embryo homogenates after E2 treatment. These data suggest that the impacts of E2 on embryonic development at this stage are complex and may involve multiple receptor and/or signaling pathways.

Introduction

Xenobiotics in the environment can alter the normal functions of the endocrine system by acting as antagonists or agonists to hormonal receptors, and/or alter the synthesis/metabolism of endogenous hormones (Guillette et al., 1995; Sonnenschein and Soto, 1998). For example, phenolic xenobiotic compounds structurally similar to the endogenous hormone, 17β-estradiol (E2), may alter the regulation of a variety of signal transduction events during development. Studies in zebrafish have been utilized extensively as a model to evaluate the effects of xenobiotics on development, and have shown that exposure to agents such as Bisphenol-A (BPA) and the natural hormone E2 during development resulted in a range of gross malformations, including curved body axis, yolk- sac edema, and pericardial edema (Brion et al., 2004; Duan et al., 2008; Saili et al., 2012). Similar cardiac phenotypes have been observed following polycyclic aromatic hydrocarbon (PAH) exposure in zebrafish embryos (Incardona et al., 2004). Although many studies have evaluated the impacts of xenobiotics such as PAHs on heart development, the molecular mechanisms by which estrogenic compounds cause cardiotoxicity is poorly understood.

Embryonic development depends on the precise spatio-temporal expression of signaling genes, and alterations can result in abnormal phenotypes. While nuclear E2 receptors have been primarily studied in development, limited work has been reported on the G-protein-coupled estrogen receptor 1 (GPER). Activation of GPER by G1 (a GPER agonist), E2 and other estrogenic compounds increases levels of secondary messengers

such as Ca2+ (Brailoiu et al., 2013; Szego and Davis, 1967; Thomas et al., 2005), which can affect the expression of genes vital to cardiovascular development, such as *lrrc10* and *hand2* (Brody et al., 2013; Dirkx et al., 2013).

To better understand the effects of E2 and other potential phenolic contaminants that have estrogenic activities, the purpose of this study was to evaluate the role of GPER in the toxicity of E2 on zebrafish embryo development; G1 was used as a positive control for all exposures. To analyze the potential role of GPER in E2 and G1 toxicity, signal transduction and the expression of *gper* and cardiac genes, *lrrc10* and *hand2* were evaluated.

Materials and methods

Chemicals

G1 (rel-1-[4-(6-bromo-1,3-benzodioxol-5-yl)-3aR,4S,5,9bS-tetrahydro-3H-cyclopenta[c]quinolin-8-yl]-ethanone; ≥ 98% purity, Cayman Chemical, Ann Harbor, MI), G36 ((4S)-rel-4-(6-bromo-1,3-benzodioxol-5-yl)-3aR,4,5,9bS-tetrahydro-8-(1-methylethyl)-3H-cyclopenta[c]quinolone; ≥ 98% purity, Cayman Chemical); ICI 182,780182, 780 (7α,17β-[9-[(4,4,5,5,5-Pentafluoropentyl)sulfinyl]nonyl]estra-1,3,5(10)-triene-3,17-diol; ≥ 99% purity, Tocris, Minneapolis, MN) and 17β-estradiol (E2; ≥ 98% purity, Sigma-Aldrich, St. Louis, MO) were dissolved in ethanol. Stock solutions were kept at 4°C in dark conditions. Exposure solutions were prepared by diluting working

stocks in dechlorinated water at a final vehicle concentration of 0.1- 0.2% ethanol within all vehicle control and treatment groups.

Maintenance of zebrafish culture

Zebrafish (Danio Rerio) 5D adults were purchased from Oregon State University. Adults were maintained and embryos were treated according to an animal use protocol (AUP #20130005) that was reviewed and approved by the University of California, Riverside (UCR) Institutional Animal Care and Use Committee (IACUC). Adults were bred in tanks containing a mesh-spawning basket. The morning of treatment, embryos were collected 30min after the light turned on. Embryos were cleaned and microscopically evaluated for viability. The stage of the embryos was visualized before treatment to ensure that exposure was conducted at a consistent developmental stage throughout all experiments. The different stages were determined using previously published standards (Kimmel et al., 1995). The embryos were maintained at 28°C in dechlorinated water with a light:dark cycle of 14 h:10 h.

Exposure regime

After microscopic evaluation, 30–35 randomly selected embryos were placed in petri dishes (100 mm × 15 mm) for expo- sure. Treatment was initiated at 2h post fertilization (hpf) and embryos were statically exposed until 76 hpf. At this time point, there is no cardiac progenitor cell formation which allows for sufficient time to determine the embryo viability without confounding cardiac effects. The embryos were exposed to 0.1% ethanol as the solvent control and to various nominal concentrations of E2 (0.1, 2, 5, 7 and 8 μM). The concentrations were selected based on range finding studies and our

own dose response experiment (data not shown). Each dish of treatment contained 20 ml of the appropriate treatment solution. There were 4–9 replicates for each treatment depending on the specific experiment.

After exposure, the plates were incubated at 28°C in a light:dark cycle of 14h:10h. Embryos were statically exposed for 74h and were checked daily for viability based on a transparency, yellowish appearance and presence of a heartbeat. Embryos that were determined to be dead were removed immediately at each observation time. At 76 hpf, treatment was terminated and surviving embryos were used for molecular endpoints (see below) and analyzed for abnormalities. Prevalence of the following gross malformations were assessed microscopically and quantified: curved body axis, bent tail, yolk-sac edema, looping defects and pericardial edema.

To investigate the role of GPER in E2-induced toxicity expression of GPER, Hand2, and Lrrc10 mRNA was analyzed at several time points during development including the segmentation (12 hpf) and pharyngula stages (28 hpf). We also analyzed expression of these genes and Vtg mRNA at the same time point morphological responses occurred (76 hpf). Vtg was included as a positive control for ER activation.

To determine and compare whether GPER activation resulted in similar effects as E2 during development, embryos were exposed to G1, a GPER agonist. Embryos were exposed at various concentrations (0.5, 2 and 5 μM) of G1 at the same developmental time point as the E2 treatment. Doses were determined using range finding dose response experiments based on previous studies (Chandrasekar et al., 2010). To determine the contribution of GPER, co-exposure experiments were conducted with the GPER

antagonist, G36 (5 μM) and ICI 172, 780 (14 μM). Concentrations of the antagonists were selected based on the solubility of these compounds in ethanol and the highest concentration that did not cause adverse effects on embryonic development, based on a range finding dose response experiment (data not shown).

RNA isolation and RT-PCR

Post-treatment embryos at 12, 28, and 76 hpf were pooled for mRNA expression analysis. Approximately 35 embryos were pooled per treatment replicate (n=4–9) and used for total RNA extraction using RNeasy Lipid Tissue Mini Kit purchased from Qiagen (Valencia, CA). After RNA extraction, the purity and integrity of the samples were analyzed using the OD260/OD280 ratio. Using the Promega Reverse Transcription System kit (Madison, WI), 1000 ng of RNA was used for cDNA synthesis following the manufacturer's instructions. Upon completion, cDNA was stored at -20°C until qPCR was performed. qPCR was done using the iTAQ Universal SYBR green kit from BioRad (Hercules, CA). Each SYBR reaction mix had 100 ng of cDNA and a specific primer set for the genes of interest. The primer sequence is as follows:

gper forward- 5' TGG CTG TGG CAG ATC TTA TTC 3'

gper reverse- 5' CAA TGG ACT GCT GCT CAT AGA 3'

hand2 forward- 5' AGA GAT GTC TCC TCC TGA CTA TAC 3'

hand2 reverse- 5' TTC CCT GAG TTC TGC AAA GG 3'

lrrc10 forward- 5' AGG AGC TTC CTC TGG TCA TA 3'

lrrc10 reverse- 5' AGC CTA AAT GGA GCG TCT TG 3'

vtg forward- 5' CTG CAA GAG TGC AAC TGA TAG TTT C 3'

vtg reverse- 5' ACT TGC CAG TGA CTT TGT GCT T3'

ef- α forward- 5' CTA CAT CAA GAA GAT CGG CTA CAA 3'

ef- α reverse- 5' CGA CAG GGA CAG TTC CAA TAC 3'

The thermal cycling conditions used for all three genes analyzed via qPCR was as follows: The denaturation step was done at 95°C for 5 min, followed by annealing and extension at 95°C for 10 sec and at 55°C for 30 sec. This was repeated for 40 cycles. Afterwards, a melt curve analysis was done from 54-95°C in increments of 0.5°C. All primer sets displayed one peak demonstrating the specificity. Data was normalized using *ef-*α and the efficiency for all genes were optimized and monitored using PCRminer. (Zhao and Fernald, 2005)

Calcium measurement

To measure calcium, treated embryos were collected (~30-35 embryos per treatment replicate; n=6) and homogenized on ice using a lysis buffer (150 mmol L^{-1} NaCl, 1% Triton X-100, 0.5% sodium deoxycholate, 50 mmol L^{-1} Tris-HCl, 1 mmol L^{-1} EDTA, 1 mmol L^{-1} phenylmethanesulfonyl fluoride, 0.1% SDS). After incubation for 30 min on ice, lysed samples were centrifuged at 15,000 x *g* for 20 min at 4°C. The resulting supernatant was aspirated and used for the assay. Supernatant was mixed with 150 µl of the calcium reagent Arsenazo III (Sigma Aldrich, St. Louis, MO) and the absorbance determined at 650-nm with a spectrophotometer. The readings were then normalized to protein content, which was measured using a Pierce™ BCA Protein Assay Kit (Thermo Fisher Scientific, Waltham, MA) per manufacturer's instructions.

cAMP Measurements

Treated zebrafish embryos at 76 hpf (30-35 embryos per replicate, n=4-6) were snap-frozen in liquid nitrogen. cAMP concentrations was determined using Direct cAMP ELISA kit (Enzo Life Sciences, Farmingdale, NY) following the manufacturers' instructions. Proteins levels were determined using a Bradford assay (Thermo Fisher Scientific, Waltham, MA) for normalization.

Statistical Analysis

All statistical analyses were done using the statistical program R (R version 3.1.2). For parametric analyses, one-way ANOVA was used followed by a Tukey's HSD test ($p<0.05$). Data sets that were not normally distributed were analyzed using a nonparametric method, the Kruskal–Wallis one-way analysis of variance. If the Kruskal-Wallis test showed significance ($p<0.05$), then Dunn's post hoc test was used. Co-exposures were analyzed by a two-way ANOVA. Survival and deformity datasets were analyzed via logistic regression model.

Results

Sublethal malformations were observed after treatment with E2, including curved body axis, yolk-sac edema and pericardial edema (Figure 1-8). At 76 hpf, 35.5±15.9% and 61.1±28.9% of the surviving embryos exhibited pericardial edema and cardiac impairment (such as looping defects) after exposure to 7 μM and 8 μM of E2, respectively, which were both statistically significant compared to all groups (Figure 1-

1A). To assess ER activation in embryos, *vtg* expression was also analyzed at 76 hpf after treatment and an upward trend was observed following E2 treatment (Figure 1-9).

The expression of two cardiac genes *lrrc10* and *hand2* also increased after exposure to E2. The patterns of *lrrc10* and *hand2* expression were correlated with an r^2 value of 0.88. Expression of *lrrc10* transcripts at 12 hpf showed an increasing trend after exposure to 5 μM and 7 μM of E2, with a significant 9.6-fold increase observed at 8 μM E2 (Figure 1-2A). At 28 hpf, *lrrc10* expression did not significantly change (Figure 1-2B). At 76 hpf, an upward trend in *lrrc10* expression was seen after exposure to 2, 7 and 8 μM of E2, with a significant change at 5 μM exposure (Figure 1-2C). At 12 hpf, the expression of *hand2* after exposure to 8 μM of E2 resulted in a significant 5.7-fold increase (Figure 1-3A). At 28 hpf, *hand2* expression did not significantly change (Figure 1-3B). At 76 hpf, *hand2* expression showed an upward trend after exposure to 2, 7 and 8 μM of E2, but a significant change only occurred at 5 μM exposure (Figure 1-3C).

After exposure to 2 μM and 5 μM of G1 for 74 hrs, there was a significant increase in cardiac deformities (e.g., pericardial edema and looping defects). Treatment with 2 μM and 5 μM of G1 resulted in 87.7 ± 19.4% and 100 ± 0% of embryos with cardiac deformities (Figure 1-4A). After treatment with 2 μM of G1, expression of *lrrc10, hand2* and *gper* were significantly induced. Expression of *gper* resulted in a 9-fold increase compared to the vehicle control (Figure 1-4B). G1 exposure also resulted in a 8- and 9-fold increase in the expression of *lrrc10* and *hand2,* respectively (Figure 1-4C and D).

To assess whether the impacts on cardiac development were mediated through activation of GPER, E2- and G1-exposed embryos were co-exposed with the GPER antagonist G36. Exposure up to 5 μM of G36 did not cause cardiac deformities. Embryos exposed to 7 μM of E2 and 1.75 μM of G1 both caused a significant increase in the percentage of embryos that had cardiac deformities (45.4 ± 5.3% and 52.8 ± 6.1% respectively). Co-exposure of embryos to G1 and G36 decreased the abnormalities observed with G1 to 13.3 ± 2.5% (Figure 1-5A). In addition, the alterations observed in *gper*, *lrrc10* and *hand2* transcripts after G1 exposure were also abolished (Figure 1-5B and C). This suggests that expression of these genes may be associated with GPER-induced cardiotoxicity.

The increase in the expression of *gper*, *lrrc10* and *hand2* observed in the E2 exposed embryos were reduced when co-exposed with G36 (Figure 1-6B and C). However, the deformities were not rescued in the embryos that were co-exposed with E2 and G36 (Figure 1-6A). Since E2 deformities were not rescued by G36, we investigated whether the nuclear estrogen receptors were involved in E2 developmental toxicity. Embryos were co-exposed to 14 μM of ICI, 182,780 (ICI). The co-exposed samples did not significantly decrease the number of observed deformities, although levels of *vtg* mRNA was diminished confirming the concentration of ICI necessary for ER antagonism (Figure 1-7 and 2-9).

Activation of GPER enhances levels of intracellular secondary messengers such as cAMP and Ca^{2+}, which can moderate the expression of *lrrc10* and *hand2* (Brody et al., 2013; Dirkx et al., 2013). Levels of both secondary messengers were analyzed after

exposure to 2, 5 and 7 μM of E2, and G1 was used as a positive control. There was an increase in the levels of Ca^{2+} following treatment with 5 μM of G1 (Figure 1-10). However, significant changes were not seen after exposure to E2 for 74 hr at any of the concentrations analyzed (Figure 1-10). There was also no increase in cAMP after treatment with E2 and a trend towards a decrease after G1 exposure (Figure 1-11).

Discussion

Activation of GPER by the GPER agonist G1 induces similar malformations as those of embryos exposed to other estrogenic compounds (Jayasinghe and Volz, 2012). Binding of E2 or G1 to GPER can alter transcriptional regulation of genes required for development. In the present study, the role of GPER on cardiac impacts by E2 during development was evaluated. We showed that exposing zebrafish embryos to E2 and G1 during embryogenesis altered the transcription of *gper* and genes involved in cardiac development (*lrrc10* and *hand2*). Embryo lethality and developmental abnormalities such as cardiac deformities (e.g., pericardial edema) were temporally related to the altered expression patterns.

A significant increase in cardiac deformities (primarily pericardial edema) was observed after exposure to 7-8 μM of E2 at 76 hpf. Exposure to E2 (7-96 hpf) was reported to cause cardiac abnormalities in zebrafish embryos, but was observed at lower concentrations (2 μM) (Chandrasekar et al., 2010). The inconsistency in effect thresholds are likely due to experimental design differences such as different treatment vessels,

duration and developmental stage. In our study, exposure was only for 74 hrs with exposure occurring at 2 hpf. In contrast, Chandrasekar et al. (2010) exposed 7-hpf embryos to E2 for 96 hrs. Cardiac deformities have also been observed with other estrogen receptor ligands including EE2, BPA, bifenthrin, and genistein (Duan et al., 2009; Jin et al., 2009; Tse et al., 2013; Santos et al., 2014). EE2 was shown to alter heart rate and cause pericardial edema after exposure for 142 h (2-144 hpf) (Santos et al., 2014). Exposure to BPA in embryos from 8-120 hpf resulted in cardiac abnormalities at concentrations between 30-70 μM (Saili et al., 2012). Similarly, exposing 24-hpf zebrafish embryos to genistein (25 and 50 μM) for 60 hr resulted in a reduction of heart rate and increased pericardial edema (Kim et al., 2009).

Consistent with earlier studies, G1 also caused similar developmental cardiac toxicity in the current study (Jayasinghe and Volz, 2012). In addition, expression of *gper* mRNA was significantly increased following E2 treatment. Previous studies have shown that E2 induced the levels of both *gper* mRNA and protein in breast cancer cells via the epidermal growth factor receptor (EGFR) pathway (Vivacqua et al., 2009). Overexpression of GPER has been observed in breast and lung cancer cells, indicating its role in different chronic diseases (Filardo et al., 2006; Jala et al., 2012). The role of EGFR in the developmental toxicity of estrogenic compounds in zebrafish is unclear, but warrants further study.

GPER signaling is important for reproductive physiology and cardiovascular function (e.g. vasolidation) (Bopassa et al., 2010; Deschamps and Murphy, 2009; Meyer et al., 2011). In this study, E2 altered *hand2* transcripts at 12 hpf and 76 hpf and

treatment with G1 also caused altered expression of *hand2*. The transcription factor, *hand2* belongs to the beta helix-loop-helix (bHLH) family of proteins and regulates cardiac differentiation, especially during early somitogenesis, which occurs ~10-24 hpf in zebrafish (Kimmel et al., 1995; Stainier, 2001; Yelon et al., 2000). In addition, *hand2* plays a role in Notch and NFAT signaling in the endocardium (VanDusen et al., 2014). Overexpression of *hand2* in zebrafish embryos increases the number of cardiomyocyte cells and causes heart enlargement (Schindler et al., 2014). For example, mice that overexpressed *hand2* developed cardiac hypertrophy (Dirkx et al., 2013). Thus, the increase of *hand2* observed in our study may negatively affect cardiac development, but further study is needed to test this hypothesis.

Changes in the expression of *lrrc10* during development were also observed in the study after exposure to E2 at 12 hpf and 76 hpf. Transcripts of *lrrc10* were also altered by G1 exposure, showing that activation of GPER is a potential pathway for E2-induced expression of *lrrc10*. LRRC10 is a cardiac specific protein that contains leucine-rich repeat (LRR) motifs and is found in mice, humans and zebrafish. LRRC10 also has a significant role in heart function and development in mice as well as zebrafish (Brody et al., 2013; Kim et al., 2007; Nakane et al., 2004). A zebrafish study using *lrrc10* morpholinos showed that knocking down this gene caused cardiac morphogenic defects, such as cardiac looping errors, in addition to pericardial edema (Kim et al., 2007). This, along with the results from our study indicates that any disturbance in the levels of *lrrc10* may also result in abnormal development.

To verify that the altered gene expression of *gper*, *lrrc10* and *hand2* were mediated through the activation of GPER, embryos were co-exposed to the GPER antagonist, G36. Co-exposure of G1 with G36 rescued the altered expression of all three genes back to control levels. In addition, the rescue of *gper*, *lrrc10* and *hand2* expression was associated with a reduced percentage of cardiac deformities in the G1-G36 co-exposure. This shows that *gper*, *lrrc10* and *hand2* may be involved in the cardiac effects of G1.

In contrast to G1, G36 was unable to rescue the cardiac deformities induced by E2 exposure, although the expression of *gper, hand2* and *lrrc10* were reduced in the E2-G36 co-exposure. To investigate the involvement of the estrogen receptor pathway in E2 toxicity, a co-exposure study was conducted using the ER antagonist, ICI 182, 780 (ICI). Interestingly, neither ICI 182, 780 nor G36 rescued the observed cardiac effects caused by E2. While these results were unexpected, it is important to note the limitations of chemical co-exposure experiments in evaluating the mechanism of toxicity of compounds. The inability of G36 to rescue E2 cardiac deformities does not eliminate the contribution of other rapid estrogen sig- naling pathways involvement such as ERs variants (i.e. mER36) that can localize in the membrane (Razandi et al., 1999; Levin, 2002; Chaudhri et al., 2012). In addition, E2 may induce expression of additional ERs that may not be inhibited by ICI. Although these compounds are known bind to specific receptors and initial downstream effects, it is currently not possible to eliminate all other pathways that might be affected by E2 at this concentration, time-point and developmental stage. Thus, the inability of ICI 182, 780 or G36 to rescue the E2 induced morphological effects may

be due to the possibility that concentrations used for the study were insufficient to reverse E2 effects at the specific stage of development examined. Clearly, concentrations of G36 were sufficient to reduce G1-mediated effects and expression of GPER regulated cardiac genes, but morphological effects of E2 were unchanged. Concentrations of agonists and antagonists for all exposures were optimized based on solubility and overt toxicity. Antagonist concentrations above the solubility limit or that caused overt toxicity were not used. Although other studies in zebrafish adults have shown that 1 μM ICI can rescue effects of 10 nM E2, this was seen in adult male fish (Lam et al., 2011). Given that the concentrations of ICI in our study (14 μM) were more than 10-fold greater that those used in the adult male exposure, and below limits of solubility and overt toxicity, it seems likely that concentrations of ICI should have been high enough to elicit anti-estrogenic activity. In fact, the ICI-mediated inhibition of *vtg* induction by E2 is also consistent with ICI concentrations being relevant. However, the kinetic disposition of E2 and antagonists to specific molecular targets in adults relative to embryos is unknown, and suggests morphological effects may be dependent upon the time of exposure.

Alteration in the transcriptional regulation of *gper, hand2* and *lrrc10* was observed at 12 hpf and 76 hpf but not at 28 hpf. Enhanced expression at unique temporal periods may indicate sensitive windows for E2 toxicity during zebrafish development. At 12 hpf, the embryo is in the segmentation period of development. At this stage, cardiac precursor cells begin to move towards the embryonic axis and segregate (Stainier, 2001; Bakkers, 2011). At 28 hpf, ventricular and atrial chambers of the heart tube are becoming more distinct (Stainier, 2001). At 76 hpf, rapid growth of all tissues including the heart is

occurring (Staudt and Stainier, 2012). This is the time when deformities were observed in the current study. Proliferation of cardiac myocytes, and development of the primitive leaflet valves occur during 76 hpf and are critical for regulating blood flow (Scherz et al., 2008). The degree of reduced blood flow needed to cause embryo or larval mortality is unclear but would be a fruitful area of further study.

In summary, our data suggest that E2-induced cardiotoxicity in developing zebrafish embryos may not be attributed to a specific estrogen pathway. This further raises the question of the role of GPER and ERs during development. Given the widespread occurrence of structurally similar environmental pollutants, such as hydroxy-PAHs or phenolic compounds, that affect estrogen pathways, it is necessary to better characterize this pathway in vertebrate development and environmental toxicology.

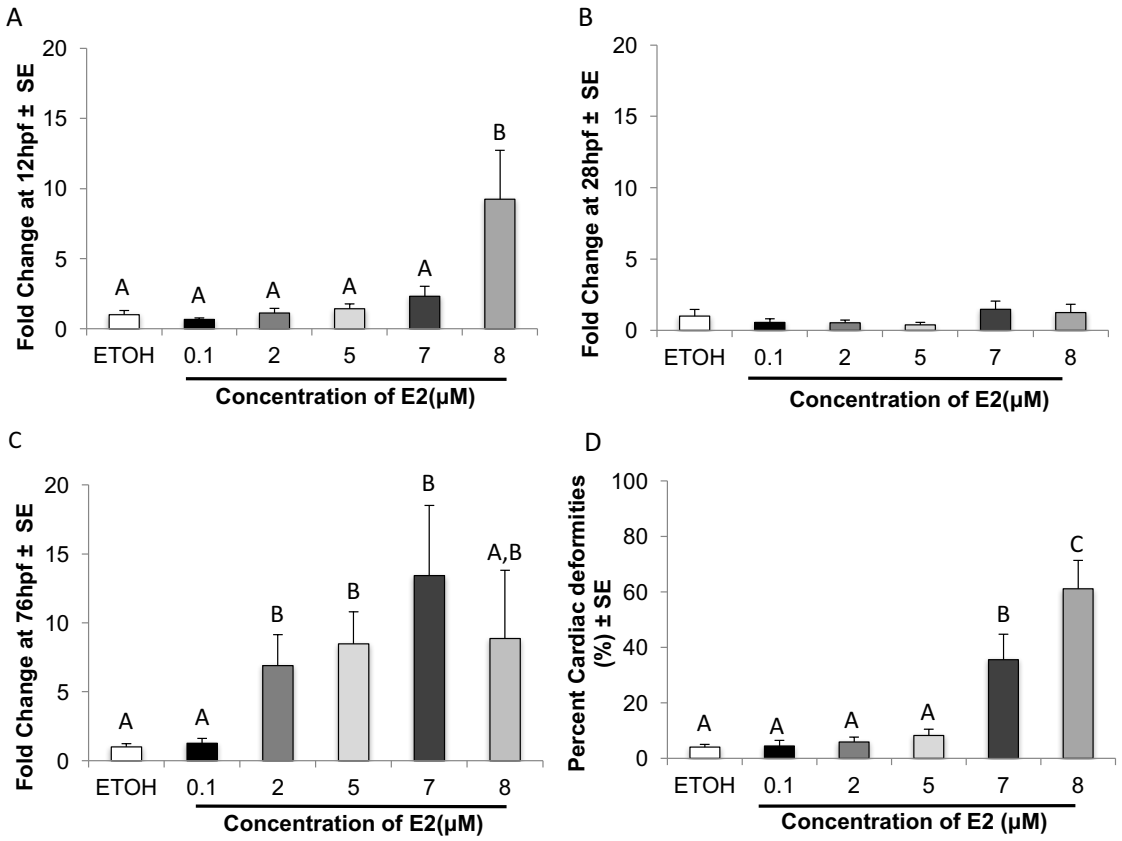

Figure 1-1. Effects of 17β–Estradiol (E2) on cardiac development and mRNA levels of GPER in zebrafish embryos at different times during development. Cumulative fold change of GPER mRNA of zebrafish embryos exposed to 0.1% ethanol (ETOH) and 0.1 μM-8 μM of E2 at 2hpf. Each graph represents different time points A) 12 hpf B) 28 hpf and C) 76 hpf. Data presented as mean ± standard error (SE) of four to nine independent replicates. (D) Average percent cardiac deformities at 76 hpf after treatment with 0.1% ethanol (ETOH) and 0.1 μM- 8 μM of E2 at 2 hpf. Data presented as mean ± standard error (SE) of four to six independent replicates. Deformities data were analyzed using a logistic regression model. Normal data was analyzed by ANOVA followed by Tukey's HSD multiple comparisons test. Data that was not normal a Wallis test was used followed by a Dunn's Multiple Comparison Test. Asterisks (*) represent the significant difference ($p<0.05$).

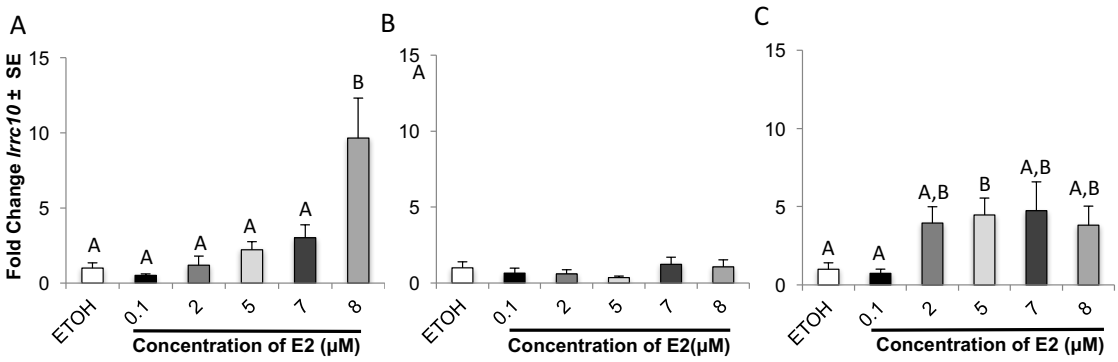

Figure 1-2. Effects of E2 on the expression of *lrrc10* in zebrafish embryos at different times during development. Cumulative fold change of *lrrc10* mRNA of zebrafish embryos exposed to 0.1% ethanol (ETOH) and 0.1 μM-8 μM of 17β-estradiol(E2) at 2 hpf. Each graph represents different time points (A) 12 hpf (B) 28 hpf and (C) 76 hpf. Data presented as mean ± standard error (SE) of four to nine independent replicates. Normal data was analyzed by ANOVA followed by Tukey's HSD multiple comparisons test. Data that was not normal a Kruskal-Wallis test was used followed by a Dunn's Multiple Comparison Test. Asterisks (*) represent the significant difference compared to control ($p<0.05$).

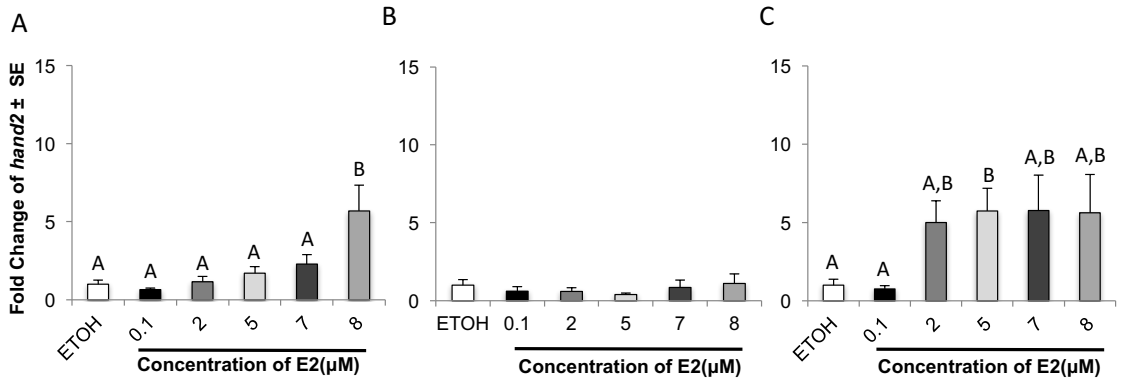

Figure 1-3. Effects of E2 on the expression of *hand2* in zebrafish embryos at different times during development. Cumulative fold change of *hand2* (A-C) mRNA of zebrafish embryos exposed to 0.1% ethanol (ETOH) and 0.1 μM-8 μM of 17β-estradiol(E2) at 2 hpf. Each graph represents different time points (A) 12 hpf (B) 28 hpf and (C) 76 hpf. Data presented as mean ± standard error (SE) of four to nine independent replicates. Normal data was analyzed by ANOVA followed by Tukey's HSD multiple comparisons test. Data that was not normal a Kruskal-Wallis test was used followed by a Dunn's Multiple Comparison Test. Asterisks (*) represent the significant difference compared to control ($p<0.05$).

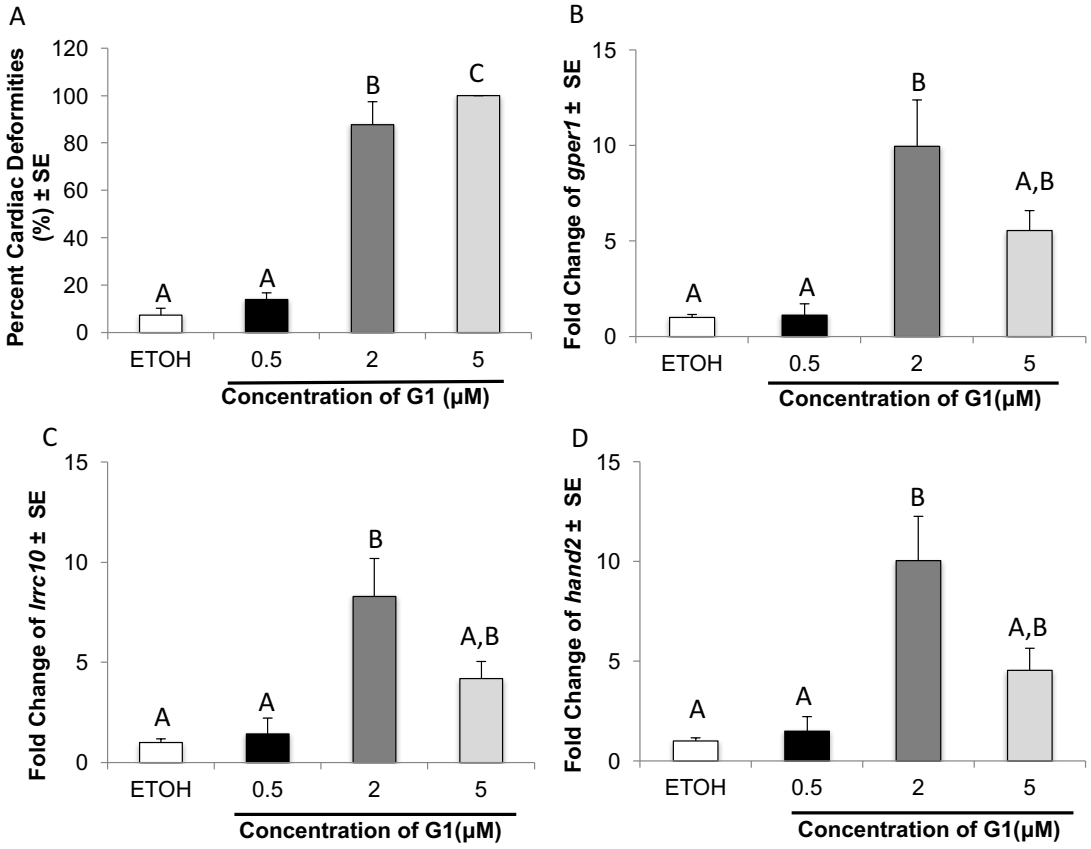

Figure 1- 4. Effects of G1 exposure on cardiac development and expression of *lrrc10*, *hand2* and *gper* in zebrafish embryos. (B-D) Cumulative fold change of *gper* (B), *lrcc10* (C) and *hand2* (D) mRNA of zebrafish embryos exposed to 0.1% ethanol (ETOH) and 0.5 µM-5 µM of G1 for 74 hr starting at 2 hpf. Data presented as mean ± standard error (SE) of four to nine independent replicates. (A) Data represents average percent cardiac deformities at 76 hpf after treatment with 0.1% ethanol (ETOH) and 0.5 µM- 5 µM of E2 at 2 hpf. Average percent cardiac deformities is presented and was analyzed via a logistic regression model. Normal data was analyzed by ANOVA followed by Tukey's HSD multiple comparisons test. Data that was not normal a Kruskal-Wallis test was used followed by a Dunn's Multiple Comparison Test. Different letters represent the significant differences ($p<0.05$).

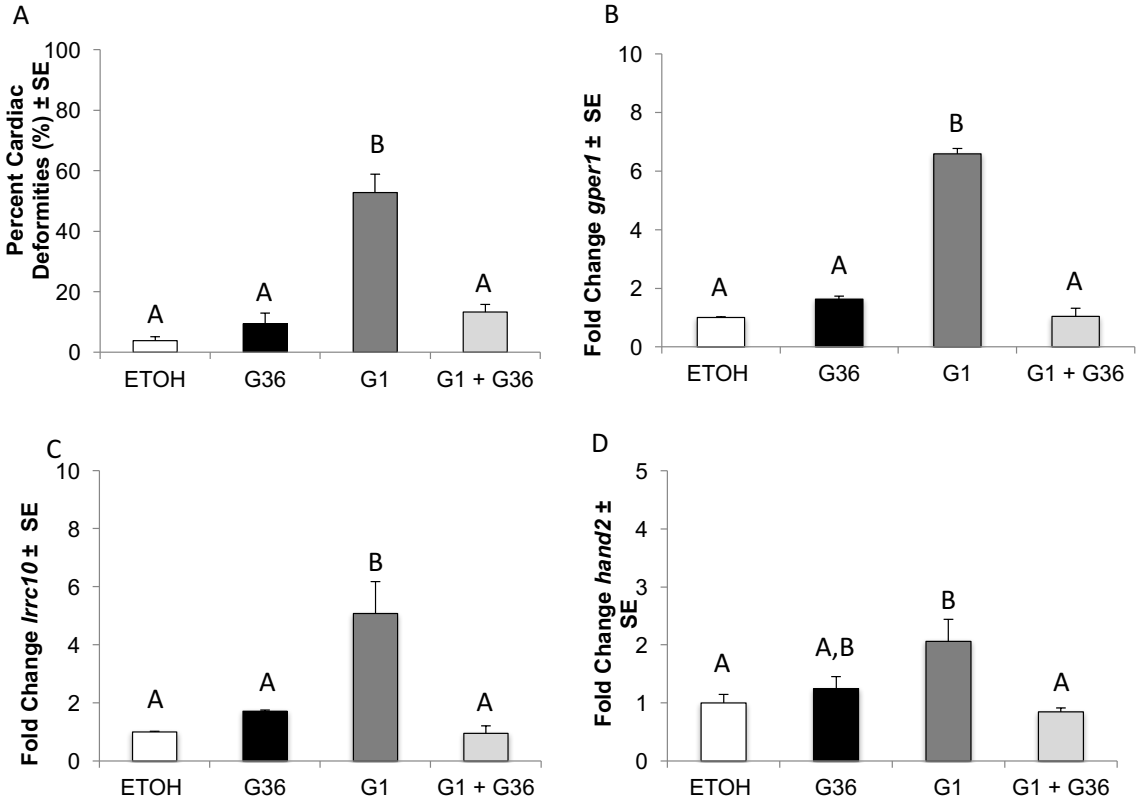

Figure 1-5. Effects of GPER agonist G1 and GPER antagonist G36 co-exposure on deformities and the expression of *lrrc10*, *hand2* and *gper* in zebrafish embryos. (A) Data represents average percent cardiac deformities at 76 hpf after treatment with 0.2% ethanol (ETOH), 5 μM of G36 and 1.75 μM of G1 for 74 hr starting at 2 hpf. (B-D) Cumulative fold change of *gper* (B), *lrrc10* (C) and *hand2* (D) mRNA of zebrafish embryos after exposure at 2 hpf. Data presented as mean ± standard error (SE) of four to nine independent replicates. Normal data was analyzed by 2-way ANOVA followed by Tukey's HSD multiple comparisons test. Deformities data was analyzed using a logistic regression model. Different letters represent the significant difference ($p<0.05$).

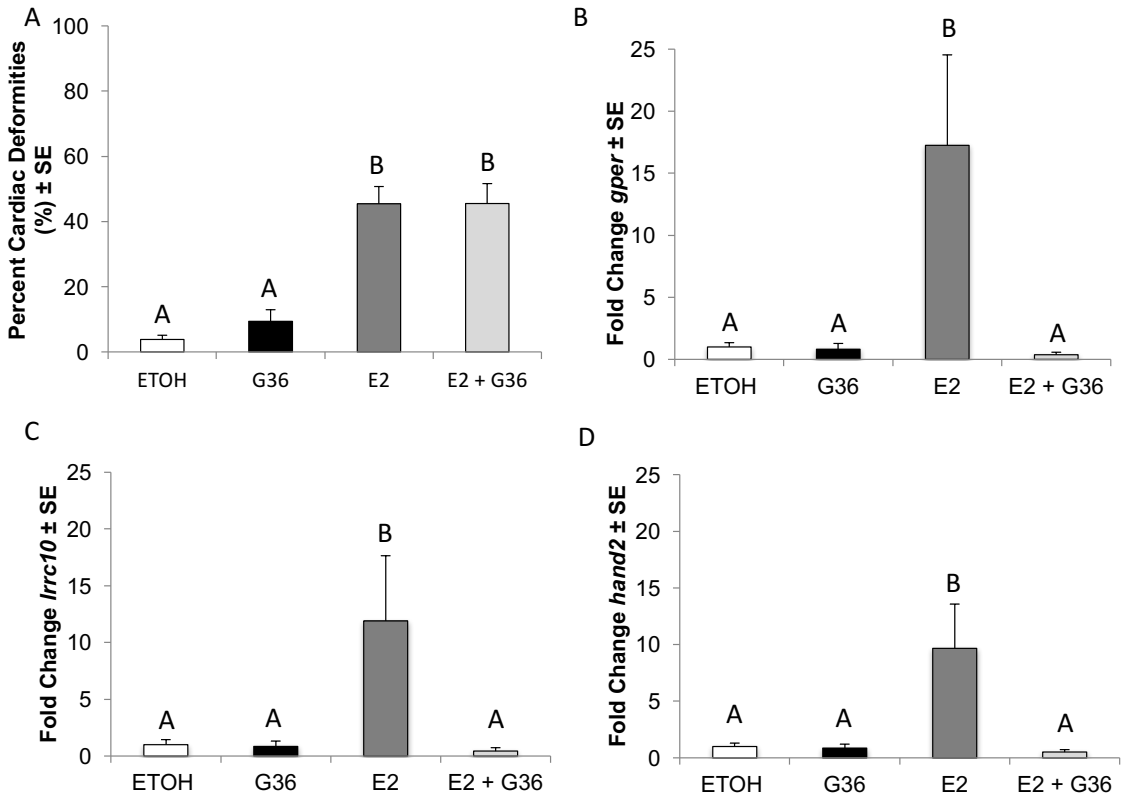

Figure 1-6. Effects of co-exposure to E2 and GPER antagonist G36 on deformities and the expression of *lrrc10, hand2* and *gper* in zebrafish embryos. (A) Data represents average percent cardiac deformities at 76 hpf after treatment with 0.2% ethanol (ETOH), 5 μM of G36 and 7 μM E2 for 74 hr starting at 2 hpf. (B-D) Cumulative fold change of *gper* (B), *lrrc10* (C) and *hand2* (D) mRNA of zebrafish embryos after exposure at 2 hpf. Data presented as mean ± standard error (SE) of four to nine independent replicates. Normal data was analyzed by 2-way ANOVA followed by Tukey's HSD multiple comparisons test. Deformities data was analyzed using a logistic regression model. Different letters represent the significant difference ($p<0.05$).

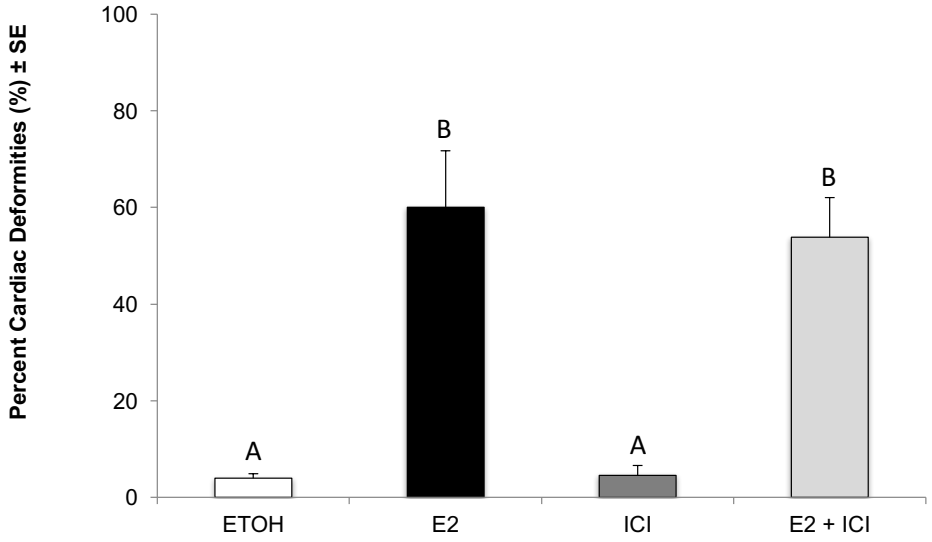

Figure 1-7. Percent of cardiac deformities after co-exposure of ER antagonist ICI 182, 780 with 17β–Estradiol (E2). Data represents average percent cardiac deformities at 76 hpf after treatment with 0.2% ethanol (ETOH), 7 μM of E2, 14 μM of ICI 182, 780 and 2 μM of Ral at 2 hpf. Data presented as mean ± standard error (SE) of four to six independent replicates. Data was analyzed using a logistic regression model. Asterisks (*) represent the significant difference ($p<0.05$).

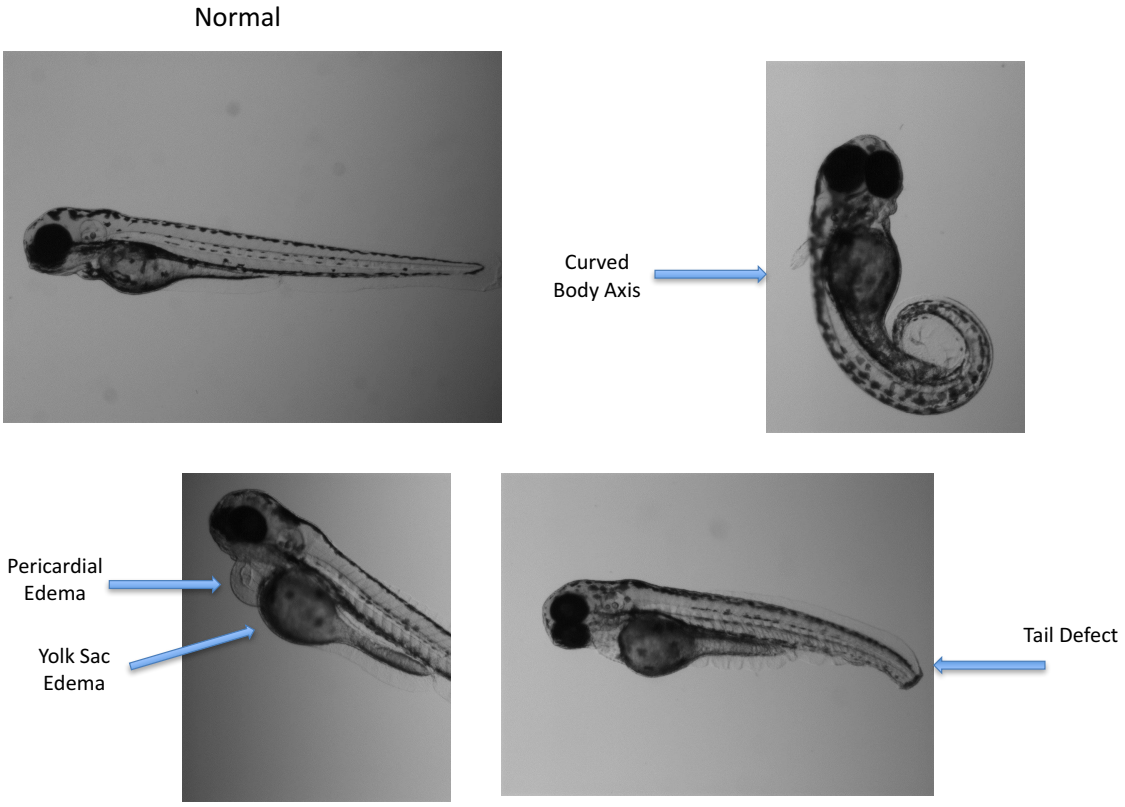

Figure 1-8. Images of sublethal malformations were observed after treatment with E2, including curved body axis, yolk-sac edema and pericardial edema at 76 hpf.

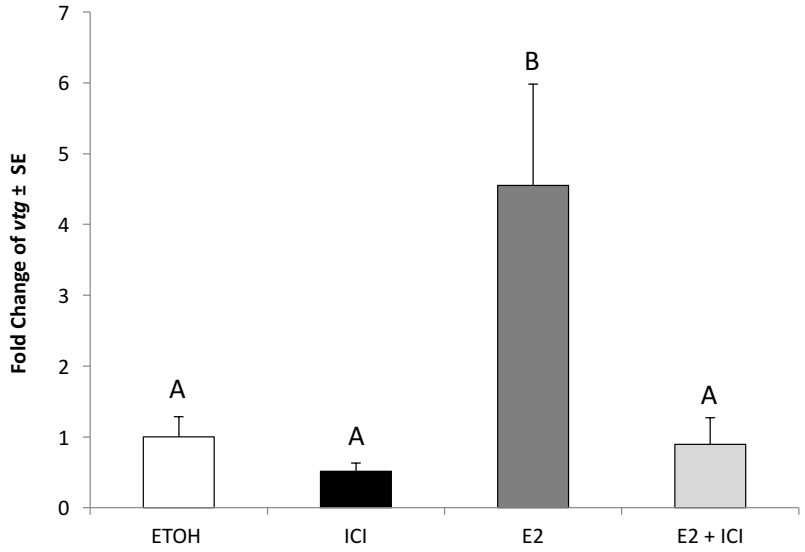

Figure 1-9. Effects of E2 on *vtg* expression in zebrafish embryos at 76 hpf. Cumulative fold change of *vtg* mRNA of zebrafish embryos exposed to 0.2% ethanol (ETOH), 7 μM of 17β-estradiol(E2), 14 μM ICI 182, 780 and co-exposed with E2 and ICI 182, 780 at 2 hpf. Data presented as mean ± standard error (SE) of four to six independent replicates. Kruskal-Wallis test was used followed by a Dunn's Multiple Comparison Test. Asterisks (*) represent the significant difference ($p<0.05$).

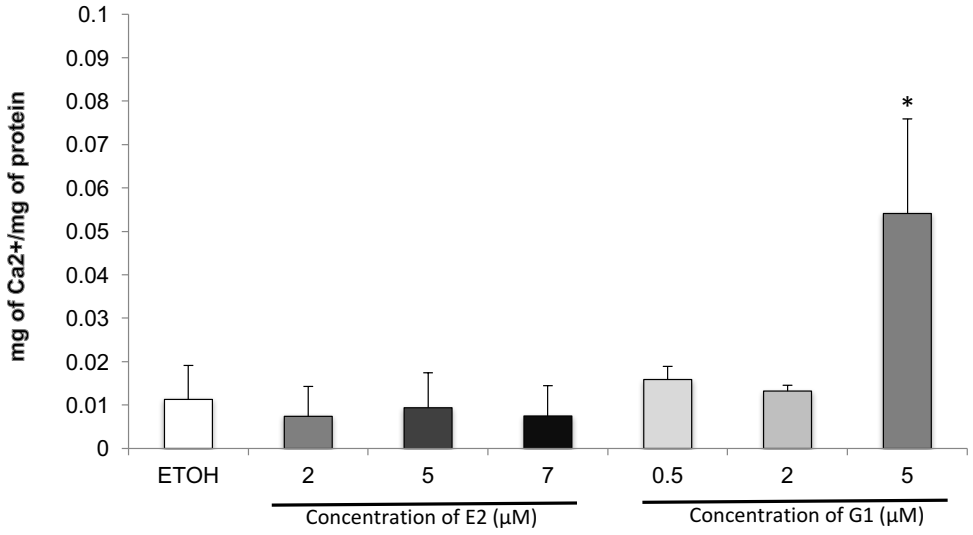

Figure 1-10. Effects on Ca^{2+} levels in zebrafish embryos after 17β–Estradiol (E2) exposure. Average levels of Ca^{2+} normalized to protein concentrations in zebrafish embryos exposed to 0.1% ethanol (ETOH) and 2μM-7μM E2 and 0.5 μM -5 μM G1 for 74hr starting at 2hpf. Data presented as mean ± standard error (SE) of six independent replicates. Data was analyzed by ANOVA followed by Tukey's HSD multiple comparisons test. Asterisks (*) represent the significant difference ($p<0.05$).

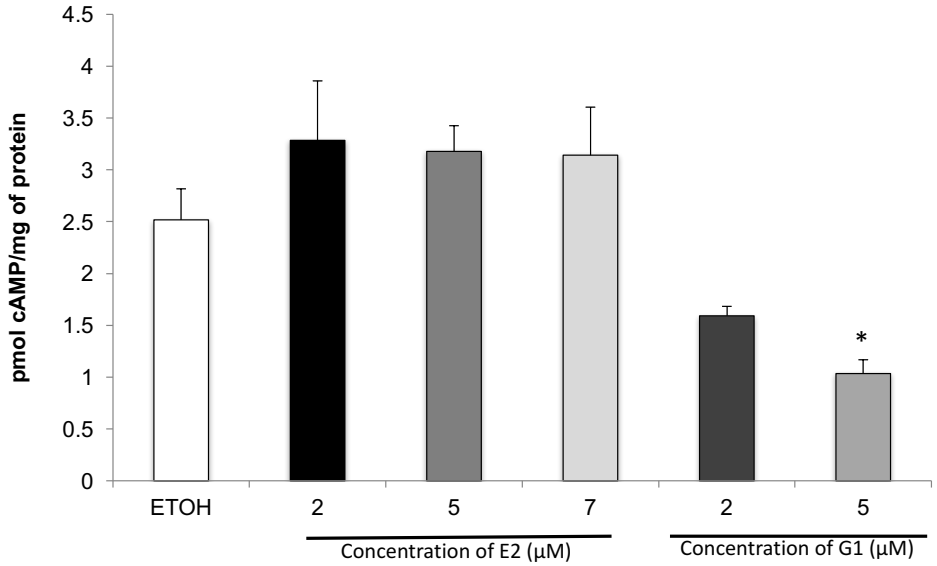

Figure 1-11. Levels of cAMP in zebrafish embryos after 17β–Estradiol (E2) and G1. Average levels of cAMP normalized to protein concentrations in zebrafish embryos exposed to 0.1% ethanol (ETOH) and 2μM-7μM E2 and 2μM -5 μM G1 for 74hr starting at 2hpf. Data presented as mean ± standard error (SE) of six independent replicates. Kruskal-Wallis test was used followed by a Dunn's Multiple Comparison Test. Asterisks (*) represent the significant difference ($p<0.05$).

References

Bakkers, J., 2011. Zebrafish as a model to study cardiac development and human cardiac disease. Cardiovasc Res. 91, 279-88.

Bopassa, J.C., Eghbali, M., Toro, L., Stefani, E., 2010. A novel estrogen receptor GPER inhibits mitochondria permeability transition pore opening and protects the heart against ischemia-reperfusion injury. Am J Physiol Heart Circ Physiol. 298, 16–23.

Brailoiu, G.C., Arterburn, J.B., Oprea, T.I., Chitravanshi, V.C., Brailoiu, E., 2013 Bradycardic effects mediated by activation of G protein-coupled estrogen receptor in rat nucleus ambiguus. Exp Physiol. 98, 679-91

Brion, F., Tyler, C.R., Palazzi, X., Laillet, B., Porcher, J.M., Garric, J., Flammarion, P., 2004. Impacts of 17beta-estradiol, including environmentally relevant concentrations, on reproduction after exposure during embryo-larval-, juvenile- and adult-life stages in zebrafish (Danio rerio). Aquat Toxicol. 68, 193-217.

Brody, M.J., Cho, E., Mysliwiec, M.R., Kim, T.G., Carlson, C.D., Lee, K.H., Lee, Y., 2013. Lrrc10 is a novel cardiac-specific target gene of Nkx2-5 and GATA4. J Mol Cell Cardiol. 62, 37-46.

Chandrasekar, G., Archer, A., Gustafsson, J.A., Andersson Lendahl, M., 2010. Levels of 17b-Estradiol Receptors Expressed in Embryonic and Adult Zebrafish Following In Vivo Treatment of Natural or Synthetic Ligands. PLoS ONE. 5, e9678.

Deschamps, A.M., Murphy, E., 2009. Activation of a novel estrogen receptor, GPER, is cardioprotective in male and female rats. Am J Physiol Heart Circ Physiol. 297, H1806-13.

Dirkx, E., Gladka, M.M., Philippen, L.E., Armand, A.S., Kinet, V., Leptidis, S., El Azzouzi, H., Salic, K., Bourajjaj, M., da Silva, G.J., Olieslagers, S., van der Nagel, R., de Weger, R., Bitsch, N., Kisters, N., Seyen, S., Morikawa, Y., Chanoine, C., Heymans, S., Volders, P.G., Thum, T., Dimmeler, S., Cserjesi, P., Eschenhagen, T., da Costa Martins, P.A., De Windt, L.J., 2013. Nfat and miR-25 cooperate to reactivate the transcription factor Hand2 in heart failure. Nat Cell Biol. 15, 1282-93.

Duan, Z., Zhu, L., Zhu, L., Kun, Y., Zhu, X., 2008. Individual and joint toxic effects of pentachlorophenol and bisphenol A on the development of zebrafish (Danio rerio) embryo. Ecotoxicol Environ Saf. 71, 774-80.

Filardo, E.J., Quinn, J.A., Frackelton, A.R. Jr., Bland, K.I., 2002. Estrogen action via the G protein-coupled receptor, GPR30: stimulation of adenylyl cyclase and cAMP-mediated

attenuation of the epidermal growth factor receptor-to-MAPK signaling axis. Mol Endocrinol. 16, 70-84.

Filardo, E.J., Graeber, C.T., Quinn, J.A., Resnick, M.B., Giri, D., DeLellis, R.A., Steinhoff, M.M., Sabo, E., 2006. Distribution of GPR30, a seven membrane-spanning estrogen receptor, in primary breast cancer and its association with clinicopathologic determinants of tumor progression. Clin Cancer Res. 12, 6359-66.

Guillette, L.J. Jr., Crain, D.A., Rooney, A.A., Pickford D.B., 1995. Organization versus activation: the role of endocrine-disrupting contaminants (EDCs) during embryonic development in wildlife. Environ Health Perspect. 103, 157-64.

Hayakawa, K., Onoda, Y., Tachikawa, C., Hosoi, S., Yoshita, M., Chung, S.W., Kizu, R., Toriba, A., Kameda, T., Tang, N., 2007. Estrogenic/antiestrogenic activities of polycyclic aromatic hydrocarbons and their monohydroxylated derivatives by yeast two-hybrid assay. J. Health Sci., 53, 562–570

Incardona, J.P., Collier, T.K., Scholz, N.L., 2004. Defects in cardiac function precede morphological abnormalities in fish embryos exposed to polycyclic aromatic hydrocarbons. Toxicol Appl Pharmacol. 196, 191-205.

Jala, V.R., Radde, B.N., Haribabu, B., Klinge, C.M., 2012. Enhanced expression of G-protein coupled estrogen receptor (GPER/GPR30) in lung cancer. BMC Cancer. 12, 624.

Jayasinghe, B.S., and Volz, D.C., 2012. Aberrant ligand-induced activation of G protein-coupled estrogen receptor 1 (GPER) results in developmental malformations during vertebrate embryogenesis. Toxicol Sci. 125, 262-73.

Jin, Y., Chen, R., Sun, L., Qian, H., Liu, W., Fu, Z., 2009. Induction of estrogen-responsive gene transcription in the embryo, larval, juvenile and adult life stages of zebrafish as biomarkers of short-term exposure to endocrine disrupting chemicals. Comp Biochem Physiol C Toxicol Pharmacol. 150, 414-20.

Kim, D.J., Seok, S.H., Baek, M.W., Lee, H.Y., Na, Y.R., Park, S.H., Lee, H.K., Dutta, N.K., Kawakami, K., Park, J.H., 2009. Developmental toxicity and brain aromatase induction by high genistein concentrations in zebrafish embryos. Toxicol Mech Methods. 19, 251-6.

Kim, K.H., Antkiewicz, D.S., Yan, L., Eliceiri, K.W., Heideman, W., Peterson, R.E., Lee, Y., 2007. Lrrc10 is required for early heart development and function in zebrafish. Dev Biol. 308, 494-506.

Kimmel, C.B., Ballard, W.W., Kimmel, S.R., Ullmann, B., Schilling, T.F., 1995. Stages of embryonic development of the zebrafish. Dev Dyn. 203, 253-310.

Lam SH, Lee SG, Lin CY, Thomsen JS, Fu PY, Murthy KR, Li H, Govindarajan KR, Nick LC, Bourque G, Gong Z, Lufkin T, Liu ET, Mathavan S. 2011. Molecular conservation of estrogen-response associated with cell cycle regulation, hormonal carcinogenesis and cancer in zebrafish and human cancer cell lines. BMC Med Genomics. 4:41.

Levin, E.R., (2002) Cellular functions of plasma membrane estrogen receptors. Steroids. 67(6):471-5.

Meyer, M.R., Prossnitz, E.R., Barton, M., 2011. The G protein-coupled estrogen receptor GPER/GPR30 as a regulator of cardiovascular function. Vascul Pharmacol. 55, 17-25.

Nakane, T., Satoh, T., Inada, Y., Nakayama, J., Itoh, F., Chiba, S., 2004. Molecular cloning and expression of HRLRRP, a novel heart-restricted leucine-rich repeat protein. Biochem Biophys Res Commun. 314, 1086-92.

Razandi, M., Pedram, A., Greene, G.L., Levin, E.R., (1999) Cell membrane and nuclear estrogen receptors (ERs) originate from a single transcript: studies of ERalpha and ERbeta expressed in Chinese hamster ovary cells. Mol Endocrinol. 13(2):307-19.

Revankar, C.M., Cimino, D.F., Sklar, L.A., Arterburn, J.B., Prossnitz, E.R., 2005. A transmembrane intracellular estrogen receptor mediates rapid cell signaling. Science. 307, 1625–1630.

Saili, K.S., Corvi, M.M., Weber, D.N., Patel, A.U., Das, S.R., Przybyla, J., Anderson, K.A., Tanguay, R.L., 2012. Neurodevelopmental low-dose bisphenol A exposure leads to early life-stage hyperactivity and learning deficits in adult zebrafish. Toxicology. 291, 83-92.

Santos, D., Matos, M., Coimbra, A.M., 2014. Developmental toxicity of endocrine disruptors in early life stages of zebrafish, a genetic and embryogenesis study. Neurotoxicol Teratol. 46, 18-25.

Scherz, P.J., Huisken, J., Sahai-Hernandez, P., Stainier, D.Y., 2008. High-speed imaging of developing heart valves reveals interplay of morphogenesis and function. Development. 135, 1179-87.

Schindler, Y.L., Garske, K.M., Wang, J., Firulli, B.A., Firulli, A.B., Poss, K.D., Yelon, D., 2014. Hand2 elevates cardiomyocyte production during zebrafish heart development and regeneration. Development. 141, 3112-22.

Sonnenschein, C., Soto, A.M., 1998. An updated review of environmental estrogen and androgen mimics and antagonists. J Steroid Biochem Mol Biol. 65, 143-50.

Stainier, DY., 2001. Zebrafish genetics and vertebrate heart formation. Nat Rev Genet. 2, 39-48.

Staudt, D., Stainier, D., 2012. Uncovering the molecular and cellular mechanisms of heart development using the zebrafish. Annu Rev Genet. 46, 397-418.

Szego, C.M., Davis, J.S., 1967. Adenosine 3',5'-monophosphate in rat uterus: acute elevation by estrogen. Proc Natl Acad Sci USA. 58, 1711-8.

Thomas, P., Pang, Y., Filardo, E.J., Dong, J., 2005. Identity of an estrogen membrane receptor coupled to a G protein in human breast cancer cells. Endocrinology. 146, 624–632.

Tse, W.K., Yeung, B.H., Wan, H.T., Wong, C.K., 2013. Early embryogenesis in zebrafish is affected by bisphenol A exposure. Biol Open. 2, 466-71.

VanDusen, N.J., Casanovas, J., Vincentz, J.W., Firulli, B.A., Osterwalder, M., Lopez-Rios, J., Zeller, R., Zhou, B., Grego-Bessa, J., De La Pompa, J.L., Shou, W., Firulli, A.B., 2014. Hand2 is an essential regulator for two Notch-dependent functions within the embryonic endocardium. Cell Rep. 9, 2071-83.

Vivacqua, A., Lappano, R., De Marco, P., Sisci, D., Aquila, S., De Amicis, F., Fuqua, S.A., Andò, S., Maggiolini, M., 2009. G protein-coupled receptor 30 expression is up-regulated by EGF and TGF alpha in estrogen receptor alpha-positive cancer cells. Mol Endocrinol. 23, 1815-26.

Yelon, D., Ticho, B., Halpern, M.E., Ruvinsky, I., Ho, R.K., Silver, L.M., Stainier, D.Y., 2000. The bHLH transcription factor hand2 plays parallel roles in zebrafish heart and pectoral fin development. Development. 127, 2573-82.

Zhao, S., Fernald, R.D., 2005. Comprehensive algorithm for quantitative real-time polymerase chain reaction. J Comput Biol. 12(8):1047-64.

Chapter 2

Developmental Toxicity Of Hydroxylated Chrysene Metabolites in Zebrafish Embryos

The text of this part of the thesis, in full, is a reprint of the material as it appears in the Journal of Aquatic Toxicology (189:77-86) published on August 2017.
Co-authors: do Amaral E Silva Müller G, Menjivar-Cervantes N, Xu EG, Volz DC, Dias Bainy AC, Schlenk D.

This research was made possible by a grant from The Gulf of Mexico Research Initiative. Data are publicly available through the Gulf of Mexico Research Initiative Information & Data Cooperative (GRIIDC) at https://data.gulfresearchinitiative.org (doi:10.7266/N77W699K) and in part by CAPES/INCT-TA and CNPq. ACDB is recipient of CNPq productivity fellowship (Grant # 307467/2013-9)

Abstract

One of the primary sources of polycyclic aromatic hydrocarbons (PAHs) in marine environments is oil. Photochemical oxidation and microbial transformation of PAH-containing oils can result in the formation of oxygenated products. Among the PAHs in crude oil, chrysene is one of the most persistent within the water column and may be transformed to 2- and 6-hydroxychrysene (OHCHR). Both of these compounds have been shown to activate (2-OHCHR) and antagonize (6-OHCHR) the estrogen receptor (ER). Previous studies in our lab have shown that estrogen can significantly alter zebrafish development. However, little is known about the developmental toxicity of hydroxylated PAHs. Zebrafish embryos were exposed to 0.5-10 μM of 2- or 6-OHCHR from 2 hours post-fertilization (hpf) until 76 hpf. A significant decrease in survival was observed following exposure to 6-OHCHR – but not 2-OHCHR. Both OHCHRs significantly increased the percentage of overall deformities after treatment. In addition to cardiac malformations, ocular and circulatory defects were also observed in embryos exposed to both compounds, while 2-OHCHR generally resulted in a higher prevalence of effect. Moreover, treatment with 2-OHCHR resulted in a significant decrease in hemoglobin levels. ER nor G-Protein coupled estrogen receptor (GPER) antagonists and agonists did not rescue the observed defects. We also analyzed the expression of cardiac-, eye- and circulation-related genes previously shown to be affected by oil. *Rhodopsin* mRNA expresssion was significantly decreased by both compounds equally. However, exposure to 2-OHCHR significantly increased the expression of the hematopoietic

regulator, *runx1* (*runt related transcription factor 1*). These results indicate the toxicity of oxygenated photoproducts of PAHs and suggest that other targets and signaling pathways may contribute to developmental toxicity of weathered oil. Our findings also demonstrate the regio-selective toxicity of hydroxy-PAHs in the effects on eye and circulatory development and raise the need to identify mechanisms and ecological risks of oxy-PAHs to fish populations.

Introduction

The Deepwater Horizon (DWH) disaster of 2010 released millions of barrels of oil into the Gulf of Mexico, which occurred at the same time and location where numerous ecologically and commercially important fish species spawn (Incardona et al., 2014). Numerous studies have shown that fish embryos are especially sensitive to oil and the primary target may be the developing heart (Incardona et al., 2013 and 2014). The induced toxicity observed with oil exposure has been attributed to polycyclic aromatic hydrocarbons (PAHs) found in oil as mixtures. In crude oil, the major PAHs responsible for cardiac effects are those that have 2-4 aromatic rings (Brette et al., 2017). In addition to cardiotoxicity, exposure to PAHs also caused yolk sac edema, reduction in jaw size, skeletal defects (lordosis or scoliosis) and neurodevelopmental abnormalities commonly referred to as blue sac disease (BSD) (Incardona et al., 2004; 2006; 2011; Heintz et al., 1999; Le Bihanic et al., 2014).

In the marine environment, PAHs can undergo weathering processes (biotic and abiotic) that can change their physical and chemical composition and alter bioavailability and toxicity. Photolytic and microbial oxidation can result in the formation of oxygenated products that have greater toxic effects on marine life and the environment (Saeed et al., 2011; Esbaugh et al., 2016; Sweet et al., 2016). Among the PAHs found in crude oil, chrysene is one of the most persistent in the water column (Tansel et al., 2011) and can undergo oxidation to produce derivatives such 2- and 6-hydroxchrysene (OHCHR).

Prior work evaluating the molecular mechanisms of PAH toxicity has been primarily focused on the aryl hydrocarbon receptor (AhR) pathway (Jayasundara et al., 2015). AhR activation during development has been shown to cause cardiovascular defects induced by certain PAHs (Scott et al., 2011). However, growing evidence suggests that certain PAH-induced developmental toxicity may be AhR-independent (Incardona et al., 2005; Goodale et al., 2013). For example, in zebrafish, knockdown of AhR using morpholinos blocked pyrene-induced cardiotoxicity, but not phenanthrane or dibenzothiophene (Incardona et al., 2005).

In vitro studies have shown that hydroxylated PAHs such as 2- and 6-OHCHR can activate or antagonize estrogen receptor, respectively (Hayakawa et al., 2008; Van Lipzig et al., 2005; Tran et al., 1996). The estrogen pathway plays a significant role in reproduction, development, and the maintenance and function of the cardiovascular system of vertebrates (Allgood Jr. et al., 2013). Estrogens can induce biological effects by binding G-protein coupled estrogen receptors (GPER) or nuclear estrogen receptors (ER) (Hall et al. 2001). Estrogen treatment during development in zebrafish caused significant cardiotoxicity (Diamante et al., 2017). However, little is known about the effects of hydroxylated PAHs in aquatic organisms. To address this issue, we evaluated the effects of the ER agonist, 2-OHCHR, and the ER antagonist, 6-OHCHR on the embryonic development of zebrafish. In addition to cardiac effects, ocular and circulatory system effects were also investigated. To gain insight into the possible pathway involved in the 2- and 6-OHCHR induced developmental abnormalities, transcriptional and circulatory defects associated with 2- and 6-OHCHR toxicity were also evaluated.

Materials and methods

Chemicals

2- and 6 hydroxychrysene (≥ 99% purity, MRI Global, Kansas City, MO), phenanthrene (≥ 98% purity, Sigma-Aldrich, St. Louis, MO), chrysene (≥ 98% purity, EMD Millipore, Billerica, MA), G36 ((4S)-rel-4-(6-bromo-1,3-benzodioxol-5-yl)-3aR,4,5,9bS-tetrahydro-8-(1-methylethyl)-3H-cyclopenta[c]quinolone; ≥ 98% purity, Cayman Chemical); ICI 182, 780 (7α,17β-[9-[(4,4,5,5,5-Pentafluoropentyl) sulfinyl]nonyl] estra-1,3,5(10)-triene-3,17-diol; ≥ 99% purity, Tocris, Minneapolis, MN) and E2 (17β-estradiol ≥ 98% purity, Sigma-Aldrich, St. Louis, MO) were dissolved in 100% ethanol. Stock solutions were kept at 4°C in dark conditions. Exposure solutions were prepared by diluting working stocks in dechlorinated water at a final vehicle concentration of 0.1 or 0.2% ethanol within all vehicle control and treatment groups.

2.2 Maintenance of zebrafish culture

Wildtype zebrafish (5D) embryos were obtained from the facility of Dr. David Volz at the University of California, Riverside (UCR). The night prior to exposure in-tank breeding traps were placed into tanks. Embryos were handled under the UCR-Institutional Animal Care and Use Committee (IACUC) approved protocol (AUP #20130005). Newly fertilized eggs were collected within 30 min of spawning. After collection, embryos were rinsed and microscopically evaluated for viability. The developmental stage of embryos was visualized before treatment to ensure that exposure was conducted at a consistent stage throughout all experiments. The different stages were

determined using previously published standards (Kimmel at al., 1995). The embryos were maintained at 28°C in dechlorinated water with a light:dark cycle of 14 hours:10 hours (hrs).

Exposure Regime

After microscopic evaluation, 30-35 embryos were randomly placed in plastic petri dishes (100 x 15mm) for exposure at 2 hours post fertilization (hpf). Working solutions were freshly prepared by spiking stock solutions into water, resulting in 0.1 or 0.2% ethanol in controls and treatment groups. The embryos were exposed to ethanol as the solvent control and to various nominal concentrations of 2- or 6-OHCHR (0.5, 3, 5, 10 μM). Embryos were also treated with E2 (3, 5 and 8 μM), chrysene (0.5, 1 and 3 μM), phenanthrene (0.5, 3 and 5 μM), E2 (3 μM), G36 (5 μM) and ICI 172, 780 (14 μM). Concentrations of the oxy-PAHs were based on relative potency of the compounds to E2 (Hawakawa et al., 2008) and the developmental toxicity of E2, which was determined from previous studies in our laboratory (Diamante et al. 2017). Similarly, the concentrations of E2, G36 and ICI 172, 780 were also selected based on our previous study (Diamante et al., 2017). These concentrations were the highest soluble concentrations that did not cause overt toxicity. For co-exposure experiments, both compounds were added at the same developmental time point (2hpf). Each treatment dish contained 20 ml of the appropriate treatment solution. Treatment was repeated with at least 3 different clutches. The number of replicate (2-4) dishes per treatment group per clutch depended on the embryo yield for that day's hatch from culture. After exposure, petri-dishes were incubated at 28°C in a light:dark cycle of 14 hrs:10 hrs until 76 hpf.

Embryos were statically exposed for 74 h and were checked daily for viability based on a transparent and yellowish appearance and presence of a heartbeat. The dead organisms were removed immediately at each observation time. At 76 hpf, treatment was terminated and surviving embryos were analyzed for abnormalities. Treatment between 2-76 hpf was chosen due to previous work in the lab that showed this stage to be sensitive for estrogenic compound exposure (Diamante et al 2017). Prevalence of the following gross malformations were assessed microscopically and quantified: curved body axis, bent tail, yolk-sac edema, pericardial edema, presence of red blood cells, cardiac looping and eye defects (diameter).

RNA isolation and RT-PCR

Treated embryos were pooled for mRNA expression analysis. Approximately 30 embryos were pooled per replicate (n=4-9 replicate pools) for total RNA extraction using the RNeasy Lipid Tissue Mini Kit purchased from Qiagen (Valencia, CA). After RNA extraction, the purity and integrity of the samples were analyzed using the OD_{260}/OD_{280} ratio. Using the Promega Reverse Transcription System kit (Madison, WI), 1000 ng of RNA was used for cDNA synthesis following the manufacturer's instructions. Upon completion, cDNA was stored at -20°C until qPCR was performed. qPCR was carried out using the iTAQ Universal SYBR green kit from BioRad (Hercules, CA). Each SYBR reaction mix had 100 ng of cDNA and a specific primer set for the genes of interest. The primer sequences are as follows:

rho forward- 5' CCCCTCAACTACATCCTGCT 3'

rho reverse- 5' CGACTTTAGCCCCATCTCAC 3'

sema3a forward- 5' CACACCTTCCAAACGCGATG 3'

sema3a reverse- 5' ATAGGATGGAAGGCTCCGGT 3'

vegfa forward- 5' TGTAATGATGAGGCGCTCGAA 3'

vegfa reverse- 5' AGGCTCACAGTGGTTTTCTT 3'

ncx1 forward- 5' CAGGGTAGAGACAAACCAATCC 3'

ncx1 reverse- 5' CAGCAATACGCCTCTCATCTT 3'

runx1 forward- 5' CCACCCTACAACACCAATCT 3'

runx1 reverse- 5' CATGGCTGACATGCCAATAC 3'

gata1 forward- 5' AGTTCAGCAGCGCTCTATTC 3'

gata1 reverse- 5' CTGTTCTGGCCGTTCATCTTA 3'

vtg forward- 5' CTGCAAGAGTGCAACTGATAGTTTC 3'

vtg reverse- 5' ACTTGCCAGTGACTTTGTGCTT 3'

ef-α forward- 5' ATACATCAAGAAGATCGGCTACAA 3'

ef-α reverse- 5' CCACAGGTACAGTTCCAATAC 3'

The thermal cycling conditions for the qPCR analysis used for all genes were as follows: The denaturation step was done at 95°C for 5 min, followed by annealing and extension at 95°C for 10 sec and at 55°C for 30 sec. This was repeated for 40 cycles. Afterwards, a melt curve analysis was carried out from 54-95°C at increments of 0.5°C. All primer sets displayed one peak demonstrating the specificity. This was done using the BioRad CFX Connect instrument (Hercules, CA). Optimization was determined by previous studies and qPCR data was normalized using *ef-α* (Diamante et al., 2017).

Imaging

Images were captured using a Leica MZ10 F stereomicroscope equipped with a DMC2900 camera and Leica Application Suite (LAS v4.6) software. Morphometric analyses of images were performed using Image J (National Institutes of Health, Bethesda, MD). Embryos were imaged in lateral recumbency and analyzed for pericardial area.

O-Dianisidine Staining

Previously published protocols for o-dianisidine staining were utilized to determine the levels of hemoglobin after exposure (Paffett-Lugassy and Zon, 2005; Leet et al., 2014). Treated embryos were transferred into clean petri dishes and were stained with an o-dianisidine solution (0.6 mg/ml o-dianisidine, 0.01 M sodium acetate (pH 4.5), 0.65% H_2O_2, and 40% ethanol) at room temperature for 30 mins covered with foil. After staining, embryos were rinsed with E-pure water and transferred into 2 ml microfuge tubes. Once embryos were rinsed, 4% paraformaldehyde was added and the embryos were fixed for 1 h at 4°C then placed in a solution containing 0.8% KOH, 0.9% H_2O_2, and 0.1% Tween-20 for 30 mins at room temperature to remove pigments. After fixation, embryos were washed with phosphate-buffered saline (PBS) and then fixed with 4% paraformaldehyde overnight at 4°C. Embryos were then kept in PBS at 4°C until imaging. Embryos were imaged in dorsal recumbancy using a Leica MZ10 F stereomicroscope equipped with a DMC2900 camera and Leica Application Suite (LAS v4.6) software (Buffalo Grove, IL). The images were then analyzed using the Adobe Photoshop software color range tool. For comparison, a sample color of the o-dianisidine stain was obtained

from the control samples and then used to measure levels of staining in the ventral side of the yolk and pericardial area among all treatment groups.

Results

To compare the toxicity of 2- and 6-OHCHR to PAHs and estrogenic compounds, embryos were separately exposed to chrysene, phenanthrene, and E2 at the same stage and for the same duration. Exposure to 2-OHCHR for 74 h did not affect embryo survival. However, average percent survival significantly decreased to 67.01 % ± 10.73 after exposure to 10 μM of 6-OHCHR. Exposure to 5 μM phenanthrene also significantly decreased embryo survival to 33.28 % ± 5.37. No effect on survival was observed after exposure to chrysene and E2 (Table 2-1).

Occurrence of malformations were quantified after exposure to 2- and 6- OHCHR, chrysene, phenanthrene and E2 for 74 h. There was an increase in the percent of overall deformities after treatment with 2- and 6-OHCHR, phenanthrene and E2. After exposure to 0.5 μM 2-OHCHR more than 60% of the surviving embryos had deformities. Over 90% of the embryos exposed to 3-10 μM of either 2-OHCHR or 6-OHCHR presented with altered development. The highest concentration of phenanthrene also caused 70% of the surviving embryos to have malformations. E2 concentrations of 5 μM and 8 μM resulted in the average percent deformities to increase to 47.44 % ± 6.25 and 100.00 % ± 0, respectively. Similar to survival measurements, parent (non-hydroxylated) chrysene did not cause any developmental malformations at the concentrations tested (Table 2-1).

To determine whether the toxicity of 2- and 6-OHCHR was tissue-specific, the deformities were separated into different categories (spinal, eye, cardiac and circulatory defects). Exposure to the highest concentration of 6-OHCHR resulted in a significant increase in spinal deformities (Figure 2-1D). 2-OHCHR treatment at 3, 5, and 10 μM also increased structural malformations from approximately 20 to 30 % (Figure 2-1D). In contrast to 2- and 6-OHCHR, spinal deformities were the most abundant malformations observed in embryos exposed to E2. Exposure to 5 and 8 μM E2 caused a 25.23 % ± 4.6 and 99.33 % ± 0.66 prevalence of spinal deformities. Chrysene and phenanthrene did not cause significant increases in spinal deformities (Figure 2-1A and B).

Previous studies have shown that PAHs (e.g., phenanthrene) and oil can target eye development (Huang et al., 2013; Xu et al., 2016). Therefore, the incidence of eye deformities (e.g., eye discoloration and size) was also evaluated. The percentage of embryos with eye deformities significantly increased after exposure to 5 μM phenanthrene and 8 μM E2, respectively (Figure 2-2B and C). Exposure to 2- and 6-OHCHR also resulted in an increase in eye deformities. Exposure to 3, 5 and 10 μM of 2-OHCHR caused eye malformations in 80-97% of the embryos. 6-OHCHR also caused abnormal eye formation at 3, 5 and 10 μM, but the percentages were significantly lower than 2-OHCHR at the same concentrations ($P \leq 0.05$) (Figure 2-2D).

Heart development has been shown in many studies to be the primary target of PAHs; thus, the occurrence of cardiac deformities (pericardial edema, looping defects) was also quantified (Incardona et al., 2004; 2011). Phenanthrene, E2, 2- and 6- OHCHR all caused an increase in the average occurrence of cardiac malformations such as looping

defects and the presence of pericardial edema. Exposure to the highest concentrations of phenanthrene (5 μM) caused approximately a 40% increase of cardiac deformities (Figure 2-3B), whereas E2 (8 μM) caused cardiac malformations in more than 70% of embryos (Figure 2-3C). Exposure to 0.5, 3, 5, and 10 μM 2-OHCHR also resulted in an increase in cardiac deformities, with a more than 3-fold increase from 0.5 to 10 μM (Figure 2-3D). In contrast, treatment with 6-OHCHR caused the prevalence of cardiac deformities to significantly increase to nearly 70% at 3-10 μM (Figure 2-3D). Exposure to 2-OHCHR caused a 2-fold increase in pericardial area (Figure 2-4). However, embryos treated with 6-OHCHR only showed a trend towards an increase in pericardial area (Figure 2-4).

Hemoglobin levels and vascular effects were also observed. Impairment of circulation was observed in the embryos exposed to E2, 2- and 6-OHCHR. Exposure to 8 μM E2 resulted in a greater than 90% increase in the prevalence of circulatory defects (Figure 2-5C). Embryos exposed to 0.5, 3, 5 and 10 μM 2-OHCHR also resulted in blood flow alterations with effect noted from 40 % to nearly 90% over the range of concentrations (Figure 2-5D). Although similar responses were observed in embryos treated with 6-OHCHR (~50% response), overall responses were not concentration-dependent (Figure 2-5D). Exposure to 3 and 5 μM 2-OHCHR caused significantly more defects than 6-OHCHR at the same concentration. Hemoglobin levels were also measured and a significant decrease was observed in the embryos treated with 2-OHCHR compared to control and 6-OHCHR (Figure 2-6).

To investigate potential contributions of ER signaling in 2- and 6-OHCHR toxicity, the expression of *vtg* was analyzed. Expression of *vtg* was significantly increased after exposure to 2- OHCHR at 0.5 μM but unchanged by 6-OHCHR (Figure 2-7A). Co-exposure of the PAHs with the ER antagonist ICI 182,780 or the GPER antagonist G36 failed to rescue any of the developmental effects noted above (Figure 2-7B and C). Since 6-OHCHR has been shown to be an ER antagonist, embryos were co-exposed to the hydroxylated chrysene and E2. However, co-exposure of embryos to E2 and 6-OHCHR did not rescue any development malformations (Figure 2-7D).

Potential molecular targets were investigated for each malformation that was observed after exposure to 2- and 6-OHCHR for 74hrs. The expression of *rho* (ocular), *nxc1* (cardiac ion exchange), *gata1* (hematopoiesis), *runx1* (hematopoiesis), *vegfa* (vasculogenesis and angiogenesis) and *sema3a* (vasculogenesis) were investigated. The genes selected were previously shown to be affected by either oil or PAH exposure (Sørhus et al., 2016; Xu et al., 2016). No significant alterations were observed in *ncx1, gata1* and *sema3a* expression. 2- and 6-OHCHR both caused a concentration-dependent decrease in expression of *rho* (Figure 2-8). However, there were no significant differences between the responses of either compound. A trend towards an increase in levels of *vegfa* mRNA was observed with 2-OHCHR treatments (Figure 2-8C), but a significant increase in *runx1* expression was observed after exposure to 10 μM of 2-OHCHR (Figure 2-8E).

Discussion

Oil spillage from minor fuel leakage to disasters, such as the DWH spill, is one of the major sources of PAHs in the environment. The effects of parent PAHs have been well studied in model organisms such as zebrafish. However, PAHs can undergo oxidation to degradates that are non-target compounds in oil studies. In this study, zebrafish embryos were used to assess the developmental effects of 2- and 6-OHCHR, chrysene, phenanthrene and E2. Exposure of zebrafish embryos to 0.5-3 μM of chrysene during embryogenesis did not result in any significant developmental defects at 76 hpf. These results are consistent with previous studies in zebrafish (Incardona et al., 2004). Conversely, both mortality and malformations were increased in the embryos that were exposed to 5 μM of phenanthrene. This is also consistent with other studies showing the toxic effects of phenanthrene on survival and development of fish (Incardona et al., 2004; Gundel et al., 2012; Butler et al., 2013; Brette et al., 2017). Interestingly, unlike the parent compound chrysene, 2- and 6-OHCHR significantly affected zebrafish development, both causing a significant increase in deformed embryos. However, only treatment with 6-OHCHR was acutely toxic to zebrafish embryos. This study is the first to show structural regio-selective toxicity of hydroxylated PAHs on development and survival of fish embryos. Previous studies have shown that oxygenated PAHs can be toxic to both vertebrates and invertebrates (Lampi et al., 2006; Knecht et al., 2013). Interestingly, oil induced toxicity was enhanced in mahi mahi embryos when co-exposed to UV light (Alloy et al., 2016; Stieglitz et al., 2016; Sweet et al., 2016). While there are

clearly higher levels of toxicity of oxy-PAHs, the mechanisms and targets for the toxicity are still somewhat unclear and warrants further investigation.

The cardiovascular system has been the most well studied target of PAHs and oil in both marine and model organisms like zebrafish (Incardona et al., 2004; Brette et al., 2014; 2017). Several studies have reported the effects of individual PAHs such as phenanthrene and dibenzothiophene on the cardiovascular system of zebrafish embryos. Incardona et al., (2004) also observed developmental toxicity induced by phenanthrene (28 μM) but at higher concentrations. This difference may be explained by initial time of exposure. In our study, exposure started at 2hpf while in the previous study it occurred at 4-8hpf. To determine if these differences are due to signaling processes at a specific stage additional studies are needed.

In contrast to other 2-4 ring PAH, chrysene failed to show cardiac defect or developmental abnormalities. However, hydroxylation at the 2 or 6 position significantly altered the cardiotoxicity of chrysene with 2-OHCHR being more active than 6-OHCHR. These data have relevance for abiotic transformation, but also biotic metabolism potentially from microbial and maternal sources. Additional metabolism studies particularly from spawning females may help quantify exposure to either metabolite in embryos.

Studies have shown that oil and PAH (e.g. phenanthrene) exposure can alter excitation-contraction coupling in cardiomyocyte cells that is important for normal heart function (Brette et al., 2014 and 2017). Altered expression of ion transporters such as *ncx1* has been previously shown to be caused by oil exposure in Atlantic haddock at 6 dpf

(Sørhus et al., 2016). In the current study, 2- or 6-OHCHR at 3dpf did not alter *ncx1* expression. Additional studies are needed to evaluate the potential alterations at later stages. The current data also does not eliminate effects on other important ion transporters such as kcnh2 and serca.

Previous studies indicated that the 2-hydroxy derivative of chrysene activated the estrogen receptor (ER) but 6-OHCHR was an antagonist using the same in vitro system (Hayakawa et al., 2008), ER signaling was evaluated as a potential target for the developmental toxicities. Consistent with the *in vitro* studies, expression of the ER regulated gene *vtg* (*vitellogenin)* was induced by 2-OHCHR, but unchanged by the 6-hydroxy metabolite. Since previous studies in our laboratory indicated that E2 caused cardiotoxicity in embryonic zebrafish (Diamante et al. 2017), we hypothesized regioselective toxicity at the developing heart would also occur. Although differences were observed between the compounds, treatment with ER and GPER antagonists concurrently with the ER active 2-OHCHR failed to rescue the morphological effects indicating ER or GPER signaling may not directly contribute to the toxicity of 2-OHCHR. Similar results were noted with E2 when embryos were co-treated with ER and GPER antagonists suggesting alternative molecular targets or complexities associated with *in vivo* endocrine effects of E2 (Diamante et al., 2017).

Regioselective toxicity was also observed in the hematopoietic and circulatory systems after exposure to 2- and 6- OHCHR. The most common defect was a significant reduction in hemoglobin levels in embryos exposed to 2-OHCHR. Similar abnormalities were also observed in embryos after treatment with phenanthrene and E2, which both

show the impaired cardiac phenotype. Similar to our study, anemia was observed after exposure to PAHs; however, little is known about the mechanisms by which this occurs (Incardona et al., 2004). Anemia has also been observed in many oiled seabirds and is thought to be due to oxidative damage (Troisi et al., 2007). Oil-treated zebrafish embryos showed effects on intersegmental blood vessel development, potentially due to disruption of neural crest signaling during embryogenesis (de Soysa et al., 2012). Interestingly, in this study we saw a trend towards an increase in levels of *vegfa* mRNA, which is an important factor in neural crest migration during vascular development (Wiszniak and Schwarz, 2014). The relevance of this pathway requires additional study to determine its contribution to the phenotype.

We also observed significant effects on the hemoglobin levels by 2-OHCHR. Runx1 is an important regulator for hematopoiesis and vasculoangiogenesis in zebrafish (Kalev-Zylinska et al., 2002), which was altered by 2-OHCHR. Runx1 is part of the runt family of transcription factors and is expressed during development in hematopoietic cells. It plays an important role in regulating the transition of endothelial cells to hematopoietic cells. A *runx1* morpholino study in zebrafish, showed defects in hematopoiesis and treated embryos lacked normal blood cell circulation (Kalev-Zylinska et al., 2002). RNAseq analysis carried out in mahi-mahi embryos exposed to oil also showed significant alterations in *runx1* (Xu et al., 2016). The specific initiation effect that alters runx1 is unknown, but the clear structural requirement suggests a unique pathway for anemia during embryonic exposure to PAHs.

Ocular effects were also observed after exposure to both hydroxylated chrysenes. 2-OHCHR had a higher incidence of eye malformations compared to 6-OHCHR. Previous studies in zebrafish showed that phenanthrene caused retinal defects (Huang et al., 2013), and recent RNAseq evaluations with mahi-mahi embryos exposed to weathered oil indicated that, in addition to alterations in genes involved in heart development, genes regulating eye development were all primarily down-regulated (Xu et al., 2016). Consistent with these results, both 2- and 6-OHCHR caused a significant decrease in *rho* expression. *rho* is a G-protein coupled receptor involved in phototransduction. Although regioselective differences were not observed, future studies should investigate the role of *rho* on PAH and oil induced ocular toxicity and the potential effects on vision-based behaviors such as feeding at various developmental stages. Altered eye morphology likely results in impaired response to visual stimulus and may diminish feeding, mating and predator avoidance (Bilotta et al., 2002; Baumann et al., 2016).

In summary, while no effect was observed in zebrafish embryos after exposure to chrysene, its two degradates/metabolites 2- and 6-OHCHR negatively affected development. Both 2- and 6-OHCHR caused cardiac, ocular and circulatory defects. The role of *rho* and *runx1* warrants further investigation in PAH and oil toxicity. These findings are consistent with observations that weathering of crude oil can result in greater developmental toxicity. The current study raises the need to further identify mechanisms that are involved in the toxicity of oxygenated PAHs to assess the potential risks of oil spills on fish populations.

Chemical	Concentration (µM)	Survival (%) ± SE	Overall deformities (%) ± SE
Ethanol	0.2%	94.19 ± 3.14	16.15 ± 3.99
2-hydroxychrysene	0.5	91.89 ± 2.24	62.84 ± 13.50 *
	3	83.89 ± 7.27	100.00 ± 0 *
	5	86.10 ± 7.23	99.43 ± 0.57 *
	10	85.99 ± 3.45	100.00 ± 0 *
6-hydroxychrysene	0.5	87.82 ± 4.72	38.60 ± 8.41
	3	77.34 ± 5.18	97.95 ± 1.19 *
	5	69.89 ± 13.09	97.74 ± 1.65 *
	10	67.01 ± 10.73 *	99.31 ± 0.69 *
Phenanthrene	0.5	98.67 ± 1.33	23.10 ± 6.32
	3	93.31 ± 1.48	42.69 ± 8.37
	5	33.28 ± 5.37 *	77.87 ± 7.34 *
Chrysene	0.5	98.15 ± 1.85	10.47 ± 1.27
	3	100 ± 0	14.09 ± 2.55
	4	96.59 ± 0.09	13.28 ± 4.84
17β-estradiol	3	99.38 ± 0.63	32.75 ± 3.97
	5	98.37 ± 1.11	47.44 ± 6.25 *

	8	97.95 ± 0.84	100.00 ± 0 *

Table 2-1. Effects of 2-hydroxychrysene, 6-hydroxychrysene, phenanthrene, chrysene and 17β–estradiol on survival and development of zebrafish embryos at 76 hpf after a 74hr exposure. Data is presented as mean ± standard error (SE) of 4 to 7 independent replicates. 2- and 6-hydroxychrysene was analyzed using Two-way ANOVA, Tukey HSD test. Phenanthrene, Chrysene and 17β–Estradiol were analyzed using a logistic regression model. Asterisks (*) represent the significant difference relative to the solvent control. Letters represents differences between the same concentrations of 2 and 6-hydroxychrysene. ($p<0.05$)

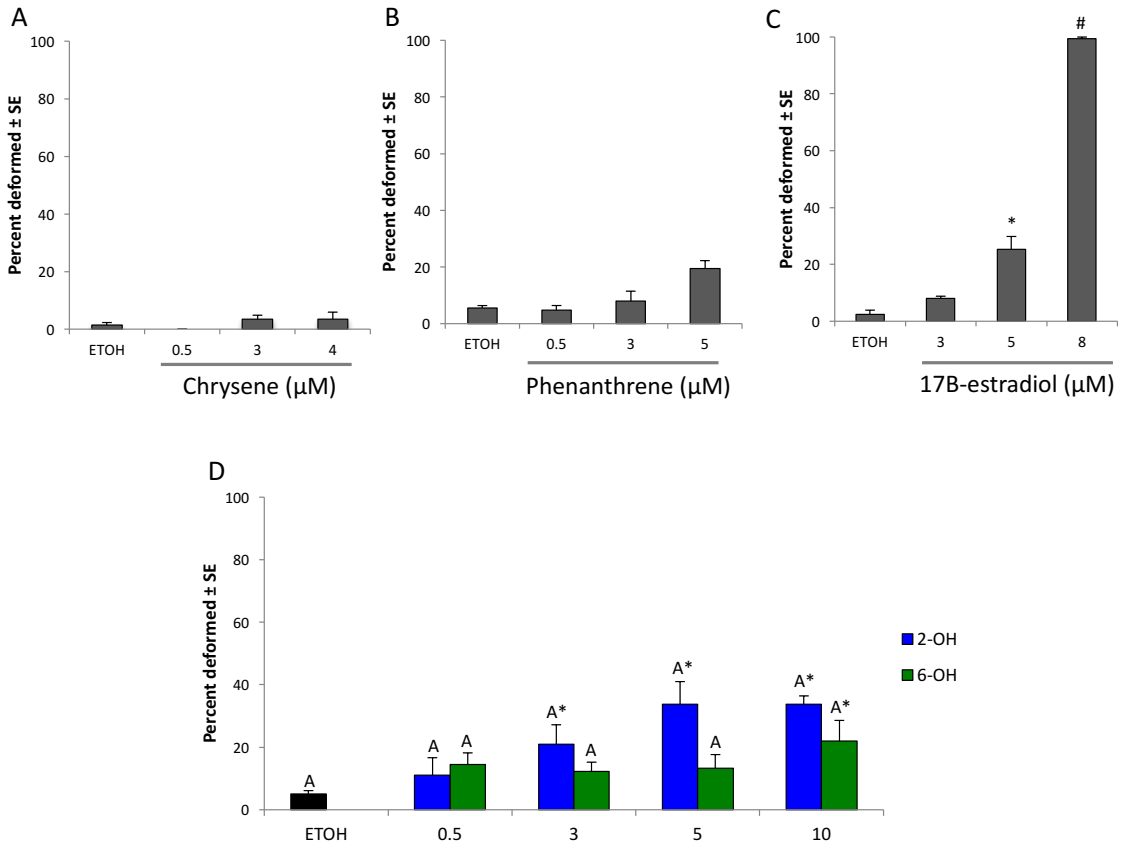

Figure 2-1. Effects of 2-hydroxychrysene, 6-hydroxychrysene, phenanthrene, chrysene and 17β–estradiol on spinal development of zebrafish embryos at 76 hpf after a 74 h exposure. (A) Chrysene, (B) Phenanthrene, (C) 17β–Estradiol and (D) 2- and 6-hydroxychrysene. A-C) Logistic regression model. D) Two -way ANOVA, Tukey HSD test. Data presented as mean ± standard error (SE) of 4 to 6 independent replicates. Asterisks represent the significant difference between the solvent control. Letters represents difference between same concentrations of 2 and 6-hydroxychrysene. ($p<0.05$)

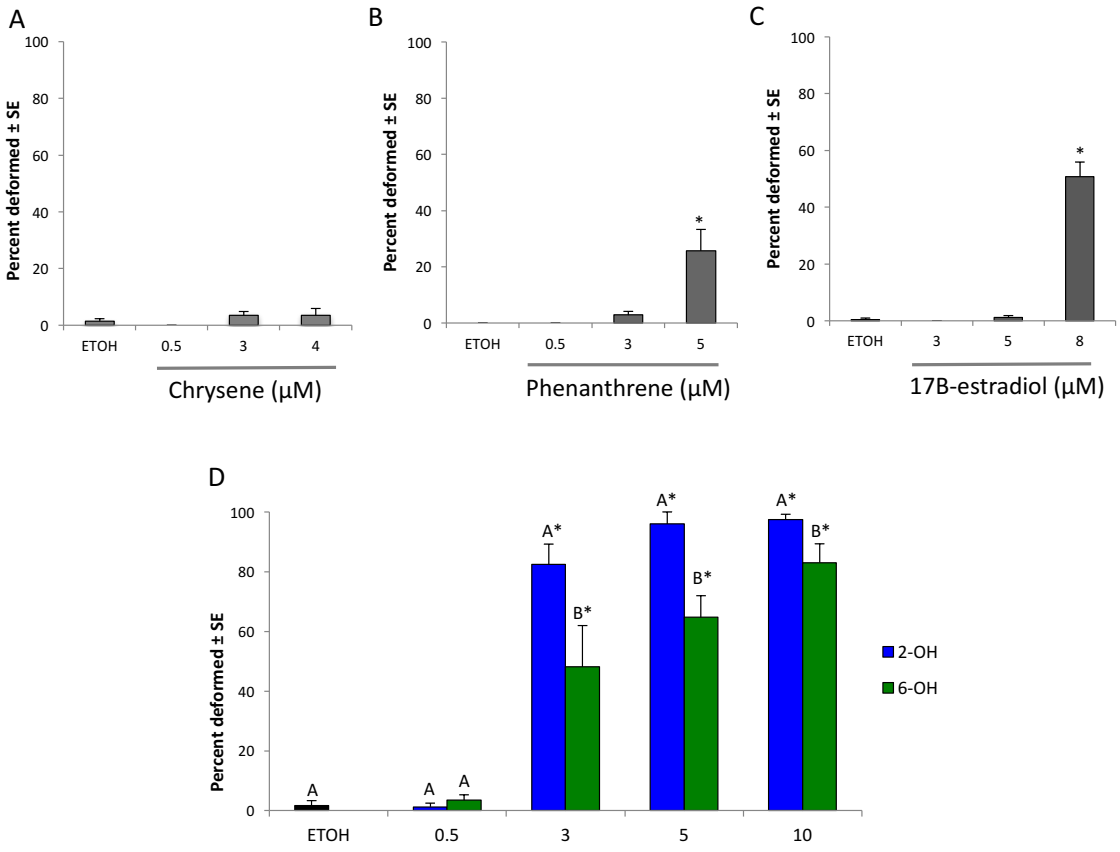

Figure 2-2. Effects of 2-hydroxychrysene, 6-hydroxychrysene, phenanthrene, chrysene and 17β–estradiol on eye development of zebrafish embryos at 76 hpf after a 74 h exposure. (A) Chrysene, (B) Phenanthrene, (C) 17β–Estradiol and (D) 2- and 6-hydroxychrysene. A-C) Logistic regression model. D) Two-way ANOVA, Tukey HSD test. Data presented as mean ± standard error (SE) of 4 to 6 independent replicates. Asterisks represent the significant difference between the solvent control. Letters represent significant difference between same concentrations of 2 and 6-hydroxychrysene. ($p<0.05$)

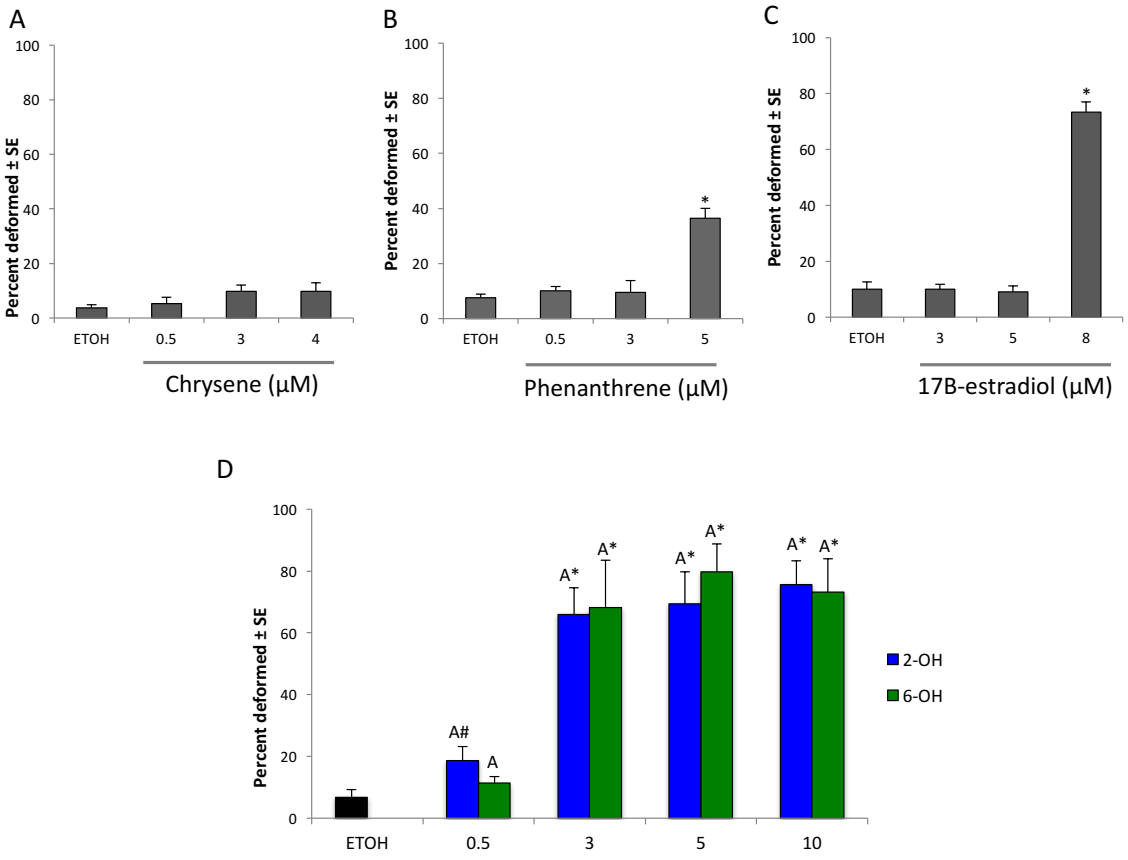

Figure 2-3. Effects of 2-hydroxychrysene, 6-hydroxychrysene, Phenanthrene, Chrysene and 17β–Estradiol on cardiac development of zebrafish embryos at 76 hpf after a 74 h exposure. (A-E) Data represents average percent cardiac deformities at 76 hpf after treatment with (A) Chrysene, (B) Phenanthrene, (C) 17β–Estradiol and (D) 2- and 6-hydroxychrysene. A-C) Logistic regression model. D) Two-way ANOVA, Tukey HSD test. Data presented as mean ± standard error (SE) of 4 to 6 independent replicates. Asterisks represent the significant difference between the solvent control. Letters represents significant difference between same concentrations of 2 and 6-hydroxychrysene. ($p<0.05$)

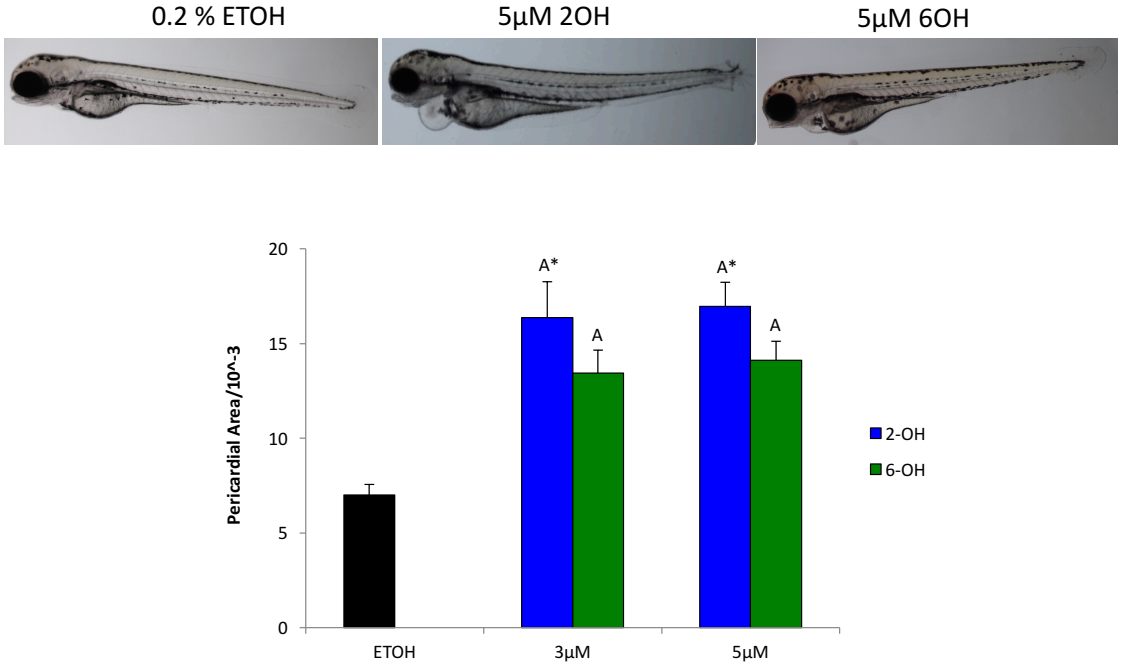

Figure 2-4. Effects of 2-hydroxychrysene and 6-hydroxychrysene on pericardial area of zebrafish embryos at 76 hpf after a 74 h exposure. Average pericardial area after treatment with 2- and 6- hydroxychrysene. Two-way ANOVA, Tukey HSD test. Data presented as mean ± standard error (SE) of 4 to 6 independent replicates. Asterisks represent the significant difference between the solvent control. Letters represents significant difference between same concentrations of 2 and 6-hydroxychrysene. ($p<0.05$)

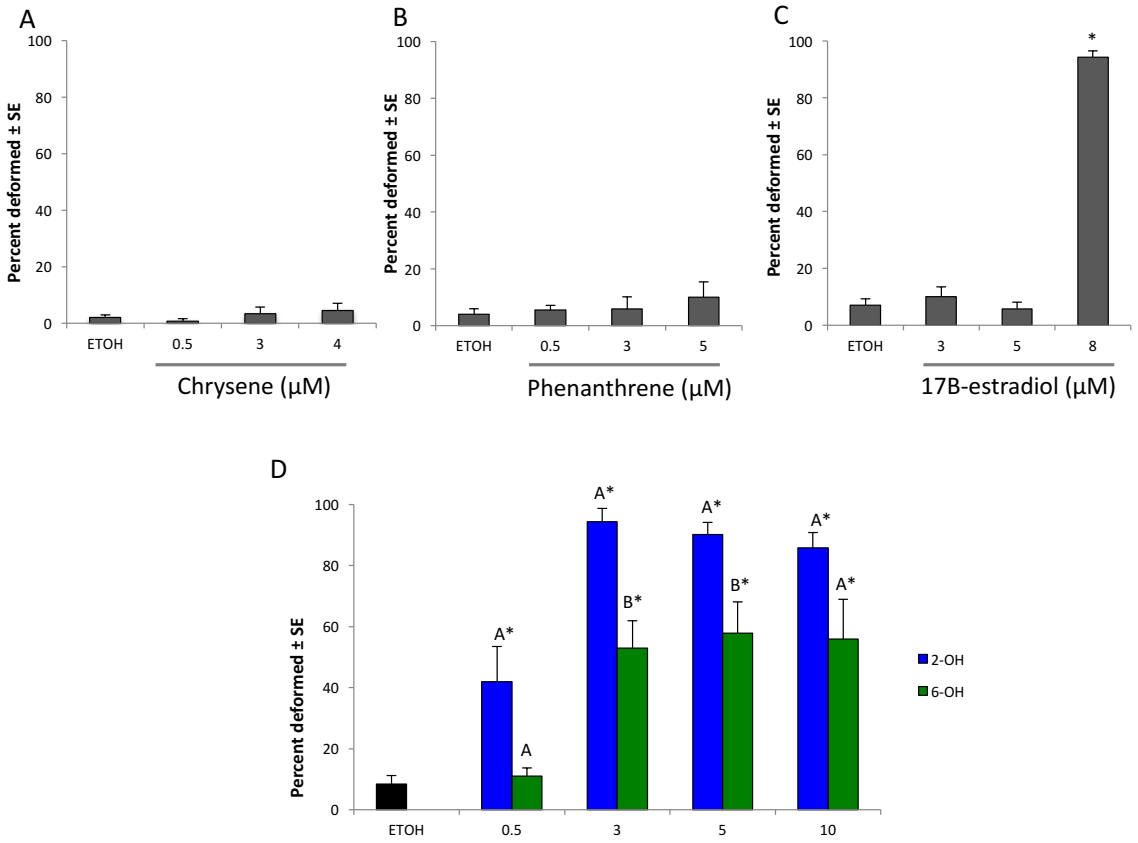

Figure 2-5. Effects of 2-hydroxychrysene, 6-hydroxychrysene, Phenanthrene, Chrysene and 17β–Estradiol on circulation of zebrafish embryos at 76 hpf after a 74 h exposure. (A-D) Data represents average percent embryos with circulatory abnormalities at 76 hpf after treatment with (A) Chrysene, (B) Phenanthrene, (C) 17β–Estradiol and (D) 2- and 6-hydroxychrysene. A-C) Logistic regression model. D) Two-way ANOVA, Tukey HSD test. Data presented as mean ± standard error (SE) of 4 to 6 independent replicates. Asterisks represent the significant difference between the solvent control. Letters represents significant difference between same concentrations of 2 and 6-hydroxychrysene. ($p<0.05$)

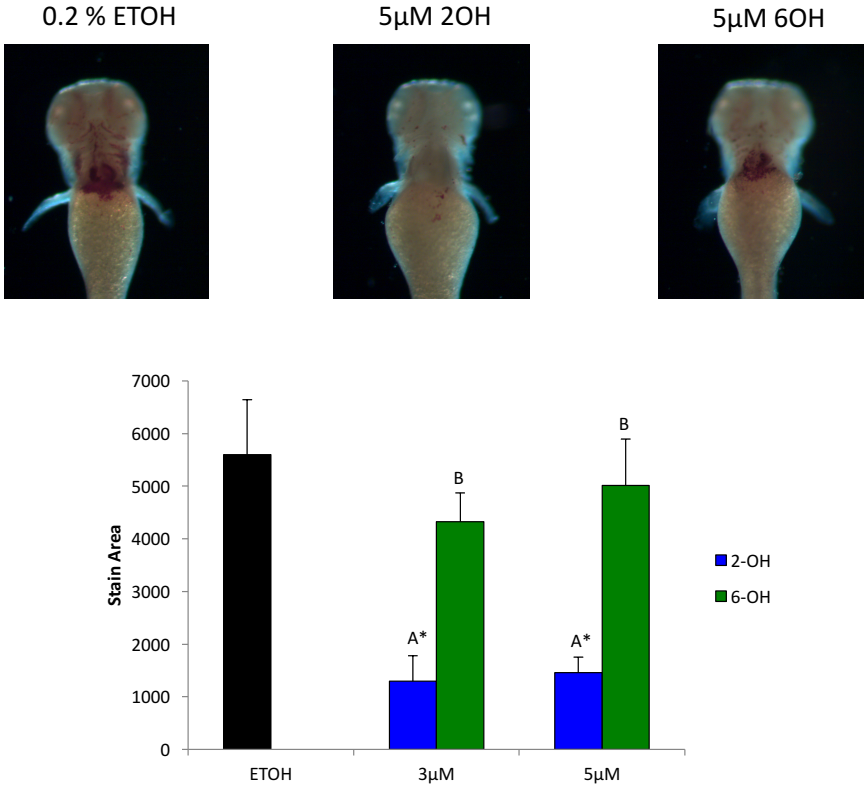

Figure 2-6. Effects of 2-hydroxychrysene and 6-hydroxychrysene on hemoglobin levels in zebrafish embryos at 76 hpf after a 74 h exposure. Average o-Dianisidine stain area in embryos exposed to 2- or 6-hydroxychrysene (3-5 µM). All embryos were oriented in dorsal recumbency for imaging. Two-way ANOVA, Tukey HSD test. Data presented as mean ± standard error (SE) of 4 to 6 independent replicates. Asterisks represent the significant difference between the solvent control. Letters represents significant difference between same concentrations of 2 and 6-hydroxychrysene. ($p<0.05$)

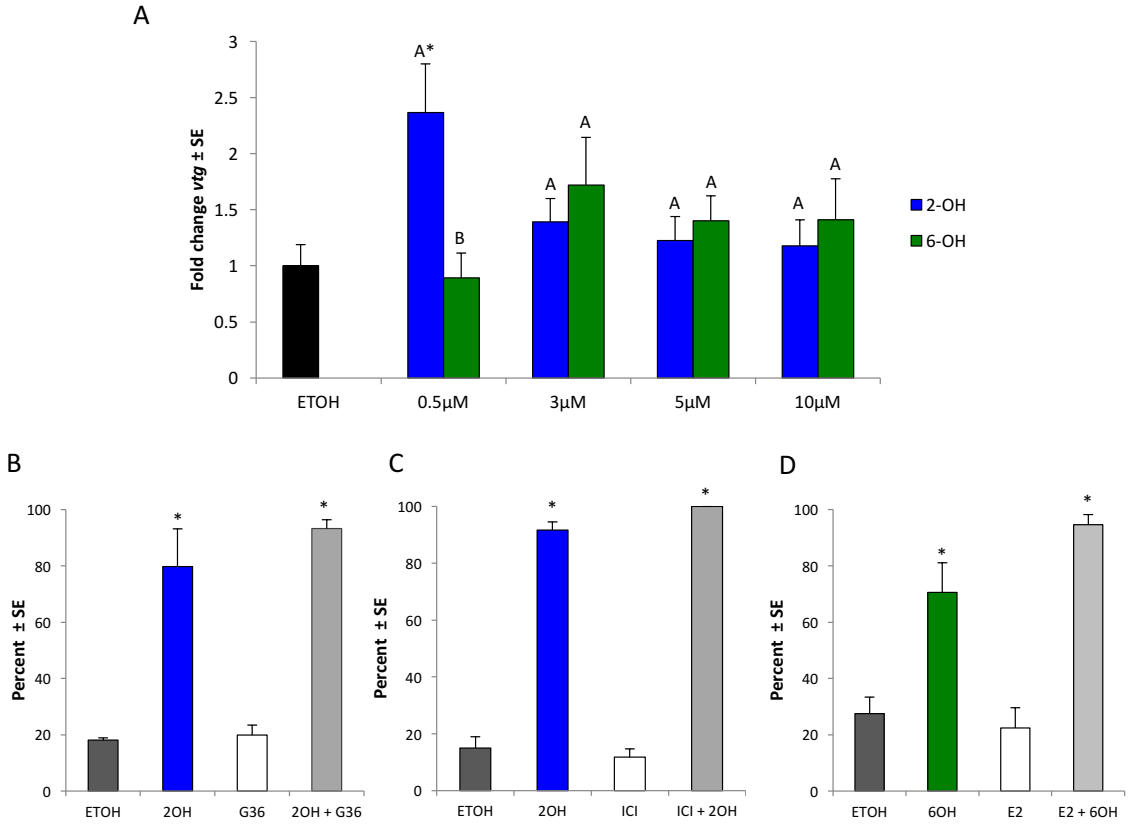

Figure 2-7. Effects of 2- and 6-hydroxychrysene on estrogen pathway signaling in zebrafish embryos at 76 hpf after a 74 hr exposure. A) Cumulative fold change of *vtg* mRNA of zebrafish embryos exposed to 0.2% ethanol (ETOH), 2-hydroxychrysene and 6-hydroxychrysene at 2hpf. B) Data represents average percent deformities at 76 hpf after treatment with 0.2% ethanol (ETOH), 3µM of 2-hydroxychrysene, 5 µM of G36 and a combination of 2-hydroxychrysene with G36 at 2hpf. C) Data represents average percent deformities at 76 hpf after treatment with 0.2% ethanol (ETOH), 3µM of 2-hydroxychrysene, 14 µM of ICI 182, 780 and a combination of 2-hydroxychrysene with ICI 182, 780 at 2hpf. D) Data represents average percent deformities at 76 hpf after treatment with 0.2% ethanol (ETOH), 3µM of 6-hydroxychrysene, 3µM of E2 and a combination of 6-hydroxychrysene with E2 at 2hpf. A-D) Two-way ANOVA, Tukey HSD test. Data presented as mean ± standard error (SE) of 4 to 6 independent replicates. A) Asterisks represent the significant difference between the solvent control. Letters represents difference between same concentrations of 2 and 6-hydroxychrysene. B-D) Symbols represent the significant difference. ($p<0.05$)

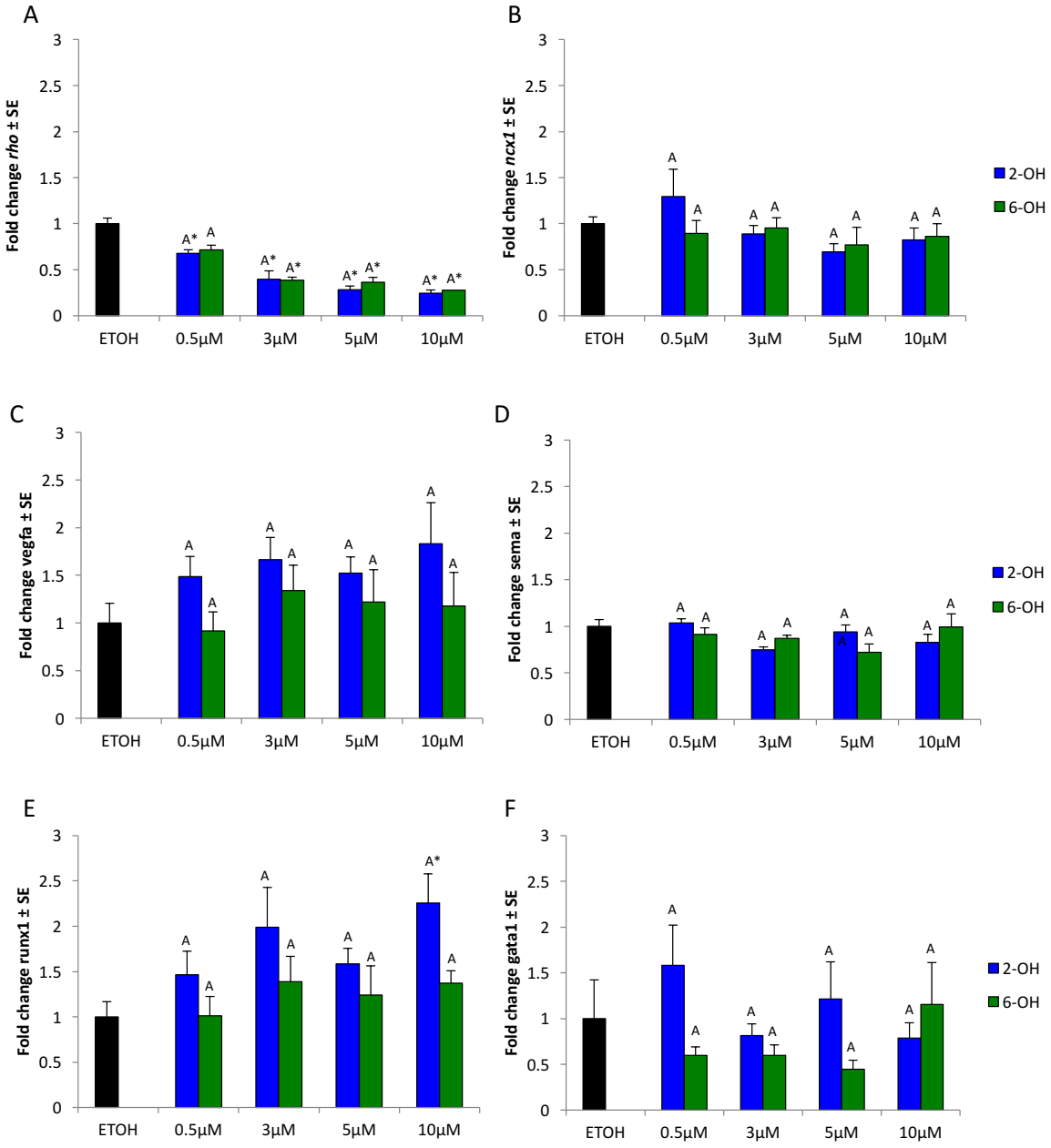

Figure 2-8. Effects of 2- and 6-hydroxychrysene on *rho, nxc1, vegfa, sema, runx1 and gata1* expression in zebrafish embryos at 76 hpf after a 74 h exposure. Cumulative fold change in zebrafish embryos exposed to 0.2% ethanol (ETOH), 2-hydroxychrysene and 6-hydroxychrysene for 74hrs. (A) *rho,* (B) *nxc1,* (C) *vegfa,* (D) *sema,* (E) *runx1 and* (F) *gata1*. Data is presented as mean ± standard error (SE) of 4 to 6 independent replicates. A-F) Two-way ANOVA, Tukey HSD test. Letters represents difference between same concentrations of 2 and 6-hydroxychrysene. Asterisks represent the significant difference. ($p<0.05$)

References

Allgood, O.E. Jr., Hamad, A., Fox, J., Defrank, A., Gilley, R., Dawson, F., Sykes, B., Underwood, T.J., Naylor, R.C., Briggs, A.A., Lassiter, C.S., Bell, W.E., Turner, J.E., (2013) Estrogen prevents cardiac and vascular failure in the 'listless' zebrafish (Danio rerio) developmental model. Gen Comp Endocrinol. 189:33-42.

Alloy, M., Baxter, D., Stieglitz, J., Mager E., Hoenig, R., Benetti, D., Grosell, M., Oris, J., Roberts, A., (2016) Ultraviolet radiation enhances the toxicity of Deepwater Horizon Oil to Mahi-mahi (Coryphaena hippurus) embryos. Env. Sci. Tech, 50:2011-2017.

Baumann, L., Ros, A., Rehberger, K., Neuhauss, S.C., Segner, H., (2016) Thyroid disruption in zebrafish (Danio rerio) larvae: Different molecular response patterns lead to impaired eye development and visual functions. Aquat Toxicol. 172:44-55.

Bilotta, J., Saszik, S., Givin, C.M., Hardesty, H.R., Sutherland, S.E., (2002) Effects of embryonic exposure to ethanol on zebrafish visual function. Neurotoxicol Teratol. 24(6):759-66.

Brette, F., Machado, B., Cros, C., Incardona, J.P., Scholz, N.L., Block, B.A., (2014) Crude oil impairs cardiac excitation-contraction coupling in fish. Science. 343(6172):772-6.

Brette, F., Shiels, H.A., Galli, G.L., Cros, C., Incardona, J.P., Scholz, N.L., Block, B.A., (2017) A Novel Cardiotoxic Mechanism for a Pervasive Global Pollutant. Sci Rep. 7:41476.

Butler, J.D., Parkerton, T.F., Letinski, D.J., Bragin, G.E., Lampi, M.A., Cooper, K.R., (2013) A novel passive dosing system for determining the toxicity of phenanthrene to early life stages of zebrafish. Sci Total Environ. 463-464:952-8.

Diamante, G., Menjivar-Cervantes, N., Leung, M.S., Volz, D.C., Schlenk, D. (2017) Contribution of G protein-coupled estrogen receptor 1 (GPER) to 17β-estradiol-induced developmental toxicity in zebrafish. Aquat Toxicol. 186:180-187.

de Soysa, T.Y., Ulrich, A., Friedrich, T., Pite, D., Compton, S.L., Ok, D., Bernardos, R.L., Downes, G.B., Hsieh, S., Stein, R., Lagdameo, M.C., Halvorsen, K., Kesich, L.R., Barresi, M.J., (2012) Macondo crude oil from the Deepwater Horizon oil spill disrupts specific developmental processes during zebrafish embryogenesis. BMC Biol. 10:40.

Esbaugh, A.J., Mager, E.M., Stieglitz, J.D., Hoenig, R., Brown, T.L., French, B.L., Linbo, T.L., Lay, C., Forth, H., Scholz, N.L., Incardona, J.P., Morris, J.M., Benetti, D.D., Grosell, M., (2016) The effects of weathering and chemical dispersion on Deepwater

Horizon crude oil toxicity to mahi-mahi (Coryphaena hippurus) early life stages. Sci Total Environ. 543(Pt A):644-51.

Goodale, B.C., Tilton, S.C., Corvi, M.M., Wilson, G.R., Janszen, D.B., Anderson, K.A., Waters, K.M., Tanguay, R.L., (2013) Structurally distinct polycyclic aromatic hydrocarbons induce differential transcriptional responses in developing zebrafish. Toxicol Appl Pharmacol. 272(3):656-70.

Gündel, U., Kalkhof, S., Zitzkat, D., von Bergen, M., Altenburger, R., Küster, E., (2012) Concentration-response concept in ecotoxicoproteomics: effects of different phenanthrene concentrations to the zebrafish (Danio rerio) embryo proteome. Ecotoxicol Environ Saf. 76(2):11-22.

Hall, J.M., Couse, J.F., Korach, K.S., (2001) The multifaceted mechanisms of estradiol and estrogen receptor signaling. J Biol Chem. 276(40):36869-72.

Hayakawa, K., Onoda, Y., Tachikawa, C., Hosoi, S., Yoshita, M., Chung, S.W., Kizu, R., Toriba, A., Kameda, T., Tang, N., 2007. Estrogenic/antiestrogenic activities of polycyclic aromatic hydrocarbons and their monohydroxylated derivatives by yeast two-hybrid assay. J. Health Sci., 53, 562–570

Heintz, R.A., Short, J.W., Rice, S.D., (1999) Sensitivity of fish embryos to weathered crude oil: Part II. Increased mortality of pink salmon (Oncorhynchus gorbuscha) embryos incubating downstream from weathered Exxon Valdez crude oil. Environ Toxicol Chem 18:494–503.

Huang, L., Wang, C., Zhang, Y., Wu, M., Zuo, Z., (2013) Phenanthrene causes ocular developmental toxicity in zebrafish embryos and the possible mechanisms involved. J Hazard Mater. 261:172-80.

Incardona, J.P., Collier, T.K., Scholz, N.L., 2004. Defects in cardiac function precede morphological abnormalities in fish embryos exposed to polycyclic aromatic hydrocarbons. Toxicol Appl Pharmacol. 196, 191-205.

Incardona, J.P., Day, H.L., Collier, T.K., Scholz, N.L., (2006) Developmental toxicity of 4-ring polycyclic aromatic hydrocarbons in zebrafish is differentially dependent on AH receptor isoforms and hepatic cytochrome P4501A metabolism. Toxicol Appl Pharmacol. 217(3):308-21.

Incardona, J.P., Gardner, L.D., Linbo, T.L., Brown, T.L., Esbaugh, A.J., Mager, E.M., Stieglitz, J.D., French, B.L., Labenia, J.S., Laetz, C.A., Tagal, M., Sloan, C.A., Elizur, A., Benetti, D.D., Grosell, M., Block, B.A., Scholz, N.L., 2014. Deepwater Horizon crude oil impacts the developing hearts of large predatory pelagic fish. Proc Natl Acad Sci U S A. 111(15), E1510-8.

Incardona, J.P., Linbo, T.L., Scholz, N.L., (2011) Cardiac toxicity of 5-ring polycyclic aromatic hydrocarbons is differentially dependent on the aryl hydrocarbon receptor 2 isoform during zebrafish development. Toxicol Appl Pharmacol. 257(2):242-9.

Incardona, J.P., Swarts, T.L., Edmunds, R.C., Linbo, T.L., Aquilina-Beck, A., Sloan, C.A., Gardner, L.D., Block, B.A., Scholz, N.L., (2013) Exxon Valdez to Deepwater Horizon: comparable toxicity of both crude oils to fish early life stages. Aquat Toxicol. 142-143, 303-16.

Jayasundara, N., Van Tiem Garner, L., Meyer, J.N., Erwin, K.N., Di Giulio, R.T., (2015) AHR2-Mediated transcriptomic responses underlying the synergistic cardiac developmental toxicity of PAHs. Toxicol Sci. 143(2):469-81.

Kalev-Zylinska, M.L., Horsfield, J.A., Flores, M.V., Postlethwait, J.H., Vitas, M.R., Baas, A.M., Crosier, P.S., Crosier, K.E., (2002) Runx1 is required for zebrafish blood and vessel development and expression of a human RUNX1-CBF2T1 transgene advances a model for studies of leukemogenesis. Development. 129(8):2015-30.

Kimmel, C.B., Ballard, W.W., Kimmel, S.R., Ullmann, B., Schilling, T.F., 1995. Stages of embryonic development of the zebrafish. Dev Dyn. 203, 253-310.

Knecht, A.L., Goodale, B.C., Truong, L., Simonich, M.T., Swanson, A.J., Matzke, M.M., Anderson, K.A., Waters, K.M., Tanguay, R.L., (2013) Comparative developmental toxicity of environmentally relevant oxygenated PAHs. Toxicol Appl Pharmacol. 271(2):266-75.

Lampi, M. A., Gurska, J., McDonald, K. I. C., Xie, F., Huang, X.-D., Dixon, D. G., Greenberg, B. M., (2006) Photoinduced toxicity of polycyclic aromatic hydrocarbons to Daphnia magna: Ultraviolet-mediated effects and the toxicity of polycyclic aromatic hydrocarbon photoproducts. Environmental Toxicology and Chemistry. 25: 1079–1087.

Leet, J.K., Lindberg, C.D., Bassett, L.A., Isales, G.M., Yozzo, K.L., Raftery, T.D., Volz, D.C., (2014) High-content screening in zebrafish embryos identifies butafenacil as a potent inducer of anemia. PLoS One. 9(8):e104190.

Le Bihanic, F., Clérandeau, C., Le Menach, K., Morin, B., Budzinski, H., Cousin, X., Cachot, J. (2014) Developmental toxicity of PAH mixtures in fish early life stages. Part II: adverse effects in Japanese medaka. Environ Sci Pollut Res Int. 21(24):13732-43.

Paffett-Lugassy, N.N., Zon, L.I., (2005) Analysis of hematopoietic development in the zebrafish. Methods Mol Med. 105:171-98.

Saeed, T., Ali, L.N., Al-Bloushi, A., Al-Hashash, H., Al-Bahloul, M., Al-Khabbaz, A., Al-Khayat, A., (2011) Effect of environmental factors on photodegradation of polycyclic aromatic hydrocarbons (PAHs) in the water-soluble fraction of Kuwait crude oil in seawater. Mar Environ Res. 72(3):143-50.

Scott, J.A., Incardona, J.P., Pelkki, K., Shepardson, S., Hodson, P.V., (2011) AhR2-mediated, CYP1A-independent cardiovascular toxicity in zebrafish (Danio rerio) embryos exposed to retene. Aquat Toxicol. 101(1):165-74.

Sørhus, E., Incardona, J.P., Karlsen, Ø., Linbo, T., Sørensen, L., Nordtug, T., van der Meeren, T., Thorsen, A., Thorbjørnsen, M., Jentoft, S., Edvardsen, R.B., Meier, S., (2016) Crude oil exposures reveal roles for intracellular calcium cycling in haddock craniofacial and cardiac development. Sci Rep. 6:31058.

Stieglitz, J.D., Mager, E.M., Hoenig, R.H., Benetti, D.D., & Grosell, M., (2016) A novel system for embryo-larval toxicity testing of pelagic fish: Applications for impact assessment of Deepwater Horizon crude oil. Chemosphere. 162:261-268.

Sweet, L.E., Magnuson, J., Garner, T.R., Alloy, M.M., Stieglitz, J.D., Benetti, D., Grosell, M., Roberts, A.P., (2016) Exposure to ultraviolet radiation late in development increases the toxicity of oil to mahi-mahi (Coryphaena hippurus) embryos. Environ Toxicol Chem. 2016 Nov 16. doi: 10.1002/etc.3687.

Tansel, B., Fuentes, C., Sanchez, M., Predoi, K., Acevedo, M., (2011) Persistence profile of polyaromatic hydrocarbons in shallow and deep Gulf waters and sediments: effect of water temperature and sediment-water partitioning characteristics. Mar Pollut Bull. 62(12):2659-65.

Tran, D.Q., Ide, C.F., McLachlan, J.A., Arnold, S.F., (1996) The anti-estrogenic activity of selected polynuclear aro-matic hydrocarbons in yeast expressing human estrogen estrogenreceptor. Biochem. Biophys. Res. Commun. 229, 102– 108.

Troisi, G., Borjesson, L., Bexton, S., Robinson, I. (2007) Biomarkers of polycyclic aromatic hydrocarbon (PAH)-associated hemolytic anemia in oiled wildlife. Environ Res. 105(3):324-9.

van Lipzig, M.M., Commandeur, J.N., de Kanter, F.J., Damsten, M.C., Vermeulen, N.P., Maat, E., Groot, E.J., Brouwer, A., Kester, M.H., Visser, T.J., Meerman, J.H., (2005) Bioactivation of dibrominated biphenyls by cytochrome P450 activity to metabolites with estrogenic activity and estrogen sulfotransferase inhibition capacity. Chem Res Toxicol. 18(11):1691-700.

van Lipzig, M.M., Vermeulen, N.P., Gusinu, R., Legler, J., Frank, H., Seidel, A., Meerman, J.H., (2005) Formation of estrogenic metabolites of benzo[a]pyrene and

chrysene by cytochrome P450 activity and their combined and supra-maximal estrogenic activity. Environ Toxicol Pharmacol. 19(1):41-55.

Wiszniak, S.E., Schwarz, Q.P., (2014) Neural crest cells in vascular development, Neural Crest Cells: Evolution, Development and Disease. Academic press. pp. 314-330

Xu, E.G., Mager, E.M., Grosell, M., Pasparakis, C., Schlenker, L.S., Stieglitz, J.D., Benetti, D., Hazard, E.S., Courtney, S.M., Diamante, G., Freitas, J., Hardiman, G., Schlenk, D., (2016) Time- and Oil-Dependent Transcriptomic and Physiological Responses to Deepwater Horizon Oil in Mahi-Mahi (Coryphaena hippurus) Embryos and Larvae. Environ Sci Technol. 50(14):7842-51.

Chapter 3

Regulation of microRNAs in mahi-mahi (*Coryphaena hippurus*) exposed to Deepwater Horizon oil

Co-authors: Xu G, Chan S, Mager E, Grosell M, Schlenk D

This research was made possible by a grant from The Gulf of Mexico Research Initiative.

Abstract

Deepwater Horizon (*DWH*) oil causes developmental cardiotoxicity in a number of fish species, but the molecular mechanisms are still not well understood. MicroRNAs (miRNA) play key roles in a number of diverse biological processes including heart development. In our study, we evaluated the effects of *DHW* oil on miRNA expression in mahi-mahi (*Coryphaena hippurus*) embryos exposed to weathered slick oil and non-weathered source oil. miRNAs were sequenced and annotated either using the *Fugu rubripes* genome (term as Fugu-guided approach) or aligned and annotated to known mature animal miRNAs (miRBase) using the Basic Local Alignment Search Tool (BLAST) method (termed as the phylogenetic-guided approach). Using the phylogenetic-guided approach, more differentially expressed (DE) miRNAs were identified in all treatment groups at all stages. Exposure of embryos to slick oil resulted in more DE miRNAs than source oil at all developmental stages 24 hpf, 48 hpf, and 96 hpf. There was also an increase in the number of DE miRNA as development progressed, with 96 hpf having the highest number of DE miRNAs. miR-21b, miR-7641 and miR-92b, were the a few common DE miRNAs at all stages. The expression of miRNAs and their target mRNA was further compared using advanced bioinformatics with subsequent target organ predictions based on their interactions. Gene ontology (GO) analysis on the target mRNAs was consistent with pathway analysis of miRNAs, predicting disruption of cardiovascular system development after oil exposure and showed that specific miRNA–mRNA interactions may contribute to these effects. Slick oil caused an overexpression of

miR-133a, which correlated to the decrease in the expression of genes related to the cardiovascular system such as KCNH2. This work is the first study linking miRNAs and mRNAs in fish responsive to *DWH* oil exposure, providing a new opportunity for better understanding of the molecular mechanism(s) of oil toxicity.

Introduction

In 2010, the largest oil disaster in US history occurred with the explosion of the MC252 well of the *Deepwater Horizon* oil rig, releasing millions of barrels of oil into the Gulf of Mexico. In marine environments, oil spills are one of the primary sources of polycyclic aromatic hydrocarbons (PAHs), which are teratogenic, carcinogenic and mutagenic to many different organisms, especially fish (Pashin et al., 1979; Carls et al., 1999; Heintz et al., 1999; Incardona et al 2004; 2011; 2013). The timing and location of the *Deepwater Horizon* oil spill overlapped with the spawning season of economically and ecologically relevant fish species including *Coryphaena hippurus* (mahi), which spawn during the spring and summer months (Gibbs et al., 1959). Oil derived PAHs from the *Deepwater Horizon* spill have been shown to negatively affect development of mahi as well as other pelagic fish like the bluefin tuna (*Thunnus maccoyii*), yellowfin tuna (*Thunnus albacares*) and yellowtail amberjack (*Seriola lalandi*) (Incardona et al., 2014; Mager et al., 2014; Esbaugh et al., 2016).

In fish, the developing heart is known to be a primary target for PAHs derived from oil. Cardiac effects include pericardial edema and bradycardia following embryonic exposure to *DWH* oil (Incardona et al., 2014; Esbaugh et al., 2016; Stieglitz et al., 2016). In mahi, impaired looping and atrial contractility were observed along with altered expression of genes such as *atrial myosin heavy chain* (*amhc*) and *ventricular myosin heavy chain* (*vmhc*) after oil exposure (Edmunds et al., 2015). Oil exposure can also affect Ca^{2+} and K^{+} currents in isolated fish cardiomyocytes which may lead to

developmental effects in the heart (Brette et al., 2014). Collectively, the effects induced by PAHs during development can translate into adverse effects on later life stages, potentially altering overall fitness of an organism.

PAH induced developmental toxicity can be mediated through the activation of the aryl hydrocarbon receptor (AhR) (Incardona et al., 2005; Jayasundara et al., 2015). PAHs with high receptor affinity can bind and activate AhR resulting in the transcription of genes involved in metabolism, such as cytochrome P4501A, as well as a host of other pathways regulating development. However, PAHs that are poor AhR ligands can also cause developmental toxicity in fish (Incardona et al., 2005; Goodale et al., 2013). Similarly, transcriptomic studies in fish have also indicated a number of non-AhR-pathways involved in oil toxicity; however, it is unclear how many of the transcripts are regulated (Xu et al., 2016; Sørhus et al., 2016).

Gene expression can be regulated through the binding of transcription factors to promoter regions of specific genes. However, expression of mRNA can also be post-transcriptionally controlled with microRNAs (miRNA), which are small non-coding RNAs (Bartel, 2004). Transcriptional regulation by miRNAs is complex for two related reasons: first, one miRNA can target many mRNAs, and second, a single mRNA can be targeted by multiple miRNAs. miRNA play a key role during embryogenesis and in regulating other biological processes such as cell differentiation, apoptosis, and metabolism. In addition, recent studies have also shown that oil can regulate miRNA expression through methylation of miRNA promoters (Huang et al., 2016; Bianchi et al., 2017).

Based on the differential expression of genes observed after oil treatment, we sought to investigate the role of miRNA in the transcriptomic changes induced by oil in embryonic and larval fish. In this study, miRNA sequencing was performed in early life stage mahi exposed to two different types of *Deepwater Horizon* oil; source and slick (weathered). miRNA and mRNA profiles were evaluated at different developmental time points including the pharyngula embryonic stage (24 hpf), the yolk-sac larva stage (48 hpf), and the free-swimming larva stage (96 hpf) after exposure. Novel and known miRNAs were identified using single species and phylogeny based miRNA reference-genome-guided annotation approaches and compared with mRNAs with two bioinformatics tools. Several genes known to be important in the functional impacts of oil, were shown to be regulated by specific miRNA indicating a significant role in PAH induced developmental toxicity in mahi.

Materials and Methods

Oil Preparation

Preparation of high-energy water accommodated fraction (HEWAF) of each oil type was obtained from adding 1g of oil into 1L of 35ppt filtered and UV sterilized seawater. Oil and water were blended for 30s with the resulting solution subsequently placed into a glass separatory funnel and allowed to settle for 1 hour. The lower layer (~100ml) was then drained from the funnel and discarded. The remaining solution (~800ml top layer) was collected and used for exposures and was considered the 100%

HEWAF stock solution. The stock solution was then diluted to the desired concentration for treatment using 35ppt seawater. The two oil types used for the study were source and weathered oil from the *Deepwater Horizon* spill. Source oil was collected right over the well from the subsea containment system (sample ID: SO-20100815-Mass-001 A0075K). Weathered oil referred to as slick oil was collected from a surface skimming operation (sample ID: OFS-20100719-Juniper-001 A0091G).

Embryo collection and treatment

Embryos used for the study were collected from mahi broodstock. The adult mahi were captured using a hook and line angling technique from the coast of Miami, FL. The broodstock are then acclimated and kept at the University of Miami Experimental Hatchery (UMEH) of the Rosenstiel School of Marine and Atmospheric Science, in a recirculating aquaculture system. Embryos were collected and prepared using the standard UMEH method (Stieglitz et al., 2012). Embryos were treated for 1 hour with a 37ppm formaldehyde solution and rinsed with filtered and UV-sterilized seawater. Stage and quality of the embryos were assessed microscopically (Xu et al., 2016). After collection and assessment, each treatment had 30-24 embryos which were exposed to diluted HEWAF of slick and source oil (3 replicates per treatment). The embryos were exposed to each oil at the same time (~6 hpf) concurrently. Pooled embryo and larvae (n=3) were removed from oil at each of the following time points: 24, 48 and 96 hpf. The 3 stages were chosen because they mark important stages during development. At 24 hpf, the embryo forms a heart tube, which starts to beat. By 48 hpf, the ventricle and atrium is

discernable and the yolk sac diminishes in size. At the last stage (96 hpf), the larvae have undergone morphogenesis and are free swimming (Xu et al., 2017). During the treatment, health of the embryos and larvae were monitored and dead animals were removed. Water quality was also monitored throughout the experiment and PAH concentrations were measured (Xu et al., 2016 (Supplemental data)). Pooled embryos and larvae were placed in RNAlater at -80℃ until RNA extraction.

miRNA isolation, library construction and sequencing

miRNAs of pooled samples were isolated using the miRNeasy mini kit and RNeasy Mini Elute Cleanup Kit from Qiagen (Valenica, CA). The quality and concentration of miRNA was determined using the Agilent 2100 small RNA chip (Santa Clara, CA). miRNA libraries were made using the New England Biolabs NEBNext Multiplex Small RNA Sample Prep kit (Ipswich, MA) following the manufacturer's protocol. The PCR amplified cDNA libraries were then purified using the Qiagen QIAQuick PCR Purification Kit (Valencia, CA) according to the manufacturer's manual. The purified libraries were size-selected using Beckman Coulter SPRIselect beads (Indianapolis, IN). The size distribution and concentration of the libraries were determined using the Agilent High Sensitivity DNA Assay Chip (Santa Clara, CA). Single Read 1 x 75 sequencing was performed on an Illumina NextSEQ v2 at the Institute of Integrative Genome Biology, of the University of California, Riverside. The read data were deposited in the NCBI database (GSE102966).

Sequencing data process

Phylogenetic miRNA-annotation method

The quality of the raw sequences was evaluated by FastQC toolkit (Cambridge, UK). Adaptor sequences were trimmed off using the FASTX toolkit (Cambridge, UK), to obtain a mean Phred score ≥30. Only reads that are longer than 18 bp and shorter than 30 bp were kept for downstream alignment against known mature miRNA sequences (Figure 3-1). All mature miRNA sequences from miRbase (release 21) (Griffiths-Jones et al., 2006) were used and clustered into unique miRNA sequences. The filtered sequencing data were Fugu-guided approach against unique miRNA sequences by using Basic Local Alignment Search Tool- BLAST (Bethesda, MD) (Altschul et al., 1990). Only sequencing read that 1) had no gap in the alignment with known mature miRNA; 2) matched exactly with known miRNA's nucleotide 2–17; and 3) was at maximum 3 bp longer than known miRNA was considered as a candidate miRNA. A customized perl script was then designed to count the sequencing reads Fugu-guided approach to each unique miRNA. Differential expression analysis was conducted using DESeq2 (Love et al., 2014). miRNAs were considered differentially expressed when false discovery rate (FDR) < 0.01 (Benjamini−Hochberg correction). Identified differentially expressed miRNAs and mRNA-seq data from Xu et al. (2016) were analyzed using the microRNA Target Filter in Ingenuity Pathway Analysis (IPA) software from Qiagen (Valencia, CA) to identify experimentally demonstrated miRNA-mRNA relationships and predict the impact of expression changes of miRNA and its target mRNA on biological processes

and pathways. By matching miRNA and mRNA expression data, a miRNA was considered to be regulatory only if expression levels of miRNA and its mRNA targets are reversely correlated. As previous studies showed that slick oil increased pericardial area, altered the gene expression in cardiovascular and nervous system (Xu et al. 2016), we further filtered the DE miRNA/mRNA data and focused on cardiovascular/ocular functions and diseases in IPA. The target mRNAs identified by IPA were then used for gene ontology (GO) analysis by DAVID (Bethesda, MD) (Huang et al., 2009; 2009) (Figure 3-1).

Fugu-genome-miRNA annotation

The methods of quality assessment and filtration on the raw reads were the same as described above. The processed reads were Fugu-guided approach against the fugu (*Fugu rubripes*) genome, and both known and novel miRNAs were identified using miRDeep2, a probabilistic algorithm based on the miRNA biogenesis model and designed to detect miRNAs from deep sequencing reads (Friedländer et al., 2012; An et al., 2013). Read counts generated from miRDeep2 were used for differential expression analysis using DESeq2. The same downstream analysis using IPA and DAVID was conducted as described above (Figure 3-1). All analysis was carried out on a local server running under the Institute for Integrative Genome Biology (IIGB)'s Linux cluster, Biocluster, environment (http://manuals.bioinformatics.ucr.edu/home/hpc).

Quantitative Reverse Transcription Real-Time PCR (qPCR)

Differentially expressed miRNAs identified in the miRNAseq analysis were validated by qPCR. miRNA primers were designed using the Qiagen custom miRNA primer assay (Valencia, CA). Melt curve analysis and 1% agarose gel electrophoresis were performed to assess the specificity of the qPCR products. cDNA was generated using the Qiagen miScript II RT Kit following manufacturers' protocol (Valencia, CA). Expression was then analyzed using Qiagen miScript SYBR Green PCR Kit following manufacturer's instructions using RNU6 as the normalizing gene (Valencia, CA) and ran on the CFX Connect™ Real-Time PCR Detection System (Hercules, CA).

Results

To assess the role of miRNAs in oil toxicity during development (24, 48 and 96 hpf), mahi embryos were treated with slick and source oil. The number of DE miRNA increased with time, and slick oil induced more DE miRNAs than source oil by both methods. Using the phylogenetic miRNA-annotation method, the numbers of DE miRNAs were 46, 101 and 178 at 24 hpf, 48 hpf and 96 hpf, after source oil exposure, respectively (Table 3-1). At 24 hpf, the majority of DE miRNAs were down-regulated (37 down-regulated and 9 up-regulated), while at 48hpf, there were 48 down-regulated and 53 up-regulated miRNAs. By 96hpf, there were more up-regulated (137) than down-regulated (41) miRNAs (Table 3-1 and Figure 3-2). Exposure to slick oil at 24 hpf, altered expression of 139 miRNA (104 were down-regulated and 35 were up-regulated).

At the 48hpf there were 213 DE miRNAs; of these 138 were down-regulated and 75 were up-regulated. At 96hpf, of the 213 DE miRNAs, there were more over-expressed (143) than under-expressed (70) miRNAs (Table 3-1 and Figure 3-2). The Fugu-guided annotation method identified less DE miRNAs than the phylogenetic method. At 24 hpf, there were 25 DE miRNAs after source oil exposure (18 up-regulated and 7 down-regulated). At the 48hpf, there were 20 down-regulated and 4 up-regulated miRNAs. At 96hpf, there were 78 down-regulated and 87 up-regulated (Table 3-1 and Figure 3-2). Similar to phylogenetic method, more DE miRNAs were identified after slick oil exposure than source oil exposure. There was a total of 42 DE miRNA at the 24hpf after slick oil exposure (38 up-regulated and 4 down-regulated). At 48hpf there were 82 DE miRNA, with 40 down-regulated and 42 up-regulated. At 96hpf, there were 254 DE miRNAs, 126 were down-regulated and 128 were up-regulated (Table 3-1 and Figure 3-2). The expression of a subset of miRNAs were confirmed by qRT-PCR at 96 hpf of mahi-mahi exposed to slick oil (Figure 3-10).

There were about 25-35% identified DE miRNA that were common between the two annotation methods. At 24hpf, there were 6 common DE miRNAs after exposure to source and 14 common DE miRNAs in the slick oil data. At 48hpf, the source oil data showed 7 common DE miRNAs and the slick oil data showed 27 common miRNAs. At the 96hpf there were 48 and 65 similar DE miRNA after exposure to source and slick oil, respectively (Table 3-1). Several miRNAs were consistently up- or down- regulated at all three developmental stages. Using the phylogenetic method, 28 and 70 miRNAs were differentially expressed at all developmental stages after source and slick oil exposure,

respectively (Figure 3-3). Using the Fugu method, 3 miRNAs were DE at all stages, namely miR-21b, miR-7641 and miR-92b, after source oil exposure. Slick oil data showed 13 similar DE miRNAs at all stages (Figure 3-3 and Table 3-2). Several common miRNAs (e.g. miR-21b, miR-7641 and miR-92b) were consistently differentially expressed at all stages between the two methods (Table 3-2).

IPA identified miRNA-mRNA networks in both oil types at the three stages (Figure 3-4, 3-5 and 3-6) based on the reverse expression of miRNAs and their target mRNAs. The fugu method showed that at 96hpf of source oil exposure, miR-133 (regulating 81 genes), miR-214 (regulating 81 genes) and miR-20 (regulating 57 genes) were the top 3 DE miRNA targeting the largest number of DE mRNA (Figure 3-6B). For the phylogenetic method, the top 3 for source oil were miR-15 (regulating 73 genes), let-7 (regulating 56 genes) and miR125 (regulating 22 genes). Using the fugu method, IPA identified miR-15 (regulating 179 genes), miR-34 (regulating 173 genes) and miR-133 (regulating 84 genes) as the top 3 DE miRNA having the highest number of target DE mRNA after slick oil exposure (Figure 3-6D), and miR-15 was also among the top 3 for slick oil using the phylogenetic method (Figure 3-6C).

Xu et al., (2016) showed that slick oil increased pericardial area and altered expression of a number of DE expressed genes related to the cardiovascular system as well as vision related pathways and diseases. Therefore, miRNA-mRNA relationships were further filtered for cardiovascular system associated functions and pathways at the 48hpf and 96hpf after slick oil treatment (Table 3-5 and 3-6). The phylogenetic method

identified the top miRNAs ranked by the number of DE mRNA to be miR-15b, miR-155 and miR-98 at 48hpf, while the top 3 miRNA ranked in the number of DE mRNA were miR-142-3p, miR-365 and miR-144-3p by the Fugu method (Table 3-4). At 96hpf, for the fugu method, the top 3 miRNAs for slick oil were miR-34a-5p, miR-15b and miR-133b (Table 3-6). miR-133 expression was also correlated to ion transporter genes such as *kcnh2* (Figure 3-7). For the phylogenetic method, miR-15b, let-7e and miR-30c were the top three (Table 3-6). In addition, using IPA, the miRNA-mRNA networks were also filtered for ocular functions and ophthalmic diseases. The phylogenetic method identified let-7e, miR-15b and miR-30c as the top 3 miRNA correlated to the most DE mRNAs. For the Fugu method, miR-34a-5p, miR-15b and miR-20b were identified as the highest-ranking miRNAs (Table 3-7).

To determine the biological impact of the miRNA-mRNA expression, a GO term analysis (molecular function, cellular component, biological process) was conducted by analyzing the target mRNAs using DAVID (Figure 3-8 and 3-9; Table 3-8 and 3-9). Using the phylogenetic method, the top enriched biological processes were transcription and cellular proliferation terms; however, cardiac related terms were also identified for slick oil (cardiac muscle hypertrophy in response to stress (ranked 18) and heart development (rank 28)) (Figure 3-9A). For source oil, DAVID identified terms related to regulation of transcription as well as heart development as the top ranked terms (Figure 3-8A). Similar to the phylogenetic method, annotation based on Fugu also predicted regulation of transcription, heart development, and cell proliferation as the top enriched terms for both slick and source oil at 96hpf (Figure 3-8B and 1-9B). In addition, calcium

regulation, liver development, and ventricular septum morphogenesis were also significantly enriched (Figure 3-9B, 3-8B).

Discussion

The impacts of oil exposure on fish development have been well documented and the cardiovascular system has been reported to be a primary target associated with oil exposure. (Esbaugh et al., 2016; Incardona and Scholz, 2016; Incardona et al., 2014; Mager et al., 2014). Consistent with earlier studies in other fish, RNA-seq analysis in mahi has shown that exposure of embryos to *DWH* oil resulted in the altered regulation of genes associated with the cardiovascular system in addition to Ca^{2+} homeostasis, EIF2 signaling and phototransduction pathways (Xu et al., 2016). To determine the contribution of epigenetic regulation of transcription, this study evaluated the effects of oil on miRNA expression.

Previous studies have indicated that weathered slick oil caused more severe developmental defects than source oil (Xu et al., 2016). Similarly, more DE miRNA were observed after slick oil exposure compared to source oil exposure of the mahi embryos at all stages. As reported previously, a higher number of 3-ring PAHs and likely oxy-PAHs are present in slick oil (Xu et al., 2016). OxyPAHs have demonstrated higher cardiac toxicity than parent compounds (Knecht et al., 2013; Diamante et al., 2017) and oil treated with UV-light (Sweet et al., 2016).

Three ring PAHs, such as phenanthrene, have been shown to target the heart during development in fish (Incardona et al., 2004; 2005). Previously documented effects in the heart include looping defects, arrhythmia and bradycardia (Incardona et al., 2004;

2005; 2011). Recent studies have also shown that ion gradients important for normal excitation-contraction coupling are altered after exposure to oil, and contribute to the cardiotoxic effects (Brette et al., 2014). Brette et al., 2017 showed that Ca^{2+} and K^{+} currents were disrupted in the cardiomyocytes of bluefin and yellowfin tuna and that the main driver of these effects is phenanthrene. One hypothesis for the ionic alterations is the diminished expression of ion transporter genes (*kcnh2* and *ncx1*) within cardiac myocytes (Sørhus et al., 2016). However, the pathway by which oil can alter the expression of *kcnh2* and *ncx1* is still unknown. miRNA-mRNA network analysis in our study clearly showed that DE of *kcnh2* was correlated to the DE of miR-133. Similarly, a study in mice has shown that miR-133 is involved in the cardiac hypertrophy induced by phenanthrene (Huang et al., 2016). Whether miR-133 also plays a role in the alteration of ion influxes such as Ca^{+} induced by oil warrants further investigation.

miR-7641 showed the highest increase of expression at all developmental stages of mahi treated with oil. In human stem cells, miR-7461 has been shown to be involved in regulating the expression of CXCL1, a vasculogenic chemokine important for endothelial cell differentiation (Yoo et al., 2013). In our miRNA-mRNA network analysis, miR-7641 correlated with the diminished expression of positive regulatory domain containing 16 (PRDM6), a zinc finger transcriptional repressor. Deletion of PRDM6 caused cardiovascular defects in mice (Gewies et al., 2013). PRDM6 also plays a role in smooth muscle cell proliferation by regulating the expression of myocardin and GATA-6 (Davis et al., 2006). GATA transcription factors such as GATA6 are involved in regulating cardiac hypertrophy. Overexpression of GATA-6 has been shown to induce

hypertrophic characteristics in cardiomyocytes (Liang et al., 2001). Interestingly, in support of this miRNA-mRNA network, GATA-6 was upregulated after oil exposure in mahi mahi (Xu et al., 2016).

Slick oil exposure also upregulated miR-15b which regulated the highest number of DE mRNAs. Members of the miR-15 family have been shown to play an important role in normal heart development by repressing cell proliferation through genes regulating cell cycle such as checkpoint kinase 1 (CHEK1) (Porrello et al., 2013). In mahi, CHEK1 mRNA was downregulated, suggesting proliferation was impaired within embryos. Whether this occurred specifically in the heart or other targets deserves further study.

In addition to heart defects, eye related processes and diseases were identified in previous RNA-seq analysis in mahi (Xu et al., 2016). Although eye related processes were not observed in the GO term analysis using DE miRNA, some miRNA-mRNA networks were linked to ophthalmic disease. IPA showed that eye related genes such as the downregulated mRNA of phosphatase and tensin homolog (PTEN) and neurogenic locus notch homolog protein 2 (NOTCH2) genes were inversely correlated to several upregulated miRNAs (miR-34a, miR-15 and miR-23). PTEN is a phosphatase involved in tumor suppression (Chalhoub and Baker, 2009) and eye development (Chaffee et al., 2016; Huang et al., 1999). Notch2 encodes a transmembrane receptor involved in cell differentiation (Hoppe and Greenspan, 1990; Artavanis-Tsakonas et al., 2001). In mice, a NOTCH2 loss of function mutation caused abnormal eye vasculature, which can lead to several eye diseases such as cataracts and eye degeneration (McCright et al., 2001).

Cataract formation was one of the top diseases identified in the slick oil RNA-seq analysis (Xu et al., 2016). With the growing evidence that the eye is negatively affected by parental and oxygenated PAHs (Huang et al., 2013; Diamante et al., 2017), the need to further evaluate the role of miRNAs in ocular development is apparent.

Overall, this study shows that exposure to both source and slick oil can alter the expression of miRNAs during mahi embryonic development. Both oil types resulted in an increase of DE miRNA as development progressed. Similar to the toxicological effects seen between the two oil types (Xu et al., 2016), a more pronounced change of miRNA expression was observed after slick oil exposure than source oil. IPA identified miRNA-mRNA networks involved in cardiovascular and ocular functions and diseases for both oil types, and GO term analysis also indicated heart development and ion regulation terms were affected after oil exposure. To our knowledge, this is the first study linking miRNAs and mRNA in fish responsive to crude oil exposure, providing a new opportunity for understanding mechanisms of oil induced toxicity.

Acknowledgements.

This research was made possible in part by a grant from BP/The Gulf of Mexico Research Initiative to the RECOVER Consortium.

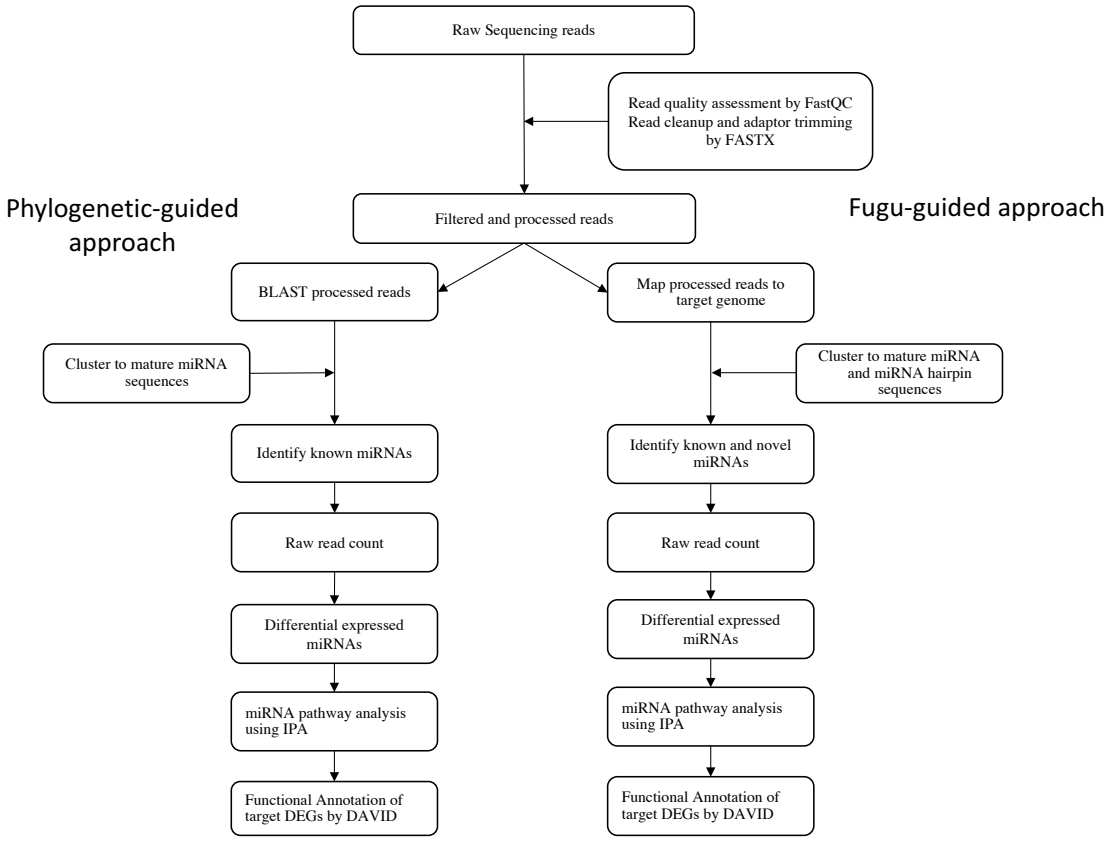

Figure 3-1. Schematic of bioinformatics pipeline. Flow diagram of steps used to identify differentially expressed miRNAs and the inversely correlated putative target genes.

Phylogenetic-guided approach

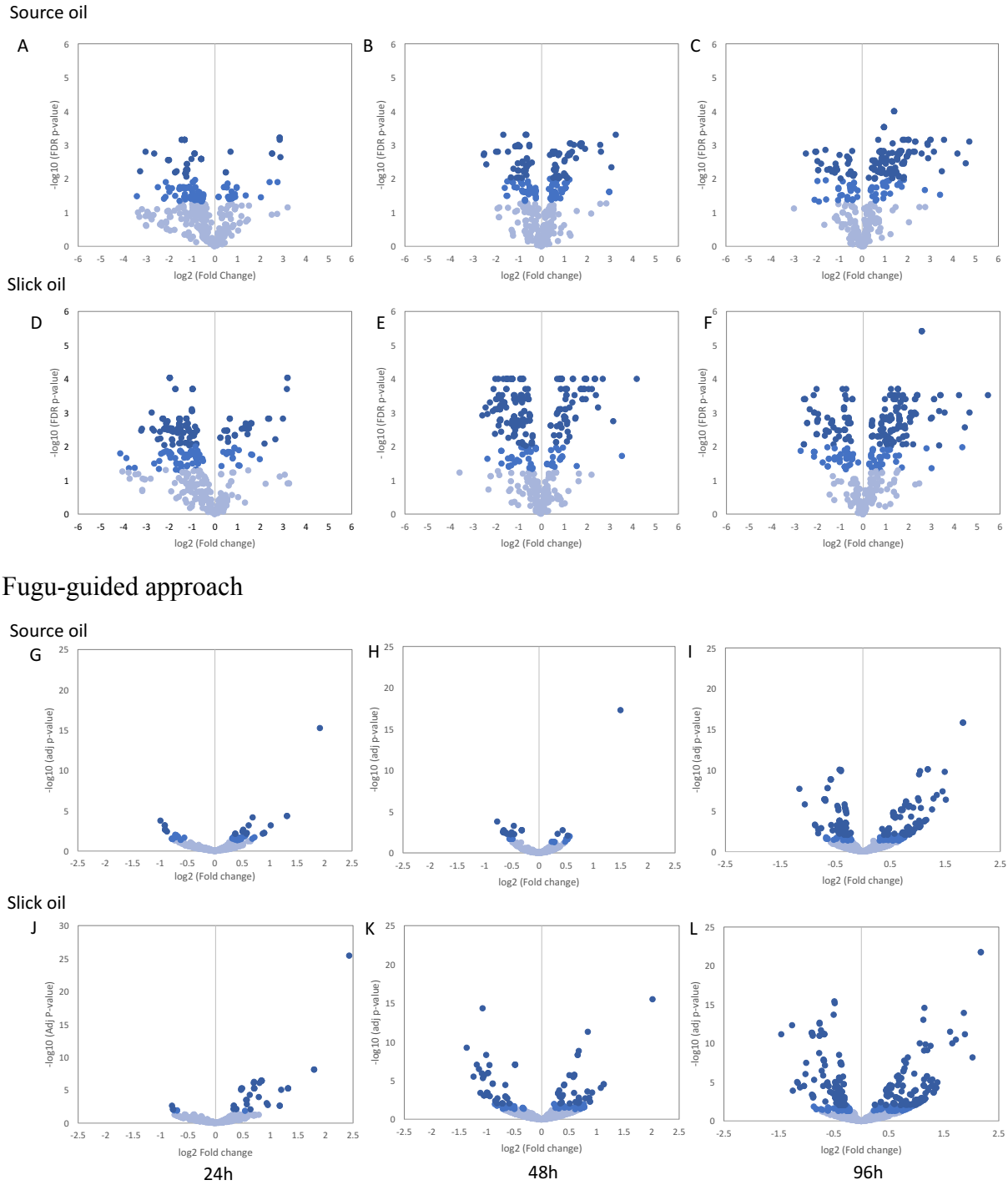

Figure 3-2. Transcript expression profiles of miRNAs using the phylogenetic-guided approach and Fugu-guided approach. The plots show relative expression of genes in

source oil (A-C and G-I) and slick oil (D-F and J-L) treated larvae compared with control at 24 (A, D, G, J), 48 (B, E, H, K) and 96 (C, F, I, L) hpf. The X-axis plots log2 fold change and the Y-axis is the –log10 adjusted p-value. Light blue dots represent non-significant genes, whereas blue indicate genes with an adjusted p value < 0.05 and dark blue dots indicate significant differentially expressed genes with a p value < 0.01.

Method		**Phylogenetic-guided approach**			**Fugu-guided approach**			**Both**	
Oil Type		**Source**	**Slick**		**Source**	**Slick**		**Source**	**Slick**
24 hours	upregulated	9	35		18	38			
	downregulated	37	104		7	4			
	Total	46	139		25	42		**6**	**14**
48 hours	upregulated	53	75		4	42			
	downregulated	48	138		20	40			
	Total	101	213		24	82		**7**	**27**
96 hours	upregulated	137	143		87	128			
	downregulated	41	70		78	126			
	Total	178	213		165	254		**48**	**65**

Table 3-1. Number of upregulated and downregulated miRNA after slick and source oil exposure using both methods.

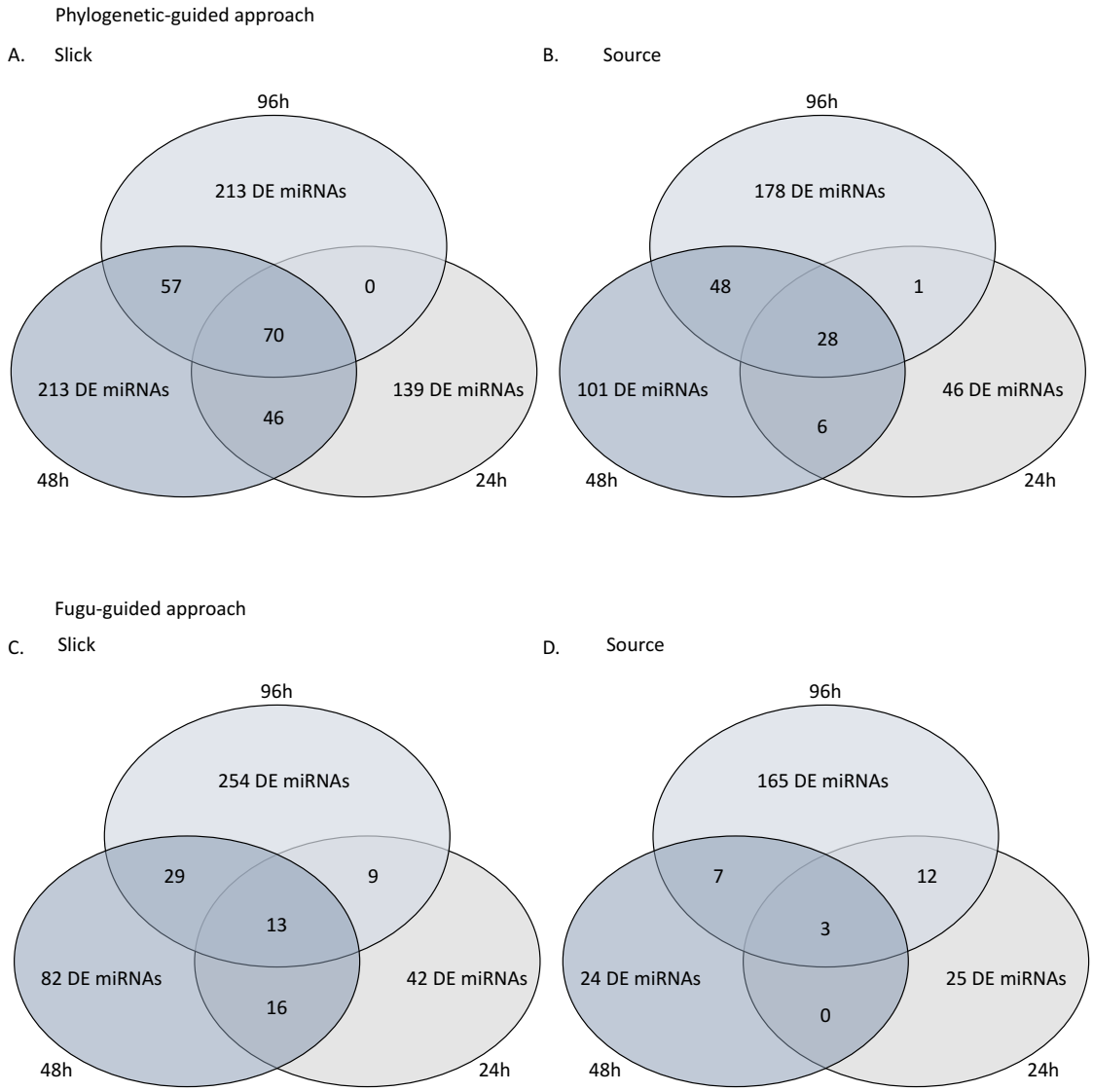

Figure 3-3. Venn Diagrams of differentially expressed miRNA at the 3 different stages after slick and source oil exposure. Venn diagram showing the number of shared differentially expressed (DE) miRNA at 24h, 48 and 96h time points identified using the phylogenetic-guided approach method after slick (A) and source oil (B) exposure. Venn diagram showing the number of shared DE miRNA at 24h, 48 and 96h time points identified using the Fugu-guided approach method after slick (C) and source oil (D) exposure.

	Source oil		
	log_2 fold change		
DE miRNA	24h	48h	96h
miR-21b-3p	-0.994	-0.650	-1.055
miR-7641	1.918	1.504	1.513
	Slick oil		
	log_2 fold change		
DE miRNA	24h	48h	96h
miR-204	0.840	0.594	0.456
miR-204b	0.838	0.588	0.466
miR-211	0.839	0.589	0.459
miR-21b-3p	-0.794	-1.065	-0.651
miR-365	1.794	1.126	1.138
miR-7641	2.434	2.020	2.023
miR-92a	0.703	0.675	0.352
miR-92b	0.799	0.840	0.512

Table 3-2. List of differentially expressed (DE) miRNA at all 3 stages after source and slick oil exposure observed using both methods.

Fugu-guided approach	Source oil		
	log_2 fold change		
DE miRNA	24h	48h	96h
miR-21b-3p	-0.994	-0.650	-1.055
miR-7641	1.918	1.504	1.513
miR-92b	0.690	0.438	0.398
	Slick oil		
	log_2 fold change		
DE miRNA	24h	48h	96h
miR-204	0.840	0.594	0.456
miR-204-5p	0.836	0.589	0.460
miR-204a	0.830	0.576	0.456
miR-204a-5p	0.831	0.590	0.451
miR-204b	0.838	0.588	0.466
miR-211	0.839	0.589	0.459
miR-21b-3p	-0.794	-1.065	-0.651
miR-365	1.794	1.126	1.138
miR-365-5p	1.794	1.126	1.138
miR-462	0.789	0.677	1.615
miR-7641	2.434	2.020	2.023
miR-92a	0.703	0.675	0.352
miR-92b	0.799	0.840	0.512

Table 3-3. List of differentially expressed (DE) miRNA at all 3 stages after source and slick oil exposure observed using the Fugu-guided approach.

Phylogenetic-guided approach method	Source oil		
	log_2 fold change		
	24hpf	48hpf	96hpf
let-7e	-1.7434	-0.7699	-2.0334
let-7j	-1.7388	-0.7751	-2.0319
miR-10	0.4854	0.5351	0.8327
miR-101	-2.0261	-1.1258	-1.1067
miR-101a	-2.0242	-1.1263	-1.1068
miR-101b	-2.0124	-1.1315	-1.1066
miR-101c	-2.0499	-1.1492	-1.1482
miR-10a	0.4872	0.5339	0.8285
miR-148a	-1.2666	-1.0114	-0.6001
miR-192	-1.4593	-0.5255	-0.3976
miR-212	2.518	1.2579	1.7847
miR-212a	2.5098	1.2777	1.8605
miR-215	-1.4563	-0.5315	-0.3926
miR-21b	-2.6572	-2.4195	-2.469
miR-222	-0.8853	-0.6592	-0.5647
miR-222a	-0.9004	-0.6788	-0.5784
miR-222b	-0.8867	-0.6838	-0.5616
miR-3529	-0.597	-0.6555	-0.4272
miR-3596c	-1.6828	-0.8182	-2.0562
miR-365	2.8375	1.7834	2.0212
miR-365a	2.8468	1.7587	2.0464
miR-365b	2.8526	1.7533	2.0463
miR-7	-0.597	-0.6555	-0.4272
miR-7641	2.8821	2.5911	2.0696
miR-79	-1.2519	-0.6177	-0.658
miR-7a	-0.597	-0.6554	-0.4272
miR-7b	-0.597	-0.6555	-0.4272
miR-7d	-0.5992	-0.6594	-0.4264

Phylogenetic-guided approach method	Slick oil		
	log_2 fold change		
	24hpf	48hpf	96hpf
let-7	-1.2922	-0.8742	-1.9785
let-7b	-1.2934	-0.8921	-2.0075
let-7e	-2.1423	-1.5277	-2.5494
let-7f	-1.1662	-0.841	-1.5536
let-7g	-1.1892	-0.8539	-2.0011
let-7h	-2.6822	-2.0904	-2.3378
let-7j	-2.1258	-1.5345	-2.5467
miR-10	0.6506	0.9036	1.1709
miR-10a	0.6526	0.9044	1.1676
miR-10b	0.526	0.895	1.1921
miR-10c	0.526	0.8949	1.1921
miR-10d	0.5397	0.6963	1.1092
miR-135b	-1.8884	-1.2121	-0.5222
miR-142	-1.3748	-1.2515	-0.8364
miR-142a	-1.3838	-1.2395	-0.8295
miR-142b	-1.3838	-1.2395	-0.8295
miR-148a	-1.5406	-1.3119	-0.6252
miR-153	-2.1492	-1.8185	-0.729
miR-153b	-2.076	-1.1796	-0.7633
miR-153c	-2.1309	-1.7879	-0.7403
miR-1623	2.651	4.1818	5.4896
miR-192	-1.7281	-0.9191	-0.6277
miR-204	1.595	1.7349	2.581
miR-204b	1.5978	1.7428	2.5786
miR-211	1.6116	1.7397	2.5774
miR-212	2.3795	1.3772	1.4604
miR-212a	2.3441	1.3886	1.5411
miR-214	2.1767	2.7037	4.2208
miR-215	-1.7333	-0.9178	-0.6231
miR-216	-1.9593	-1.7943	-1.352
miR-216a	-1.949	-1.8029	-1.357
miR-218	-1.6156	-1.1949	-0.4603

miR-2188	-0.9755	-1.2702	-1.5935
miR-218a	-1.6145	-1.1924	-0.4593
miR-218b	-1.6145	-1.1924	-0.4593
miR-21b	-2.7746	-2.5925	-1.6744
miR-222	-0.9928	-0.799	-0.5474
miR-222a	-1.012	-0.8201	-0.5641
miR-222b	-1.013	-0.8164	-0.5577
miR-235	1.3531	1.358	1.1899
miR-25	0.248	0.8472	0.7698
miR-301a	-1.5584	-1.1739	-1.3651
miR-301b	-1.5351	-1.1687	-1.3963
miR-301d	-1.1166	-1.206	-1.1927
miR-310	1.5645	1.8038	1.7525
miR-311	1.5664	1.8013	1.7423
miR-311a	1.4921	2.0771	1.3409
miR-3120	-1.208	-1.137	-0.7881
miR-313	1.4353	1.9104	1.6456
miR-3529	-0.9826	-1.0017	-0.5859
miR-3596b	-1.5691	-1.1585	-2.1584
miR-3596c	-2.0719	-1.5471	-2.5846
miR-365	3.1612	2.3589	2.3672
miR-365a	3.1867	2.3534	2.3764
miR-365b	3.1793	2.3496	2.3824
miR-499	-2.2095	-1.8567	-2.0273
miR-499a	-2.2095	-1.8573	-2.0302
miR-499b	-2.2084	-1.8553	-2.0294
miR-7	-0.9826	-1.0017	-0.5859
miR-7641	2.9898	2.3953	2.1069
miR-79	-1.5705	-0.9117	-0.8305
miR-7a	-0.9826	-1.0017	-0.5859
miR-7b	-0.9826	-1.0017	-0.5859
miR-7d	-0.9855	-1.0029	-0.5869
miR-9	-1.5187	-0.7967	-0.6511
miR-92	1.3969	1.9573	1.5254
miR-92a	0.2487	0.8501	0.7754
miR-92b	1.3977	1.9595	1.53
miR-92c	1.3972	1.959	1.5255

miR-92d	1.1773	1.0561	1.0116

Table 3-4. List of differentially expressed (DE) miRNA at all 3 stages after source and slick oil exposure using the phylogenetic-guided approach method.

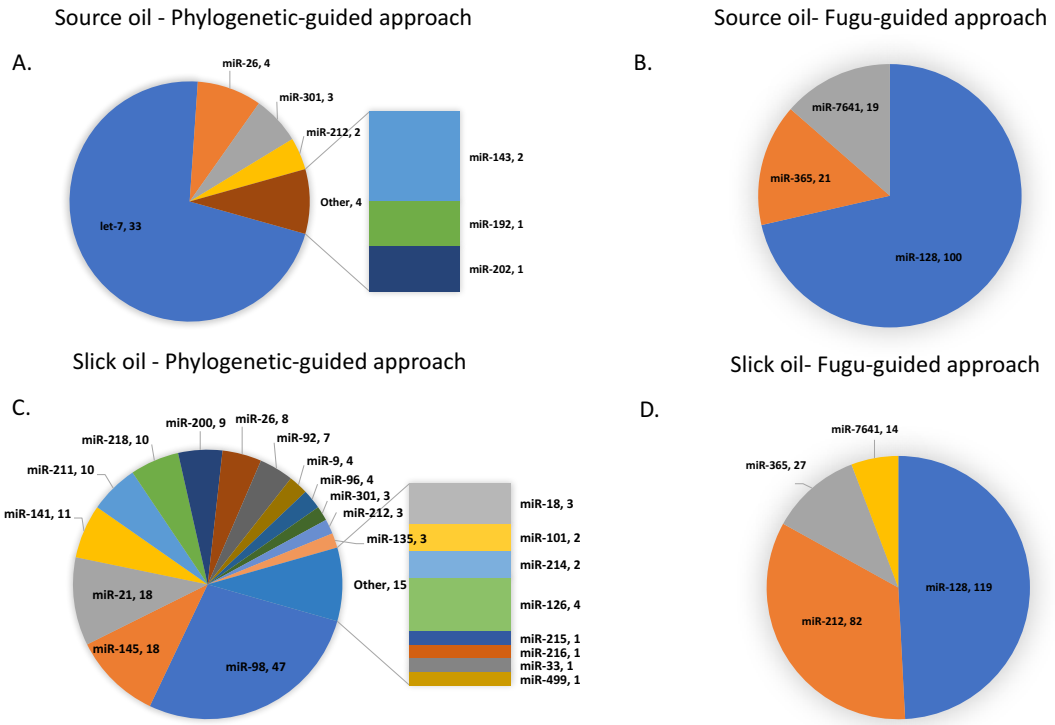

Figure 3-4. Visual distribution of the number of differentially expressed mRNA correlated to differentially miRNA identified using IPA at 24h. Pie chart showing the number of correlated mRNA and miRNA at 24h after source (A and B) and slick (C and D) oil exposure.

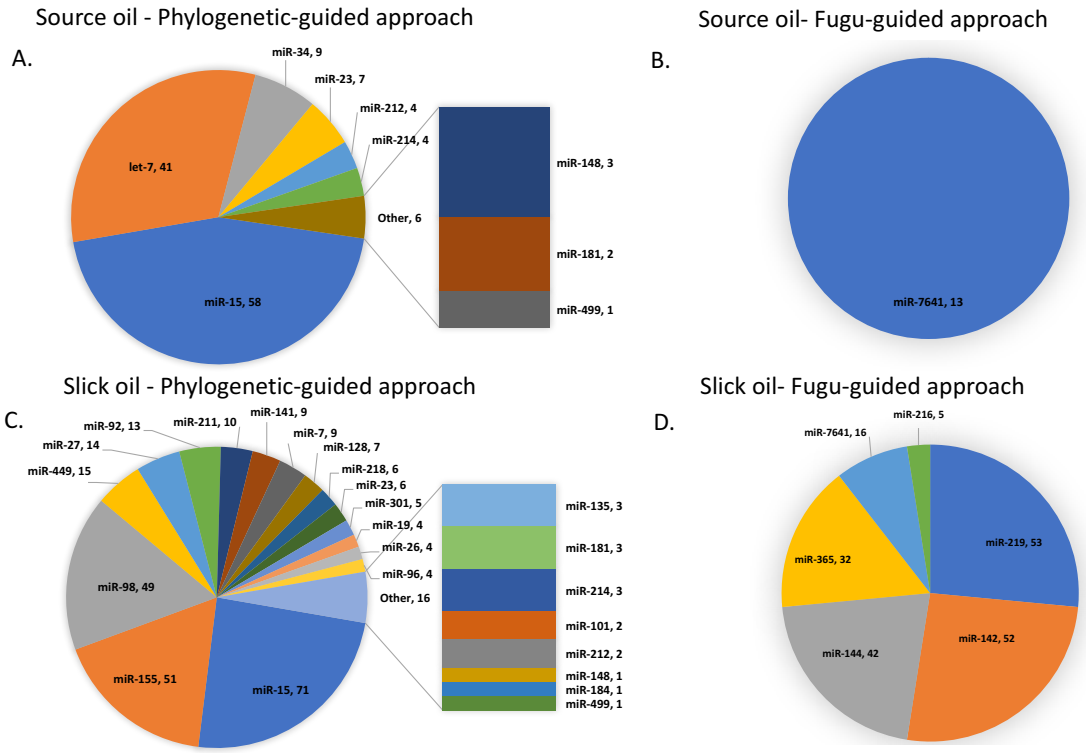

Figure 3-5. Visual distribution of the number of differentially expressed mRNA correlated to differentially miRNA identified using IPA 48h. Pie chart showing the number of correlated mRNA and miRNA at 48h after source (A and B) and slick (C and D) oil exposure.

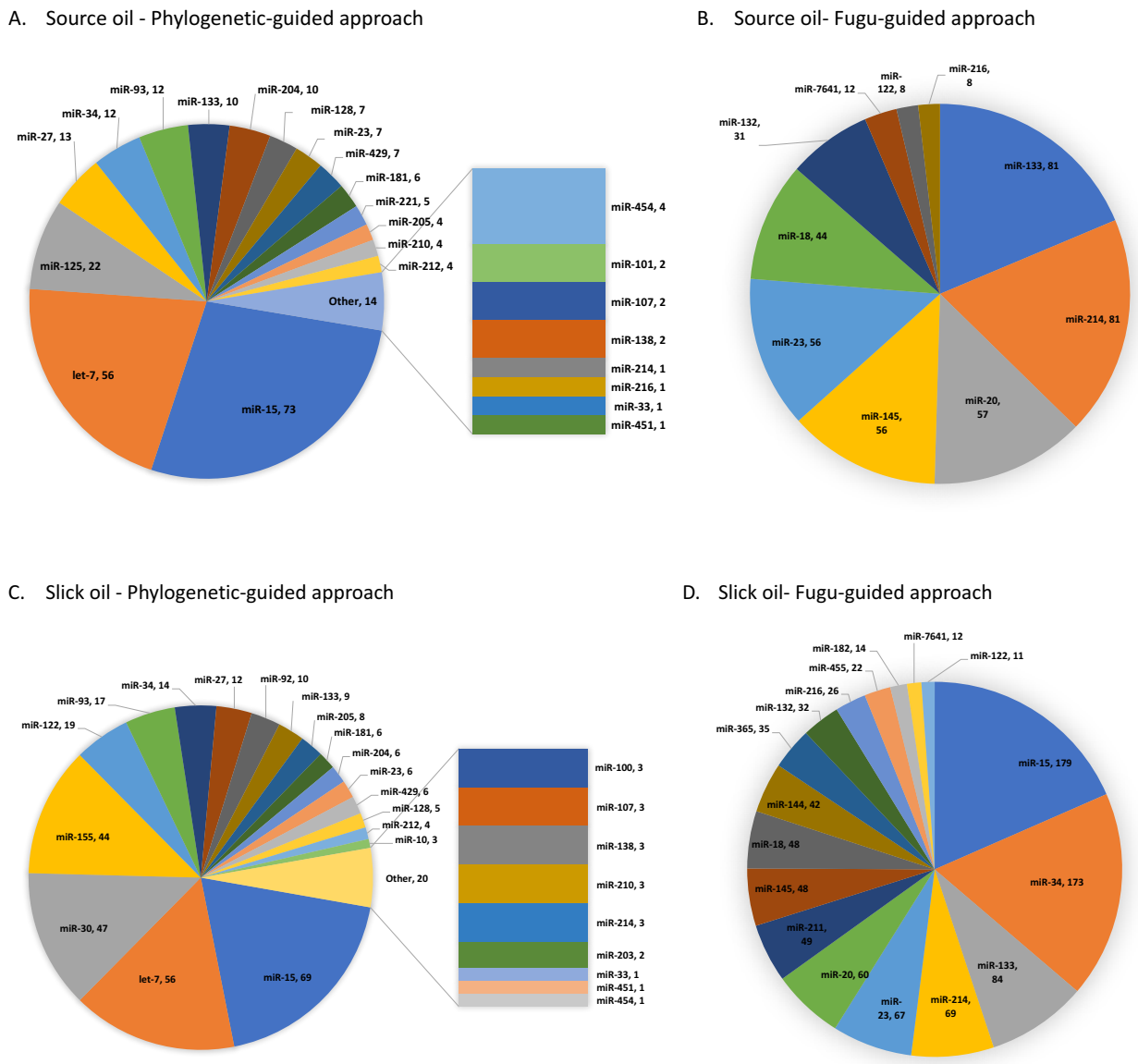

Figure 3-6. Visual distribution of the number of differentially expressed mRNA correlated to differentially miRNA identified using IPA at 96h. Pie chart showing the number of correlated mRNA and miRNA at 96h after source (A and B) and slick (C and D) oil exposure.

Phylogenetic-guided approach Slick Oil (48h)			
DE miRNA	**log_2 FC**	**DE mRNA**	**GENE ID**
miR-15b	1.505	37	ARHGDIA, ATF6, BCL2, BDNF, CA12, CCNE1, CDC25A, CDK6, CHEK1, CHORDC1, DMTF1, DNAJB4, E2F3, EGFR, F2, FGFR1, FNDC3B, GRB2, HACE1, IGF1, IGF2R, ITGA2, KCNN4, LAMC1, MAPK3, MSH2, MYB, PHLDB2, PLK1, PMS1, PRIM1, PRIMPOL, SHOC2, SLC12A2, TPI1, UGDH, WT1
miR-155	1.13	22	AGTR1, ARL5B, BACH1, CSF1R, F2, GNA13, IKBKE, JARID2, MAF, MYB, MYD88, MYO10, PDE3A, PICALM, PPL, PRKCI, PTPRJ, RCN2, RHOA, SYNE2, TAB2, TRAM1
miR-98	-1.67	16	BCL2L1, CCND1, CDKAL1, DRD3, FANCD2, GYS1, HMGA2, IGF2BP2, IGF2BP3, MTRR, PTGS2, RDH10, SIGMAR1, SLC25A1, SLC25A32, WNT1
miR-449b	-1.188	13	CCND1, CREB1, FOXP1, JAG1, MAP2K1, MET, MYCN, NOTCH2, SIRT1, TP53, TRPS1, VEGFA, WNT1
miR-27b	1.112	10	FBXW7, FOXO1, GRB2, IGF1, NOTCH1, PDPK1, PPARG, RUNX1, SMAD3, ST14
miR-141	-1.613	8	CTNNB1, CYP1B1, DLX5, ERBB21P, MAP2K4, PITX2, ZEB2, ZFPM2
miR-92b	1.96	8	CCNE2, FBXW7, IKZF1, ITGA5, ITGB3, MYLIP, PTEN, VSNL1
miR-211	1.74	6	BMP1, CTSC, ERF, MMP9, SHC1, SPARC
miR-218	-1.195	5	ARAF, CTSB, PIK3C2A, PLCG1, RICTOR
miR-23b	1.951	5	CXCL12, HES1, NOTCH1, PTEN, SMAD3
miR-7	-1.002	5	FOS, MAPKAP1, PAK1, RAF1, SYNE1
miR-128	-2.012	4	AFF1, KMT2A, LDLR, SNAP25
miR-19a	-1.776	4	BMPR2, CCND1, ERBB4, NR4A2
miR-135b	-1.212	3	APC, JAK2, TRPS1
miR-214	2.704	3	FGF16, GPD1, PTEN
miR-101	-1.484	2	MYCN, PTGS2
miR-301a	-1.174	2	SMAD4, ZFPM2
miR-212	1.377	2	MMP9, RB1
miR-181a	-1.796	2	GRIA2, HOXA11
miR-26a	-1.82	2	EPHA2, PTGS2
miR-96	-1.305	2	ADCY6, MITF
miR-184	1.059		AKT2

miR-499	-1.857	1	SOX6
Fugu-guided approach Slick Oil (48h)			
DE miRNA	**log_2 FC**	**DE mRNA**	**GENE ID**
miR-142-3p	-1.046	20	AKT1S1, ANK3, ANKRD11, APC, ARNTL, BAZ1A, BCL2L1, COG4, FLVCR1, GAB1, HGS, HMGA2, LIFR, LMO3, MYLK, NKX2-3, PDE4B, RICTOR, S1PR3, ZBTB41
miR-365	1.126	11	ACVR1, ADM, ARRB2, CPT2, DFFB, ESRRA, GAA, NR3C2, P2RY1, TFDP1, UBAC2
miR-144-3p	-1.111	10	FST, GABRA1, MEF2A, MSX1, PLA2G4A, PLAT, SMAD9, SYNCRIP, TBC1D9B, TNFSF11,
miR-219b-5p	-1.05	10	CHRNA7, CYP7B1, DLX3, DNAH3, DOK6, FAM20A, GUCY1B3, PPP1CB, TOMM7, UCKL1
miR-219-5p	-1.176	9	CACNB3, DOK6, ISL1, KCNA4, LEF1, PI4KA, PLCG2, RECK, RORB
miR-7641	2.02	5	BIRC5, EMC8, NOSTRIN, PRDM6, TCF21
miR-216a	-1.364	3	BECN1, CA6, KLHL8
miR-144-5p	-1.011	1	RGS5

Table 3-5. Enriched IPA cardiovascular disease of differentially expressed (DE) miRNA and inversely correlated genes at the 48h stage after slick oil treatment using the both phylogenetic-guided approach and Fugu-guided approach method. Ranked by the number of DE gene inversely correlated. Fold change (FC).

Phylogenetic-guided approach Slick oil (96h)			
DE miRNA	**log $_2$ FC**	**DE mRNA**	**GENE ID**
miR-15b	3.381	31	ABCF2, BCL2, BDNF, CDC25A, CDK5RAP1, CHEK1, DMTF1, DNAJB4, E2F3, FGFR1, FNDC3B, GALNT13, IGF1, ITGA2, MAP2K1, MSH2, MYB, NAA15, NOTCH2, PHLDB2, PLK1, PMS1, PRIM1, PRIMPOL, RECK, SHOC2, SLC12A2, SLC7A1, TXN2, WT1, ZYX
let-7e	-2.549	23	CAPG, CASP3, CCND1, CDK6, DAD1, DRD3, F2, FANCD2, HMGA2, ITGB3, LIN28A, MTRR, PRDM1, PRRC2A, PTGS2, RABGAP1L, RDH10, RHOG, SLC25A1, TGFBR1, THBS1, TUSC2, WNT1
miR-30c	1.021	22	ATP2A2, ATRX, CBFB, CDCP1, CHD1, CTGF, DOCK7, ITGA2, MAT2A, MBNL1, MYO10, NT5E, PPP3CA, RBMS1, RUNX2, SLC12A4, SLC4A7, SLC7A1, SLC9A3R2, TNRC6A, TP53, TRPS1
miR-155	1.908	19	AGTR1, CBFB, CYR61, IKBKE, INPP5D, JARID2, LPL, MAF, MYB, MYO10, NT5E, PDE3A, PICALM, PPL, PTPRJ, SLA, SYNE2, TAB2, TRAM1
miR-93	1.344	13	ARID4B, BCL2, BMPR2, CAMTA1, E2F1, E2F3, ITCH, MYLIP, PKD2, PTEN, RB1, RBL2, RUNX1
miR-34a	3.124	12	BCL2, E2F3, FOXP1, MAP2K1, MYB, MYC, NOTCH1, NOTCH2, TAGLN, TP53, TRPS1, WISP2
miR-122	-2.585	8	ADAM17, ALDOA, AP3M2, CCNG1, CERS6, EGLN3, GPX7, SLC7A11
miR-92b	1.53	8	BMPR2, CCNE2, IKZF1, ITGA5, MYLIP, PTEN, VSNL1, ZEB2
miR-205	1.812	7	ATP1A1, MED1, PRKCE, PTEN, TRPS1, ZEB1, ZEB2
miR-27b	1.577	7	IGF1, MEF2C, NOTCH1, PHB, PXN, RUNX1, THRB
miR-133b	1.228	5	CDK13, CTGF, KCNH2, KLF15, RUNX2
miR-181a	-1.297	5	ESR1, GATA6, HOXA11, MMP14, TIMP3
miR-23b	2.318	5	CXCL12, FBXO32, NOTCH1, PTEN, TRPS1
miR-429	2.292	4	PTEN, RERE, ZEB1, ZEB2
miR-100	1.278	3	FGFR3, MTOR, PLK1
miR-128	-2.451	3	AFF1, LDLR, TGFBR1
miR-138	1.33	3	ALDH1A2, ROCK2, VCAN
miR-204	2.581	3	ATP2B1, SHC1, TRPS1
miR-10b	1.192	2	KLF4, NF1

miR-212	1.46	2	RB1, TJP1
miR-203	1.043	2	ABL1, RUNX2
miR-210	1.453	2	E2F3, FGFRL1
miR-214	4.221	2	GPD1, PTEN
miR-454	1.602	1	DICER1
miR-451	1.795	1	MIF
miR-33a	1.598	1	ABCA1
Fugu-guided approach Slick oil (96h)			
DE miRNA	**$\log_2$ FC**	**DE mRNA**	**GENE ID**
miR-34a-5p	1.282	59	ACBD3, ADRA1D, AGTR1, AIRE, AMER1, ASB4, ATG5, ATMIN, BCL2, CA7, CACNB3, CAV3, CBFA2T3, CCNE2, CLIC5, DGAT1, E2F3, FGF23, FOXP1, FUT9, GABRA3, GNAO1, GRIN2B, HTR2C, IKBKE, KCND3, KCNJ8, KIAA1462, KLF4, LEF1, MAP2K1, MARCH8, MYADM, MYB, MYC, NDST1, NGB, NOTCH1, NOTCH2, NTRK3, OVOL2, PDGFRA, PER2, PIGQ, RECK, ROCK1, SAMD12, SERPINF2, STAB2, STRN3, SYT1, TAGLN, TP53, TRPS1, UBP1, WISP2, XYLT1, ZDHHC17, ZHX2
miR-15b	1.042	58	ABCF2, AKT3, ALKBH3, AMER1, ATXN2, BCL2, BDNF, CARM1, CCND2, CDC25A, CDK5R1, CDK5RAP1, CHEK1, DMTF1, DNAJB4, E2F3, E2F7, FASN, FGFR1, FNDC3B, GALNT13, IGF1, INSR, ITGA2, KIF1B, MAP2K1, MSH2, MYB, MYLK, NAA15, NDP, NOTCH2, NSMF, PHLDB2, PLEKHA5, PLK1, PMS1, PRIM1, PRIMPOL, RBMS1, RECK, RGS5, RPS6KA3, RSPO3, RUNX1T1, SALL4, SHOC2, SLC12A2, SLC7A1, SMURF2, TACC1, TFRC, TXN2, UNC80, WT1, ZBTB16, ZMYM2, ZYX,
miR-133b	1.142	26	BICC1, CDK13, COL8A1, CTGF, FLI1, FOXC1, FRMPD1, KCNH2, KLF15, MAML1, PER2, PTH1R, RARB, RUNX2, SGMS2, SLC24A4, SLC6A1, SLC6A6, SNRK, SP3, SV2A, SYT1, TMOD3, TUBB1, VKORC1, WASF2
miR-145-5p	1.318	23	ACBD3, AHNAK, CASZ1, CBFB, CCNA2, CLINT1, DAB2, DDC, FLI1, IKBKAP, IRS1, ITGB8, KCNA4, KLF4, KLF5, MAP3K1, MKL2, MYC, PLCE1, PPP3CA, RASA1, SPTB, TFRC
miR-23b	1.169	23	ACVR1C, ATP11C, BORA, C15orf41, CA2, CCM2, CXCL12, DLGAP1, FBXO32, MYH1, NDUFA2, NOTCH1, NR6A1, PKP4, PROK2, PTEN, SCG5, SIX1, SST, TFRC, TMED5, TRPS1, ZNF91
miR-214	2.177	21	AKAP13, ATF2, CD276, CDK5R1, CIT, DFFB, GPD1, HECTD4, HNF1A, LHX6, MAP3K9, MYDGF, NAA15, OPRK1, PTEN, PTH1R, SAMD12, SEPT4, SIGMAR1,

			TMED5, VDR
miR-20b	1.297	19	ARID4A, ARID4B, BCL2, BMPR2, CAMTA1, E2F1, E2F3, F3, ITCH, MASTL, MYLIP, NR4A3, PKD2, PTEN, RB1, RBL2, RUNX1, SAMD12, VLDLR
miR-211-5p	1.142	15	ATP2B1, BIN1, DVL3, FOXC1, NEBL, NOP10, PDE3A, PHOX2B, PIK3CB, SF3B1, SHC1, SLC43A1, TRPS1, ZEB2, ZNF521
miR-18a-3p	1.389	13	C3orf18, CASP7, CDH20, CPS1, CRELD1, FOXJ1, HTR2C, KCNAB2, KRAS, NOTCH2, PDGFB, PROK1, VHL
miR-34b-5p	1.306	12	ACTL6A, CAV1, CDC25A, DNM1L, FUT9, MAT2A, MYC, PER2, PFKFB1, RGS4, WISP2, XYLT1
miR-144	-1.256	11	ARL15, FST, MEF2A, NFE2L2, PLA2G4A, PLAT, PTHLH, SMAD9, TBC1D9B, TBX1, TNFSF11
miR-132-3p	1.723	9	CALU, PNKD, RASA1, RB1, SDF2, SLC6A1, TGFB2, TJP1, TTK
miR-365b-3p	1.163	9	ADM, CPT1A, CPT2, DFFB, PAX6, RAPGEF4, TFDP1, TMOD3, UBAC2
miR-455-3p	1.143	8	AGTR1, BUD13, LRP6, PAX6, RARB, SUCLA2, TFRC, TTK
miR-122-3p	1.359	7	COL11A2, CXCR3, FGFR4, MAT2A, NEK8, RAPH1, TFRC
miR-216	-1.165	3	BECN1, CA6, KLHL8
miR-7641	2.023	3	EMC8, FHL5, PRDM6
miR-144-5p	-1.457	2	CTSV, F2R
miR-182-3p	-1.001	2	HAND1, SLC16A10
miR-216b-5p	-1.11	1	DLX2

Table 3-6. Enriched IPA cardiovascular disease of differentially expressed (DE) miRNA and inversely correlated genes at the 96h stage after slick oil treatment using the both phylogenetic-guided approach and Fugu-guided approach method. Ranked by the number of DE gene inversely correlated. Fold change (FC).

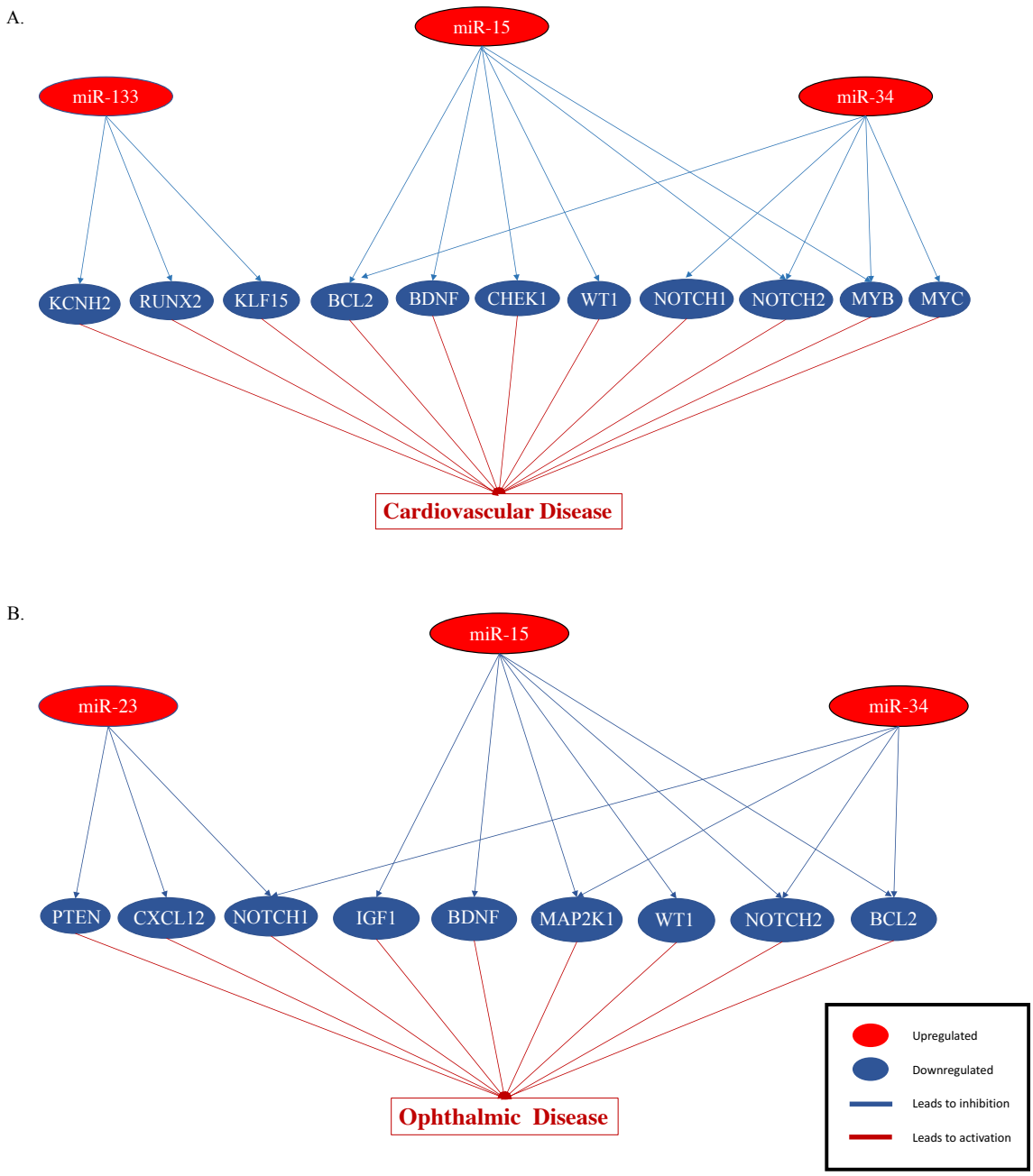

Figure 3-7. Ingenuity Pathway Analysis of correlated miRNA and mRNA network related to A) cardiovascular disease and B) Ophthalmic disease at 96h after slick oil exposure.

Phylogenetic-guided approach Slick oil (96h)			
DE miRNA	**log $_2$ FC**	**DE mRNA**	**GENE ID**
let-7e	-2.549	14	CASP3, CCND1, DRD3, DUSP12, F2, FANCD2, ITGB3, MTRR, NF2, PTGS2, RDH10, SLC1A4, TGFBR1, THBS1
miR-15b	3.381	9	BCL2, BDNF, CADM1, CDC14B, IGF1, MAP2K1, NOTCH2, PRIMPOL, WT1
miR-30c	1.021	8	ANPEP, CTGF, GPD2, MBNL1, P4HA2, PPP3CA, SLC4A7, TP53
miR-93	1.344	6	BCL2, CRIM1, E2F1, PTEN, RB1, RBL2
miR-34a	3.124	6	BCL2, FOXP1, MAP2K1, NOTCH1, NOTCH2, TP53
miR-155	1.908	4	AGTR1, CYR61, LPL, MAF
miR-429	2.292	4	BAP1, PTEN, RERE, ZEB1
miR-23b	2.318	4	CXCL12, NOTCH1, POU4F2, PTEN
miR-27b	1.577	4	IGF1, MEF2C, NOTCH1, THRB
miR-122	-2.585	3	ADAM17, EGLN3, SLC7A11
miR-205	1.812	3	MED1, PTEN, ZEB1
miR-128	-2.451	2	LDLR, TGFBR1
miR-212	1.46	2	RB1, TJP1
miR-133b	1.228	2	CTGF, PTBP2
miR-181a	-1.297	2	ESR1, TIMP3
miR-214	4.221	2	POU4F2, PTEN
miR-100	1.278	1	MTOR
miR-10b	1.192	1	NF1
miR-454	1.602	1	DICER1
miR-138	1.33	1	VCAN
miR-203	1.043	1	ABL1
miR-204	2.581	1	ITGB4
miR-33a	1.598	1	ABCA1
miR-92b	1.53	1	PTEN
Fugu-guided approach Slick oil (96h)			
DE miRNA	**log $_2$ FC**	**DE mRNA**	**GENE ID**
miR-34a-5p	1.282	26	ADRA1D, AGTR1, AIRE, ATG5, BCL2, BEST1, CA7, FOXP1, GABRA3, GNAO1, GRIN2B, HTR2C, LEF1, MAP2K1, MTMR10, NDST1, PVRL1, NGB, NOTCH1, NOTCH2, NTRK3, OVOL2, PDGFRA, PER2, TP53, TWIST2

miR-15b	1.042	17	BCL2, BDNF, CADM1, CCND2, CDC14B, IGF1, INSR, KIF21A, MAP2K1, NDP, NOTCH2, PRIMPOL, SALL4, SCN8A, SIX6, TENM2, WT1
miR-20b	1.297	12	BCL2, CRIM1, E2F1, F3, MYT1L, PTEN, RB1, RBL2, SLC17A7, TBC1D20, TOPORS, VLDLR
miR-133b	1.142	10	COL8A1, CTGF, FOXC1, PDE8B, PER2, PTBP2, RARB, SLC6A6, SOBP, TUBB1
miR-23b	1.169	8	B4GAT1, CA2, CXCL12, KCNV2, NOTCH1, POU4F2, PTEN, SIX1
miR-18a-3p	1.389	7	HTR2C, KRAS, NOTCH2, NYX, PDGFB, POMGNT1, VHL
miR-145-5p	1.318	6	DDC, GLIS1, IRS1, ITGB8, MAP3K1, PPP3CA
miR-214	2.177	6	HNF1A, PVRL1, POU4F2, PTEN, TUBGCP6, VDR
miR-455-3p	1.143	6	AGTR1, IMPG1, KCNJ13, LRP6, PAX6, RARB
miR-132-3p	1.723	5	RB1, SAP30L, SOX5, TGFB2, TJP1
miR-34b-5p	1.306	5	ALX4, CAV1, DNM1L, OLFM2, PER2
miR-144	-1.256	4	FST, PLA2G4A, PLAT, TENM3,
miR-211-5p	1.142	4	FOXC1, ITGB4, PHOX2B, SF3B1
miR-144-5p	-1.457	3	CTSV, F2R, TFG
miR-182-3p	-1.001	2	HYAL1, TRIM44
miR-216	-1.165	2	BECN1, CA6
miR-365b-3p	1.163	2	EFEMP1, PAX6
miR-122-3p	1.359	1	COL11A2

Table 3-7. Enriched IPA ophthalmic disease of differentially expressed (DE) miRNA and inversely correlated genes at the 96h stage after slick oil treatment using the both phylogenetic-guided approach and Fugu-guided approach method. Ranked by the number of DE gene inversely correlated. Fold change (FC).

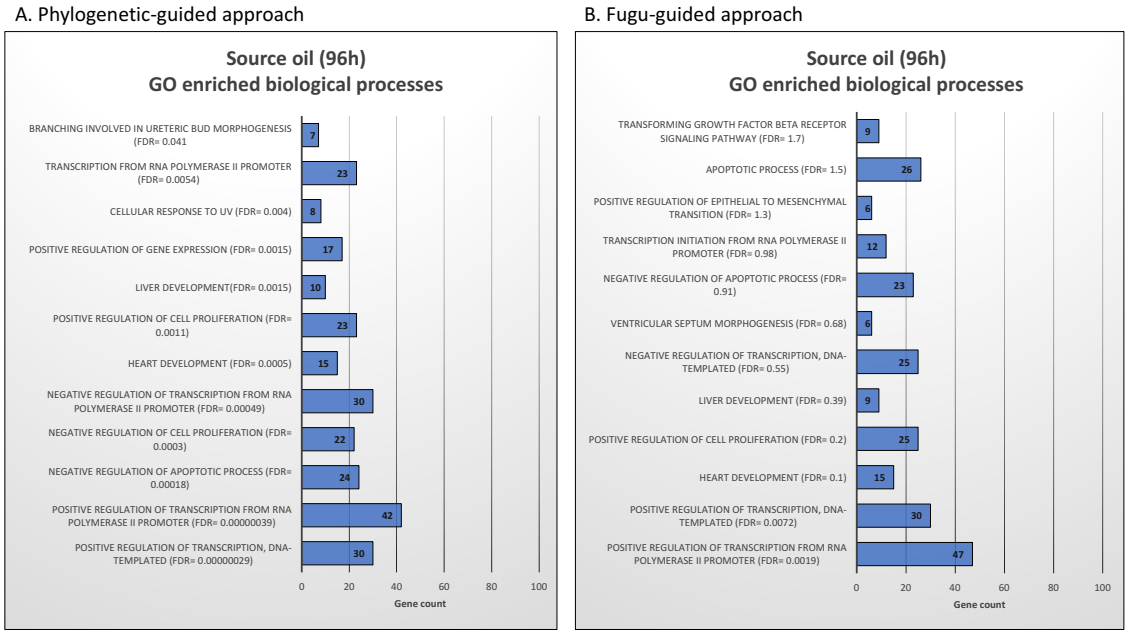

Figure 3-8. GO analysis of enriched biological processes of the correlated differentially expressed mRNA at 96h after source oil exposure. Gene count and FDR p-value associated with the GO category from DAVID are presented in the bar graph.

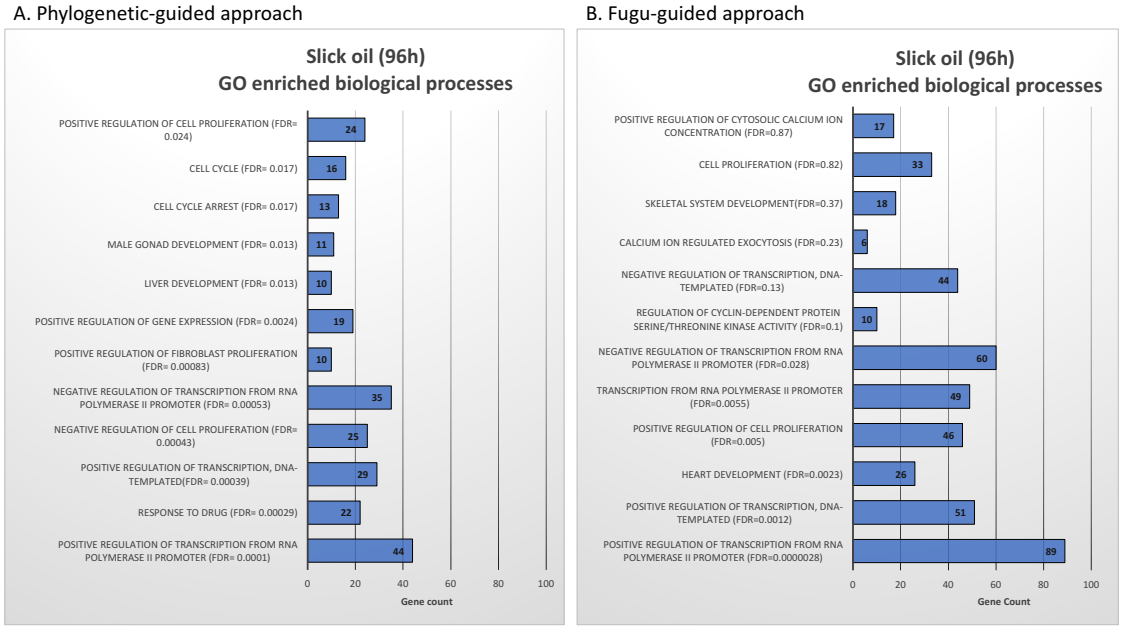

Figure 3-9. GO analysis of enriched biological processes of the correlated differentially expressed mRNA at 96h after slick oil exposure. Gene count and FDR p-value associated with the GO category from DAVID are presented in the bar graph.

Source oil (96h)					
Fugu-guided approach			Phylogenetic-guided approach		
Cellular component term	**Gene Count**	**FDR**	**Cellular component term**	**Gene Count**	**FDR**
cytosol	102	2.00E-01	cytosol	80	2.30E-05
transcription factor complex	13	1.50E+00	cytoplasm	109	3.50E-05
nucleoplasm	82	4.00E+00	nucleus	110	1.40E-04
nuclear chromatin	12	4.50E+00	nucleoplasm	65	3.40E-03
axon	13	4.60E+00	nuclear chromatin	13	1.20E-02
cell-cell contact zone	4	7.30E+00	focal adhesion	18	2.20E-02
membrane	65	1.10E+01	receptor complex	10	6.00E-02
cytoplasm	135	1.50E+01	extracellular exosome	58	4.80E-01
holo TFIIH complex	3	2.70E+01	plasma membrane	75	2.00E+00
endoplasmic reticulum	28	2.70E+01	membrane	45	3.40E+00
cell-cell adherens junction	14	2.90E+01	myelin sheath	8	5.10E+00
perinuclear region of cytoplasm	22	3.50E+01	SMAD protein complex	3	5.90E+00
Molecular function term	**Gene Count**	**FDR**	**Molecular function term**	**Gene Count**	**FDR**
protein binding	241	6.50E-04	protein binding	178	1.90E-10
transcription coactivator activity	15	1.80E+00	protein kinase binding	21	4.80E-04
transcription cofactor activity	7	6.70E+00	RNA polymerase II core promoter proximal region sequence-specific DNA binding	17	5.80E-02
transcriptional activator activity, RNA polymerase II core promoter proximal region sequence-specific binding	13	8.80E+00	transcriptional activator activity, RNA polymerase II core promoter proximal region sequence-specific binding	13	1.80E-01
neurotransmitter:sodium symporter activity	4	9.50E+00	chromatin binding	17	1.80E-01
transcription regulatory region DNA binding	12	1.10E+01	identical protein binding	25	1.90E-01
protein serine/threonine kinase activity	17	1.30E+01	RNA polymerase II transcription factor activity, sequence-specific DNA binding	11	2.10E-01

transcription factor binding	14	1.40E+01	transcription factor activity, sequence-specific DNA binding	29	2.60E-01
sequence-specific DNA binding	21	1.50E+01	core promoter binding	7	3.80E-01
protein kinase activity	16	1.80E+01	sequence-specific DNA binding	19	5.10E-01
protein homodimerization activity	26	2.50E+01	RNA polymerase II transcription factor binding	6	6.90E-01
transcription factor activity, sequence-specific DNA binding	32	2.70E+01	insulin-like growth factor I binding	4	7.80E-01

Table 3-8. Top cellular component and molecular function terms at the 96h stage after source oil treatment using DAVID. Ranked by p-value.

Slick oil (96h)					
Fugu-guided approach method			Phylogenetic-guided approach method		
Cellular component term	**Gene Count**	**FDR**	**Cellular component term**	**Gene Count**	**FDR**
nucleoplasm	173	4.90E-03	nucleus	145	3.00E-07
Golgi membrane	48	1.40E-01	nucleoplasm	88	5.70E-06
cytoplasm	282	1.60E-01	cytosol	94	2.80E-04
neuron projection	24	5.90E-01	cytoplasm	129	1.20E-03
synapse	19	1.80E+00	melanosome	11	1.20E-02
nucleus	282	2.00E+00	extracellular exosome	77	2.20E-02
cell-cell adherens junction	28	2.00E+00	membrane	63	5.00E-02
cell junction	36	2.20E+00	cell surface	24	7.70E-02
transcription factor complex	19	3.70E+00	focal adhesion	19	1.80E-01
synaptic vesicle membrane	9	4.10E+00	apical plasma membrane	16	2.00E-01
cytosol	175	1.40E+01	cell-cell adherens junction	16	6.00E-01
intracellular membrane-bounded organelle	38	1.50E+01	intracellular membrane-bounded organelle	21	2.00E+00
Molecular function term	Gene Count	FDR	**Molecular function term**	Gene Count	FDR
protein binding	492	7.30E-07	protein binding	233	6.30E-16
protein kinase activity	36	4.40E-02	protein kinase binding	22	7.00E-03
RNA polymerase II transcription factor activity, sequence-specific DNA binding	21	2.10E-01	core promoter binding	9	2.70E-02
protein kinase binding	34	5.40E-01	protein domain specific binding	15	3.70E-02
protein serine/threonine kinase activity	33	1.10E+00	integrin binding	10	1.70E-01
phosphoprotein binding	8	1.30E+00	miRNA binding	5	2.30E-01
transcription factor activity, sequence-specific DNA binding	67	1.40E+00	chromatin binding	19	3.90E-01
transcription regulatory region DNA binding	22	1.50E+00	protein tyrosine phosphatase activity	9	6.50E-01
GTPase activator activity	26	2.00E+00	transcription regulatory region DNA binding	13	7.20E-01
ATP binding	95	2.20E+00	transcription factor binding	15	9.60E-01
transcriptional activator activity, RNA polymerase II	13	2.20E+00	fibroblast growth factor binding	5	1.00E+00

transcription regulatory region sequence-specific binding					
transcriptional activator activity, RNA polymerase II core promoter proximal region sequence-specific binding	23	2.30E+00	ATP binding	45	1.10E+00

Table 3-9. Top cellular component and molecular function terms at the 96h stage after slick oil treatment using DAVID. Ranked by p-value.

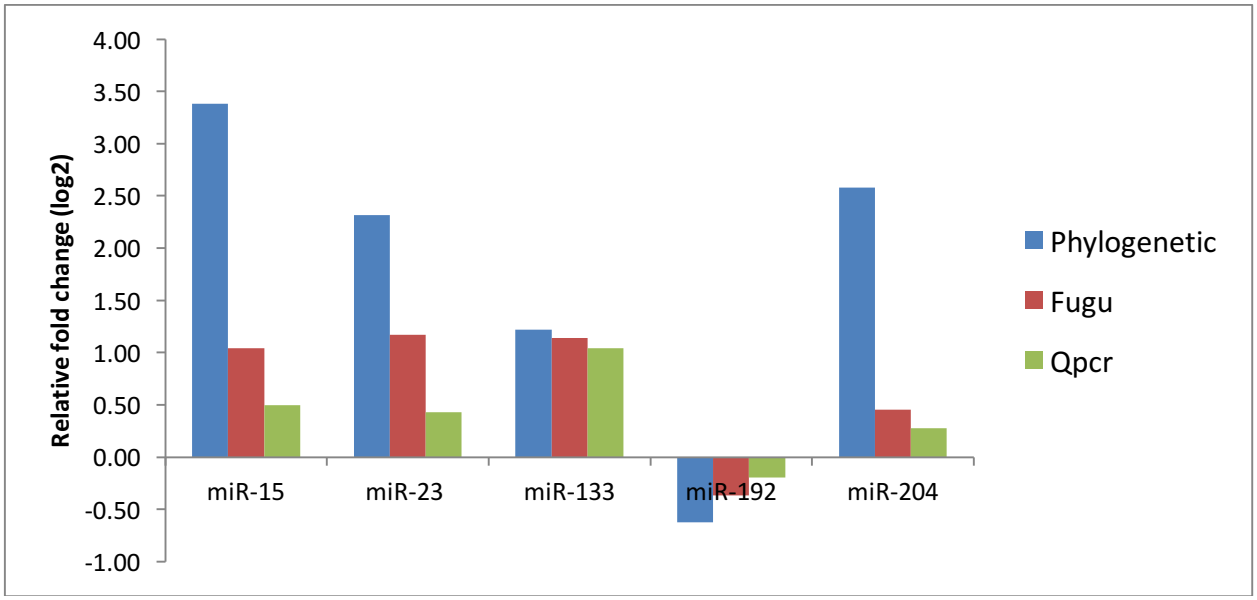

Figure 3-10.
A comparison of relative fold change of miRNA in 96 hpf larvae after slick oil exposure as determined by miRNAseq and qPCR. Mean ± SD (N=3).

References

Altschul, S.F., Gish, W., Miller, W., Myers, E.W. & Lipman, D.J. (1990) "Basic local alignment search tool." J. Mol. Biol. 215:403-410.

An, J., Lai, J., Lehman, M.L., Nelson, C.C. (2013) miRDeep*: an integrated application tool for miRNA identification from RNA sequencing data. Nucleic Acids Res. 2013 Jan;41(2):727-37.

Artavanis-Tsakonas, S., Delidakis, C., Fehon, R.G., (1991) The Notch locus and the cell biology of neuroblast segregation. Annu Rev Cell Biol. 7:427-52.

Bartel, D.P. (2004) MicroRNAs: genomics, biogenesis, mechanism, and function. Cell. 116(2):281-97.

Bianchi M, Renzini A, Adamo S, Moresi V. (2017) Coordinated Actions of MicroRNAs with other Epigenetic Factors Regulate Skeletal Muscle Development and Adaptation. Int J Mol Sci. 18(4).

Brette, F., Machado, B., Cros, C., Incardona, J.P., Scholz, N.L., Block, B.A., (2014) Crude oil impairs cardiac excitation-contraction coupling in fish. Science. 343(6172):772-6.

Brette, F., Shiels, H.A., Galli, G.L., Cros, C., Incardona, J.P., Scholz, N.L., Block, B.A., (2017) A Novel Cardiotoxic Mechanism for a Pervasive Global Pollutant. Sci Rep. 7:41476.

Carls, M. G., Rice, S. D. and Hose, J. E., (1999) Sensitivity of fish embryos to weathered crude oil: Part I. Low-level exposure during incubation causes malformations, genetic damage, and mortality in larval pacific herring (*Clupea pallasi*). Environmental Toxicology and Chemistry. 18: 481–493.

Chaffee, B.R., Hoang, T.V., Leonard, M.R., Bruney, D.G., Wagner, B.D., Dowd, J.R., Leone, G., Ostrowski, M.C., Robinson, M.L., (2016) FGFR and PTEN signaling interact during lens development to regulate cell survival. Dev Biol. 410(2):150-63.

Chalhoub, N., Baker, S.J., (2009) PTEN and the PI3-kinase pathway in cancer. Annu Rev Pathol. 4:127-50.

Davis, C.A., Haberland, M., Arnold, M.A., Sutherland, L.B., McDonald, O.G., Richardson, J.A., Childs, G., Harris, S., Owens, G.K., Olson, E.N., (2006) PRISM/PRDM6, a transcriptional repressor that promotes the proliferative gene program in smooth muscle cells. Mol Cell Biol. 26(7):2626-36.

Diamante, G., do Amaral E Silva Müller, G., Menjivar-Cervantes, N., Xu, E.G., Volz, D.C., Dias Bainy, A.C., Schlenk, D., (2017) Developmental toxicity of hydroxylated chrysene metabolites in zebrafish embryos. Aquat Toxicol. 189:77-86.

Edmunds, R.C., Gill, J.A., Baldwin, D.H., Linbo, T.L., French, B.L., Brown, T.L., Esbaugh, A.J., Mager, E.M., Stieglitz, J., Hoenig, R., Benetti, D., Grosell, M., Scholz, N.L., Incardona, J.P., (2015) Corresponding morphological and molecular indicators of crude oil toxicity to the developing hearts of mahi mahi. Sci Rep. 5:17326.

Esbaugh, A.J., Mager, E.M., Stieglitz, J.D., Hoenig, R., Brown, T.L., French, B.L., Linbo, T.L., Lay, C., Forth, H., Scholz, N.L., Incardona, J.P., Morris, J.M., Benetti, D.D., Grosell, M., (2016) The effects of weathering and chemical dispersion on Deepwater Horizon crude oil toxicity to mahi-mahi (Coryphaena hippurus) early life stages. Sci Total Environ. 543(Pt A):644-51.

Friedländer, M. R., Mackowiak, S. D., Li, N., Chen, W., & Rajewsky, N. (2012). miRDeep2 accurately identifies known and hundreds of novel microRNA genes in seven animal clades. Nucleic Acids Research, 40(1), 37–52.

Friedländer, M.R., Chen, W., Adamidi, C., Maaskola, J., Einspanier, R., Knespel, S., Rajewsky, N. (2008) Discovering microRNAs from deep sequencing data using miRDeep. Nat Biotechnol. 2008 Apr;26(4):407-15.

Gewies, A., Castineiras-Vilarino, M., Ferch, U., Jährling, N., Heinrich, K., Hoeckendorf, U., Przemeck, G.K., Munding, M., Groß, O., Schroeder, T., Horsch, M., Karran, E.L., Majid, A., Antonowicz, S., Beckers, J., Hrabé de Angelis, M., Dodt, H.U., Peschel, C., Förster, I., Dyer, M.J., Ruland, J. (2013) Prdm6 is essential for cardiovascular development in vivo. PLoS One. 8(11):e81833.

Gibbs, R.H.Jr., Collette, BB., (1959) On the identification, distribution, and biology of the dolphins, Coryphaena hippurus and C. equiselis. Bull Mar Sci. 9:117–152.

Goodale, B.C., La Du, J., Tilton, S.C., Sullivan, C.M., Bisson, W.H., Waters, K.M., Tanguay, R.L., (2015) Ligand-Specific Transcriptional Mechanisms Underlie Aryl Hydrocarbon Receptor-Mediated Developmental Toxicity of Oxygenated PAHs. Toxicol Sci. 147(2):397-411.

Goodale, B.C., Tilton, S.C., Corvi, M.M., Wilson, G.R., Janszen, D.B., Anderson, K.A., Waters, K.M., Tanguay, R.L., (2013) Structurally distinct polycyclic aromatic hydrocarbons induce differential transcriptional responses in developing zebrafish. Toxicol Appl Pharmacol. 272(3):656-70.

Griffiths-Jones, S., Grocock, R.J., van Dongen, S., Bateman, A., Enright, A.J. (2006) miRBase: microRNA sequences, targets and gene nomenclature. Nucleic Acids Res. 34(Database issue):D140-4.

Heintz, R.A., Short, J.W., Rice, S.D., (1999) Sensitivity of fish embryos to weathered crude oil: Part II. Increased mortality of pink salmon (Oncorhynchus gorbuscha) embryos incubating downstream from weathered Exxon Valdez crude oil. Environ Toxicol Chem 18:494–503.

Hoppe, P.E., Greenspan, R.J., (1990) The Notch locus of Drosophila is required in epidermal cells for epidermal development. Development. 109(4):875-85.

Huang, da W., Sherman, B.T., Lempicki, R.A. (2009) Bioinformatics enrichment tools: paths toward the comprehensive functional analysis of large gene lists. Nucleic Acids Res. 37(1):1-13.

Huang, da W., Sherman, B.T., Lempicki, R.A. (2009) Systematic and integrative analysis of large gene lists using DAVID bioinformatics resources. Nat Protoc. 4(1):44-57.

Huang, H., Potter, C.J., Tao, W., Li, D.M., Brogiolo, W., Hafen, E., Sun, H., Xu, T., (1999) PTEN affects cell size, cell proliferation and apoptosis during Drosophila eye development. Development. 126(23):5365-72.

Huang, L., Wang, C., Zhang, Y., Wu, M., Zuo, Z., (2013) Phenanthrene causes ocular developmental toxicity in zebrafish embryos and the possible mechanisms involved. J Hazard Mater. 261:172-80.

Huang, L., Xi, Z., Wang, C., Zhang, Y., Yang, Z., Zhang, S., Chen, Y., Zuo, Z., (2016) Phenanthrene exposure induces cardiac hypertrophy via reducing miR-133a expression by DNA methylation. Sci Rep. 6:20105

Incardona, J.P., Carls, M.G., Teraoka, H., Sloan, CA., Collier, T.K., Scholz, N.L. (2005) Aryl Hydrocarbon Receptor–Independent Toxicity of Weathered Crude Oil during Fish Development. Environ Health Perspect. 113(12): 1755–1762.

Incardona, J.P., Collier, T.K., Scholz, N.L., 2004. Defects in cardiac function precede morphological abnormalities in fish embryos exposed to polycyclic aromatic hydrocarbons. Toxicol Appl Pharmacol. 196, 191-205.

Incardona, J.P., Gardner, L.D., Linbo, T.L., Brown, T.L., Esbaugh, A.J., Mager, E.M., Stieglitz, J.D., French, B.L., Labenia, J.S., Laetz, C.A., Tagal, M., Sloan, C.A., Elizur, A., Benetti, D.D., Grosell, M., Block, B.A., Scholz, N.L., 2014. Deepwater Horizon crude oil impacts the developing hearts of large predatory pelagic fish. Proc Natl

Acad Sci U S A. 111(15), E1510-8.

Incardona, J.P., Linbo, T.L., Scholz, N.L., (2011) Cardiac toxicity of 5-ring polycyclic aromatic hydrocarbons is differentially dependent on the aryl hydrocarbon receptor 2 isoform during zebrafish development. Toxicol Appl Pharmacol. 257(2):242-9.

Incardona, J.P., Scholz, N.L. (2016) The influence of heart developmental anatomy on cardiotoxicity-based adverse outcome pathways in fish. Aquatic Toxicology. 177: 515-525.

Incardona, J.P., Swarts, T.L., Edmunds, R.C., Linbo, T.L., Aquilina-Beck, A., Sloan, C.A., Gardner, L.D., Block, B.A., Scholz, N.L., (2013) Exxon Valdez to Deepwater Horizon: comparable toxicity of both crude oils to fish early life stages. Aquat Toxicol. 142-143, 303-16.

Jayasundara, N., Van Tiem Garner, L., Meyer, J.N., Erwin, K.N., Di Giulio, R.T., (2015) AHR2-Mediated transcriptomic responses underlying the synergistic cardiac developmental toxicity of PAHs. Toxicol Sci. 143(2):469-81.

Knecht, A.L., Goodale, B.C., Truong, L., Simonich, M.T., Swanson, A.J., Matzke, M.M., Anderson, K.A., Waters, K.M., Tanguay, R.L., (2013) Comparative developmental toxicity of environmentally relevant oxygenated PAHs. Toxicol Appl Pharmacol. 271(2):266-75.

Liang, Q., De Windt, L.J., Witt, S.A., Kimball, T.R., Markham, B.E., Molkentin, J.D. (2001) The transcription factors GATA4 and GATA6 regulate cardiomyocyte hypertrophy in vitro and in vivo. J Biol Chem. 276(32):30245-53.

Love, M.I., Huber, W., Anders, S. (2014) Moderated estimation of fold change and dispersion for RNA-seq data with DESeq2. Genome Biol. 15(12):550.

Mager, E.M., Esbaugh, A.J., Stieglitz, J.D., Hoenig, R., Bodinier, C., Incardona, J.P., Scholz, N.L., Benetti, D.D., Grosell, M., (2014) Acute embryonic or juvenile exposure to Deepwater Horizon crude oil impairs the swimming performance of mahi-mahi (Coryphaena hippurus). Environ Sci Technol. 48(12):7053-61.

McCright, B., Gao, X., Shen, L., Lozier, J., Lan, Y., Maguire, M., Herzlinger, D., Weinmaster, G., Jiang, R., Gridley, T., (2001) Defects in development of the kidney, heart and eye vasculature in mice homozygous for a hypomorphic Notch2 mutation. Development. 128(4):491-502.

Pashin, Y.V., Bakhitova, L.M., (1979) Mutagenic and carcinogenic properties of polycyclic aromatic hydrocarbons. Environ Health Perspect. 30:185-9.

Porrello, E.R., Johnson, B.A., Aurora, A.B., Simpson, E., Nam, Y.J., Matkovich, S.J., Dorn, G.W., 2nd, van Rooij, E., Olson, EN., (2011) MiR-15 family regulates postnatal mitotic arrest of cardiomyocytes. Circ Res. 109(6):670-9.

Porrello, E.R., Mahmoud, A.I., Simpson, E., Johnson, B.A., Grinsfelder, D., Canseco, D., Mammen, P.P., Rothermel, B.A., Olson, E.N., Sadek, H.A., (2013) Regulation of neonatal and adult mammalian heart regeneration by the miR-15 family. Proc Natl Acad Sci U S A. 110(1):187-92.

Sørhus, E., Incardona, J.P., Karlsen, Ø., Linbo, T., Sørensen, L., Nordtug, T., van der Meeren, T., Thorsen, A., Thorbjørnsen, M., Jentoft, S., Edvardsen, R.B., Meier, S., (2016) Crude oil exposures reveal roles for intracellular calcium cycling in haddock craniofacial and cardiac development. Sci Rep. 6:31058.

Stieglitz, J.D., Benetti, D.D., Hoenig, R.H., Sardenberg, B., Welch, A.W., Miralao, S. (2012) Environmentally conditioned, year-round volitional spawning of cobia (Rachycentron canadum) in broodstock maturation systems. Aquacult Res. 43:1557–1566.

Stieglitz, J.D., Mager, E.M., Hoenig, R.H., Benetti, D.D., & Grosell, M., (2016) A novel system for embryo-larval toxicity testing of pelagic fish: Applications for impact assessment of Deepwater Horizon crude oil. Chemosphere. 162:261-268.

Sweet, L.E., Magnuson, J., Garner, T.R., Alloy, M.M., Stieglitz, J.D., Benetti, D., Grosell, M., Roberts, A.P., (2016) Exposure to ultraviolet radiation late in development increases the toxicity of oil to mahi-mahi (Coryphaena hippurus) embryos. Environ Toxicol Chem. 2016 Nov 16. doi: 10.1002/etc.3687.

Xu, E.G., Mager, E.M., Grosell, M, Stieglitz, J.D., Hazard, E.S., Hardiman, G., Schlenk, D. (2017) Developmental transcriptomic analyses for mechanistic insights into critical pathways involved in embryogenesis of pelagic mahi-mahi (Coryphaena hippurus). PLoS One. 12(7):e0180454.

Xu, E.G., Mager, E.M., Grosell, M., Pasparakis, C., Schlenker, L.S., Stieglitz, J.D., Benetti, D., Hazard, E.S., Courtney, S.M., Diamante, G., Freitas, J., Hardiman, G., Schlenk, D., (2016) Time- and Oil-Dependent Transcriptomic and Physiological Responses to Deepwater Horizon Oil in Mahi-Mahi (*Coryphaena hippurus*) Embryos and Larvae. Environ Sci Technol. 50(14):7842-51.

Yoo, J.K, Jung, H.Y., Kim, C.H., Son, W.S., Kim, J.K., (2013) miR-7641 modulates the expression of CXCL1 during endothelial differentiation derived from human embryonic stem cells. Arch Pharm Res. 36(3):353-8.

Conclusions

The endocrine system plays a crucial role in many signaling processes that aid in regulating normal development. Our data show that exposure to E2 and G1 cause cardiotoxicity in developing zebrafish embryos. However, the toxic effects induced by E2 was not rescued after co-exposure to ER or GPER antagonist. This further shows the complexity in endocrine signaling and raises the question of the role of GPER and ERs during development. Due to ability of these agonists and antagonists to have other potential targets, E2 induced toxicity needs to be evaluated using a more targeted approach such as morpholinos or RNAi for the specific estrogen receptors would be a relevant future study. Evaluating the pathways involved in estrogen toxicity is important due to the high number of pollutants that can alter the endocrine system.

Transformation products of chrysene such as 2-hydroxychrysene and 6-hydroxychrysene, have been shown *in vitro* to have estrogenic and antiestrogenic effects. In our study, no effect was observed in zebrafish embryos after exposure to chrysene. In contrast, its two metabolites, 2-hydroxychrysene and 6-hydroxychrysene caused cardiac, ocular and circulatory defects. However, the toxic effects of 2-hydroxychrysene and 6-hydroxychrysene do not seem to be directly mediated through the estrogen pathway. One of the most abundant deformities observed was circulatory defects, it would be interesting to investigate whether this is a primary target for 2-hydroxychrysene and if *runx1* expression is directly involved in the mechanism. Another interesting future study is to evaluate what drives the regio-selective difference between the compounds.

Preliminary data show a difference in accumulation of the 2 compounds. It would be intriguing if a difference in metabolism was involved in the regio-selective effects.

In our study, we show that exposure to both source and weathered oil can alter the expression of miRNAs during mahi-mahi development. Consistent with the toxicological effects observed, GO term analysis identified heart development and ion regulation processes to be affected after oil exposure. This study indicates that miRNAs play a role in misregulating the expression of genes involved in cardiac and ion transport induced by oil exposure that need to be elucidated. The mRNA-miRNA network generated in this study can guide many hypotheses based experiments that will contribute to the field. Studies evaluating the role of specific miRNAs on Ca^{2+} influx and transport in cardiac myocytes is important to show further understand oil toxicity. However, this also raises the question of how PAHs alter miRNA expression.

The dynamic signaling patterns that occur during early development contributes to the complexity in evaluating developmental toxicity. The zebrafish has become a useful model in better understanding the potential risks of exposed organisms to environmental pollutants. The increase in many new molecular and cellular methods as well as high throughput sequencing is beneficial in better understanding mechanisms involved in toxicological effects induced by environmental pollutants. The current study further shows the need for continued research on not only source oil, but even more so weathered oil. Studies like this can aid in identifying the risks involved when oil spills occur in areas where fish species spawn.